PRINCETON UNIVERSITY

DEPARTMENT OF AERONAUTICAL ENGINEERING

U.S. Army Transportation Research Command
Fort Eustis, Virginia

Project Number: 9-38-01-000, TK902
Contract Number: DA 44-177-TC-524

STABILITY AUGMENTATION OF GROUND EFFECT MACHINES

by
Theodor A. Dukes
Charles R. Hargraves

Department of Aeronautical Engineering
Princeton University
Instrumentation and Control Laboratory

Report No. 601 April 1962

Approved by: Dunstan Graham
Associate Professor
in Aeronautical Engineering

FOREWORD

The research in this report was conducted in the Instrumentation and Control Laboratory of the Department of Aeronautical Engineering at Princeton University.

The work was done under the sponsorship of the U.S. Army Transportation Research Command as Phase 8 of ALART. This support is gratefully acknowledged.

TABLE OF CONTENTS

page

LIST OF FIGURES

17. Effect of Cross Flow Dissipation Factor on $\frac{1}{r}\frac{\partial C_M}{\partial \theta}$

18. Effect of Lift Efficiency Factor on $\frac{1}{r}\frac{\partial C_M}{\partial \theta}$, $\beta_o = 0^\circ$

19. Effect of Lift Efficiency Factor on $\frac{1}{r}\frac{\partial C_M}{\partial \theta}$, $\beta_o = 45^\circ$

20. Experimental Values for $\frac{1}{r}\frac{\partial C_M}{\partial \theta}$

21. Experimental Moment versus Attitude Curves

22. Experimental Pitch Damping

23. Change of the Pitching Mode with Height

24. Effect of RPM on the Pitching Mode (Experimental)

25. Effect of Damping on a Statically Unstable Second Order System

26. Feedback Configurations

27. Close-up View of the Model

28. Model and Test Setup

LIST OF SYMBOLS

A	gain, augmentation factor
A_C	control gain
A_F	attitude feedback gain
A_P	pilot gain
A_R	rate feedback gain
a	nozzle area to base area ratio
B	damping force (lbs./ft./sec.)
C_{DP}	parasite drag coefficient
C_L	lift coefficient
C_M	moment coefficient
C_μ	momentum coefficient
C_b, C_h	factors defined by Equation 22
D	equivalent diameter (ft.)
g	acceleration of gravity (ft./sec.^{2})
G	general transfer function
h	height above the ground (ft.)

$\bar{h}$ normalized height = $\frac{h}{t}$

I moment of inertia (slug-ft.^{2})

J jet momentum (lbs./ft.)

$\bar{J}$ normalized jet momentum = $\frac{J}{2P_T t}$

K aerodynamic spring constant (lbs./ft.)

L lift force (lbs.)

ℓ length of the periphery (ft.)

M aerodynamic moment (ft.-lbs.); mass of GEM (slugs)

m mass flow (slug/ft.-sec.)

$\bar{m}$ normalized mass flow = $\frac{m}{\sqrt{2P_T\rho}}$

P pressure (lbs./ft.^{2})

$\bar{P}$ normalized pressure = $\frac{P}{P_T}$

P_L specific load = $\frac{L}{S}$ (lbs./ft.^{2})

$\bar{P}_L$ normalized specific load = $\frac{P_L}{P_T}$

r radius or distance (ft.)

r_g radius of gyration of saucer (ft.)

$\bar{r}$ normalized radius = $\frac{r}{t}$

S base area (ft.^{2})

s	complex variable
s_c	control lag root
s_1, s_2	pitching mode roots
T	propulsive thrust (lbs.); time constant (sec.)
t	jet thickness (ft.)
V	velocity (translational) (ft./sec.)
ν	jet velocity (ft./sec.)
W	weight of GEM (lbs.)
χ	$= \frac{1 + \sin\beta}{h}$
α	cross flow dissipation factor
β	jet inclination angle with respect to the vertical (deg.)
β_o	jet inclination angle with respect to the machine (deg.)
δ	control input
ζ	damping ratio
η_J	jet efficiency factor
η_L	base (lift) efficiency factor
θ	attitude angle

ρ	density of air (slug/ft.^{3})
ω	frequency (1/sec.)

SUBSCRIPTS

A	atmospheric
B	base
b	balanced regime
e	equilibrium
H	high side or heaving mode
J	jet
L	low side
o	overfed regime, free stream
P	pitching mode
T	total; throttle
u	underfed regime
∞	out of ground effect
θ	angle

SUMMARY

This is a study of feedback control for the stabilization of a peripheral jet ground effect machine (GEM). The study is limited to over land operation, to hovering and low forward velocities, where normal aerodynamic control surfaces are ineffective.

Expressions for the frequency and damping of the heave motion and for the attitude moment derivative are derived, using the principle of momentum balance. The influence of physical parameters and scaling on these results is discussed. The differential equations of forward flight are developed and expressed.

The results of a series of experiments on an eight foot diameter GEM model in a hover condition are in satisfactory agreement with theoretical predictions. The experiments also show considerable damping of the attitude motion.

An attitude and rate feedback control system was devised, considering the adaptability of the human pilot, and the disturbing moments. Preliminary synthesis brings out the significance of the moment control lag and the variation of the moment control effectiveness. It is suggested that open loop gain adjustments can be expected to provide satisfactory compensation for parameter changes, both in hovering and in forward flight.

1. INTRODUCTION

1.1. Background

Most low speed flying vehicles are either unstable or exhibit only marginal stability. Two outstanding examples of vehicles with stability problems are ground effect machines (GEMs) and vertical take off and landing aircraft (VTOLs). Although it is a well-known fact that aircraft need not be actually stable (i.e. return to equilibrium after any disturbance), for satisfactory flying qualities it is necessary that any divergence in the motion following a disturbance be sufficiently slow so that it can be comfortably handled by the pilot. Many GEM and VTOL configurations are sufficiently unstable, over at least a portion of the flight regime, as to be difficult if not impossible to fly. Aerodynamic stabilization in many cases proves to be inefficient. Another means for increasing the stability is the application of feedback control. Some difficulty may, however, be encountered in the application of conventional techniques to automatic stabilization because of the rapid variation of the stability derivatives during changes in flight condition.

The report which follows is confined to the problems of artificial stability augmentation of peripheral jet ground effect machines. An investigation of the literature shows that very little is known about the dynamic characteristics of this type of vehicle.

Attitude stability can be obtained in the GEM by aerodynamic means. If the GEM is operated at a height above the ground sufficiently small compared to the diameter of the machine, it is inherently stable in attitude. However, the operating height required for stability is generally incompatible with the height needed for operation over typical terrain. The range of stability

can be extended by using interior jets which effectively "compartment" the machine. Since the individual compartments tend to exhibit altitude stability, the machine becomes stable in pitch. However, as shown for example in Reference 5, considerable performance loss results from the use of internal stabilizing jets. For this reason, it was thought worthwhile to investigate feedback as a means of achieving the desired degree of stability with no significant loss of performance.

The dynamics aspect of ground effect machines has been considered previously in References 1, 2, 3 and 4, although not primarily from the point of view of feedback stabilization. Reference 1 was only of a very preliminary nature although feedback control was considered. The final results of the study proposed in Reference 2 were not available to the authors at the time of publication of this report. Reference 3 considered only machines which had been previously stabilized by means of internal jets, while Reference 4 considered only the heave motion.

During the short period of time since widespread attention was first given to the GEMs, a large amount of work has been done. However, a number of problems still remain. This is particularly true with regard to restoring moments and damping forces and moments, since most of the attention to date has been confined to predicting, and experimentally determining, the performance characteristics.

A short review in three sections is given here of the work which has been done.

1. Augmentation. A study of the general proximity effect on nozzles was made by Von Glahn in April 1957. (Reference 6). Shortly thereafter a theory was presented by Chaplin (Reference 7) which assumed the jets to be

thin and neglected the effects of viscosity. The theory was extended to thick, viscous jets in References 8 to 12. A qualitative discussion of the effects of vortices was given by Nixon and Sweeney (Reference 13). A large amount of experimental data, as well as results of experience with full scale machines, was given in the papers presented at the Princeton Symposium (Reference 14). The effects of vortices were treated theoretically in References 15 and 16.

2. Moments. A theory for the prediction of moments employing thin jets was given in Reference 17, and was extended to thick jets in Reference 18. Several experimental investigations of the static moments acting on GEMs were reported in Reference 5.

3. Forward Flight. Experimental investigations of GEMs in forward flight were given in References 19 and 20.

Available theoretical and experimental data seem to be sufficient to allow prediction of the augmentation of a hovering machine with good accuracy. The situation with regard to moments, however, is not as good. The theory in Reference 17 shows the machine to be unstable in attitude for all height to diameter ratios. The theory of Reference 18 gives results similar to those observed experimentally. However, these results are tied to certain assumptions and the sensitivity to these assumptions has not been explored.

In summary, actually very little information about stability derivatives is available in the literature. Since a fairly good understanding of the vehicle to be controlled is a necessity for a feedback control synthesis, a large part of our effort has been devoted to deriving expressions for some important stability derivatives. The validity of the theoretical results has been checked by measurements, and the results are used in a preliminary synthesis of a feedback control system for stability augmentation.

1.2. Equations of motion

If we attempted a general solution to the problem of describing the dynamics of the ground effect machine, a system of six coupled nonlinear differential equations for the six degrees of freedom would have to be solved. However, in order to concentrate on the dynamic problems which are most important from a practical engineering viewpoint, we are going to make simplifications while emphasizing those aspects which lead to a reasonable formulation of the control problem. Some of the factors which are neglected at this time may draw more attention at a later stage of development after the most important controllability problems have been solved.

The first in a series of simplifications is the assumption that the longitudinal and the lateral degrees of freedom can be considered uncoupled. The most obvious coupling terms are gyroscopic moments. A discussion of the order of magnitude and the scaling of the gyroscopic coupling is presented in Appendix A. The conclusion is that, except for single propeller ground effect machines with large specific loads, the gyroscopic coupling is practically negligible; therefore it will be neglected in the present study. Nevertheless, it should be mentioned here that the scaling of the gyroscopic coupling should be considered if the dynamics of a single propeller ground effect machine are to be investigated on a scaled model.

There is also a coupling of an aerodynamic nature between the rolling and pitching motion, due to the fact that both are coupled to the heaving motion in a similar way. It is well known that the lift does not remain the same when the GEM is not parallel to the ground; the lift is an even function of the attitude angle around any axis. On the other hand, the aero-

dynamic moment at any attitude angle is also a function of height. The mechanism of the coupling can be described in a qualitative way as follows. Assume that the machine is at a certain roll and pitch attitude angle at the same time and that the roll angle is changed. This causes a change in the lift force, therefore, the c.g. of the machine moves up or down. The change in height induces a change in the moment around the pitch axis resulting in a pitching motion. Similarly, a change in pitch angle results in a rolling motion.

The strength of this coupling depends mainly upon the slopes of the functions expressing the relationship between height and angle, and moment and height. The effect of this coupling on the dynamics is strongly influenced by the damping in heave.

The even function $L = f(\Theta)$ where Θ could be the angle around any axis, has a flat maximum at $\Theta = 0$. The change in lift with small deviations from the leveled condition has been shown experimentally to be very small. (See reference 5 and Figure 3). Experiments and theory (to be presented in subsequent sections) indicate a fairly high degree of damping in the heave motion. Considering also that at practical heights only small angles are possible, this coupling between the lateral and longitudinal degrees of freedom can be regarded as of secondary importance and is neglected in the subsequent analysis.

Other coupling terms may appear due to an added fin, tail or auxiliary thrust. Such couplings are not considered here because we are concerned primarily with low translational velocities where the ground cushion exists and where the aerodynamic forces exerted on a fin or tail are not very strong. It should be pointed out here that the effect of these additional terms on the lateral-longitudinal coupling can be, and should be, considered carefully

in the case of any particular design. We intend to concentrate on the dominant stability problem of the peripheral jet ground effect machine at and near hovering.

The above discussion, as well as experience with existing full scale GEM models, indicate that most problems of stability and controllability appear even if only three degrees of freedom are considered: the freedom in heave, in attitude around one axis, and in motion along the axis perpendicular to the attitude axis. The remainder of this study represents an approach to the analysis of the stability problems for the purpose of a preliminary synthesis of an automatic feedback system for stability augmentation.

In order to make the mathematical treatment of our problem feasible, we will use small perturbation theory. This approach enables us to investigate the necessary, but not sufficient, condition for stability of a nonlinear system; the system must be stable in the vicinity of any equilibrium point. This investigation reveals approximate quantitative information about the most important stability problems. The variation of the stability throughout the considered flight regimes will be visualized by means of root locus diagrams so that basic solutions to the feedback control problem can be suggested.

Stability in hovering will first be considered, followed by a discussion of stability in forward flight.

2. HOVERING ANALYSIS

2.1. Hovering equations

As an approximation to the stability problem in hovering, we assume that variations in attitude are sufficiently small so that any lateral or longitudinal velocities which develop are quite small, and therefore forces and moments due to horizontal velocities can be neglected. This leaves us with two coupled equations in two degrees of freedom. Using the height, h, and attitude angle with respect to horizontal, θ as perturbation variables, we can write the equations in linearized form, Laplace transformed with zero initial conditions.

For heave:

$$\left(-\frac{\partial L}{\partial h} + \frac{\partial L}{\partial \dot{h}} s + M s^2\right) h + \frac{\partial L}{\partial \theta} \theta = \frac{\partial L}{\partial \delta_T} \delta_T \qquad (1)$$

and for pitch:

$$\frac{\partial M}{\partial h} h + \left(\frac{\partial M}{\partial \theta} + \frac{\partial M}{\partial \dot{\theta}} s + I s^2\right) \theta = \frac{\partial M}{\partial \delta_\theta} \delta_\theta \qquad (2)$$

δ_T and δ_θ represent the throttle and the moment control input respectively.

For stability investigations only the homogeneous equations need to be considered. After dividing by the weight, W, we can write the heave equation in the following form.

$$\left(\frac{1}{g} s^2 + \frac{1}{P_L} \frac{\partial P_L}{\partial \dot{h}} s - \frac{1}{P_L} \frac{\partial P_L}{\partial h}\right) h + \frac{1}{P_L} \frac{\partial P_L}{\partial \theta} \theta = 0 \qquad (3)$$

where $P_L = L/S$

The moment equation can be normalized by dividing by LD where D can be any suitable dimension of the GEM

$$\left(\frac{I}{LD}s^2 + \frac{\partial C_M}{\partial \dot{\theta}}s + \frac{\partial C_M}{\partial \theta}\right)\theta + \frac{\partial C_M}{\partial h}h = 0 \qquad (4)$$

In effect, this procedure serves to define the moment coefficients.

Let us consider now a special but practically very important case. For equilibrium at the leveled condition $\partial P_L/\partial\theta = 0$ since P_L is a smooth even function of θ. Also, $(\partial M/\partial h)_{\theta=0} = 0$ since, because of symmetry, the moment at $\theta = 0$ is zero independent of the height. Therefore, in hovering with zero attitude angle, and practically also at small attitude angles, we have two uncoupled second order equations of motion for the two degrees of freedom in heave and attitude. This enables us to investigate the stabilities of the uncoupled modes as functions of height and this simplified approach will lead to basic suggestions for the solution of the stability problem in hovering. The effect of dynamic coupling and forward flight, will be discussed subsequently.

2.2. Application of momentum balance to GEMs.

2.2.1. Assumptions. In this section the momentum balance approach is used to derive the most important stability derivatives in hovering. The vortices which occur because of viscous effects are, to a certain extent, included in the analysis by lumping the averaged pressure drop under the base into a "base efficiency factor", η_L. The momentum balance approach seems to be adequate to show some of the most important mechanisms influencing the stability. The relationships to be obtained are also very useful in estimating the effects of scaling on the stability derivatives.

The momentum balance approach has been used previously by numerous authors. The method given here differs from previous presentations in that basic relationships are derived using only the momentum balance approach. Actual numerical results may differ considerably depending upon the assumptions which are made about the jet. In the following presentation different assumptions about the jet may be taken into account by making appropriate substitutions.

Some fairly general relationships concerning the base pressure and the air flow at the periphery of the base can be deduced from the assumption that the pressure difference at the periphery is kept in balance by the sum of jet moments. Following Tulin (Reference 25) we distinguish three different regimes. We shall characterize these regimes for unit length of the periphery, without specifying any method of determining the jet momentum. We shall assume that the radius of curvature of the periphery is large compared to the height of the machine above the ground, i.e., we assume the flow at each point of the periphery to be two-dimensional. (Three-dimensional correction will be made later.) We shall also assume the flow to be incompressible and inviscid. However, viscous losses will be considered in the form of efficiency factors.

2.2.2. Balanced regime. In the balanced regime the jet from the peripheral nozzle seals off the base area. At the peripheral element under consideration, air is neither entering nor leaving the base area.

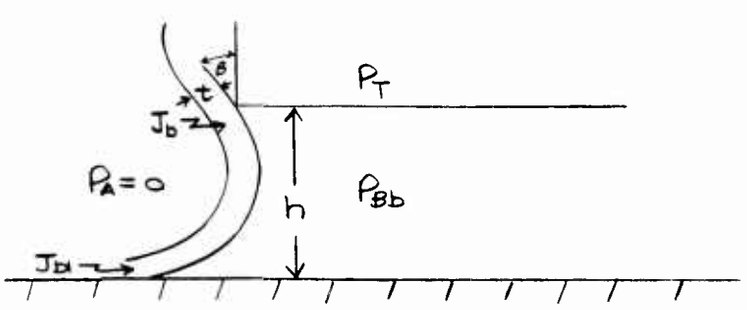

For horizontal equilibrium over a segment of the periphery of unit length,

$$P_{Bb}\, h = \eta_J \left(J_b \sin\beta + J_{b1}\right) \cong \eta_J J_b \left(1 + \sin\beta\right) \tag{5}$$

where h = the height of the nozzle section above ground

J_b = momentum of the jet leaving the nozzle

J_{b1} = final momentum of the jet

η_J = a jet efficiency factor

If the base of the machine is parallel to the ground, then $\beta = \beta_o$ where β_o is the jet inclination angle of the machine.

Equation 5 can be normalized by dividing by the jet strength out of ground effect. Using Bernoulli's equation

$$J_\infty = \rho t V_o^2 = a t P_T \tag{6}$$

Dividing (5) by (6) we get

$$\frac{1}{2} \frac{P_{Bb}}{P_T} \frac{h}{t} = \eta_J \left(\frac{J_b}{J_\infty} \sin\beta + \frac{J_{b1}}{J_\infty}\right) \tag{7}$$

Using a bar to designate normalized quantities this can be written as:

$$\frac{1}{2} \bar{P}_{Bb} \bar{h} = \eta_J \left(\bar{J}_b \sin\beta + \bar{J}_{b1}\right) \cong \bar{J}_b \left(1 + \sin\beta\right) \tag{8}$$

where the length is normalized by the nozzle width and the difference between the initial and final jet momentum has been neglected.

2.2.3. Underfed regime. In the underfed regime air is flowing out of the base area and the momentum of the escaping air must be considered.

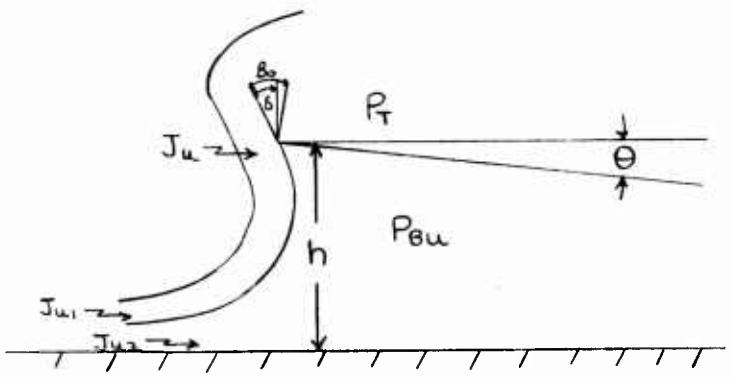

Using the subscript u for the underfed regime we can write for the horizontal equilibrium

$$\frac{1}{2}\,\bar{P}_{Bu}\,\bar{h} = \eta_J\left(\bar{J}_u \sin\beta + \bar{J}_{u1} + \bar{J}_{u2}\right) \qquad (9)$$

$$\cong \eta_J\left[\bar{J}_u\,(1+\sin\beta) + \bar{J}_{u2}\right]$$

Here $\bar{J}_{u2}$ is actually a notation for the normalized change of momentum rather than for the jet momentum.

For a leveled machine again $\beta = \beta_o$; if the base is at an angle Θ to the horizontal, $\beta = \beta_o - \Theta$. The mass flow of the escaping air must be determined from an additional equilibrium condition for the entire base area.

2.2.4. Overfed regime. In the overfed regime air is flowing into the base area. This air must be supplied by part of the nozzle jet. This weakens the total jet momentum due to diminishing of the mass flow which is turned away from the base area and due to the momentum of the air flowing into the base area.

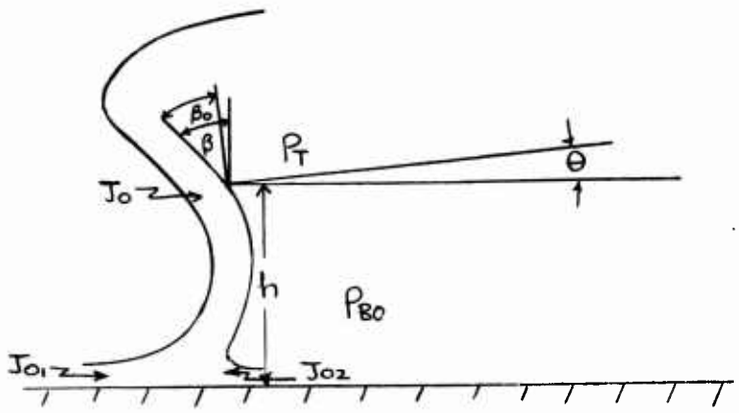

For horizontal equilibrium

$$\frac{1}{2}\,\bar{P}_{BO}\,\bar{h} = \eta_J\left(\bar{J}_o \sin\beta + \bar{J}_{o1} - \bar{J}_{o2}\right) \tag{10}$$

where again $\beta = \beta_o - \theta$. The mass flow of the air flowing into the base area must again be determined by means of an additional equilibrium condition for the base area.

Using the basic concept of these three regimes, equations for forces and moments can be determined in a form still independent of the particular choice of jet theory, but nevertheless indicating the basic relationships and important factors. It should be noted that the basic concept can be used also for other than simple peripheral jets.

2.3. Lift and augmentation.

The over-all lifting force acting on a ground effect machine with a single peripheral jet can be expressed in the following general form:

$$L = \eta_J \int_\ell J \cos\beta \, d\ell + \eta_L \int_S P_B \, dS \tag{11}$$

where J is the jet momentum per unit length of the periphery, ℓ is the length of the periphery and S is the base area enclosed by the jet. In a leveled, balanced condition the height of the jet is uniform along the periphery and $\beta = \beta_o$; the base pressure is considered uniform over the whole base area. η_L is an efficiency coefficient expressing the experimental fact that due to vortices and other losses only part of the computed pressure contributes to the lift. For the leveled balanced condition

$$L = \eta_J J_b \ell \cos\beta_o + \eta_L S P_B \tag{12}$$

Generally both J_b and P_B are functions of the height, h . We introduce now the specific load $P_L = L/S$

$$P_L(h) = \eta_J J_b(h) \frac{\ell}{S} \cos\beta_o + \eta_L P_B(h) \tag{13}$$

For determining the augmentation factor the reference is the specific lift produced by the same total head out of ground effect with $\beta_o = 0$ and the same jet efficiency factor, η_J . Out of ground effect $P_B = 0$ and with Equation 6 the augmentation can be expressed as

$$A(h) = \frac{1}{2\eta_J} \frac{P_L(h)}{P_T} \frac{S}{\ell t} = \tag{14}$$

$$= \frac{J_b(h)}{J_\infty} \cos\beta_o + \frac{\eta_L}{2\eta_J} \frac{S}{\ell t} \frac{P_B(h)}{P_T}$$

or

$$A(h) = \frac{1}{2\eta_J a}\,\bar{P}_L = \bar{J}_b \cos\beta_o + \frac{\eta_L}{2\eta_J a}\,\bar{P}_B \tag{15}$$

where $a = \frac{\ell t}{S}$ is the important physical parameter expressing the ratio of the nozzle area and the base area, and the bars indicate the jet momentum and the base pressure normalized by $2P_T t$ and P_T respectively.

We can also express the "normalized specific load" as:

$$\bar{P}_L = 2\eta_J a\,\bar{J}_b \cos\beta_o + \eta_L\,\bar{P}_B \tag{16}$$

2.4. Heaving dynamics.

2.4.1. Restoring force in heave. The equilibrium height, h_e, is determined by the condition that the lift at this height in the leveled, balanced condition be equal to the weight W.

$$P_{Le} = \frac{W}{S} = \eta_J J_b(h_e)\frac{\ell}{S}\cos\beta_o + \eta_L P_B(h_e) \tag{17}$$

A deviation from the equilibrium height gives rise to a restoring force because $L \neq W$ if $h \neq h_e$.

If we linearize for small deviations we can write

$$\Delta P_L = \frac{dP_L}{dh}\,\Delta h \tag{18}$$

The total derivative is used from here on since we are considering freedom in height only.

The specific restoring force, which is in effect the normalized "spring-constant" in heave, is defined as

$$K = - \left. \frac{dP_L}{dh} \right|_{h=h_e} \tag{19}$$

$$= - \left[\eta_J \frac{dJ_b}{dh} \frac{\ell}{S} \cos\beta_o + \eta_L \frac{dP_B}{dh} \right]_{h=h_e}$$

The derivation below is based on the following physical considerations.

1. Among the related variables $\bar{h}$, $\bar{P}_B$, $\bar{J}_b$ there is only one independent variable.

2. With our assumptions the jet is determined uniquely by the normalized base pressure, $\bar{P}_B$, therefore

$$\frac{dJ_b}{dh} = \frac{dJ_b}{dP_B} \frac{dP_B}{dh} \tag{20}$$

The change in base pressure with height, $\frac{dP_B}{dh}$, can be determined from Equation 5 by differentiating and substituting the above expression (20).

$$\frac{dP_B}{dh} = - \frac{P_B}{h} \frac{1}{1 - \frac{\eta_J}{h} \frac{dJ_b}{dP_B} (1 + \mu \sin\beta_o)} \tag{21}$$

Substituting Equation 20 and the above expression into Equation 19, we get

$$K = \eta_L \frac{P_B}{h} \quad \frac{1 + \frac{\eta_J}{\eta_L} \frac{d J_b}{d P_B} \frac{l}{s} \cos\beta_o}{1 - \frac{\eta_J}{h} \frac{d J_b}{d P_B} (1 + \mu \sin\beta_o)}$$

and normalizing by $J_\infty = 2 t P_T$ with $a = tl/s$

$$K = \eta_L \frac{P_B}{h} \quad \frac{1 + \frac{\eta_J}{\eta_L} \frac{d \bar{J}_b}{d P_B} 2a \cos\beta_o}{1 - \frac{2\eta_J}{h} \frac{d \bar{J}_b}{d P_B} (1 + \mu \sin\beta_o)} \tag{22}$$

$$= \eta_L \frac{P_B}{h} \frac{c_b}{c_h}$$

This equation also serves as a definition for c_b and c_h

The fraction in which $\frac{d \bar{J}_b}{d P_B}$ appears both in the numerator and in the denominator indicates the influence of the change of jet momentum with base pressure. If the jet would not change with the base pressure, P_B, the spring constant would be simply,

$$K = \eta_L \frac{P_B}{h} \tag{23}$$

The correction term in the denominator expresses the fact that this full K cannot develop. For example, downward motion from equilibrium results in some weakening of the jet and less restoring pressure can develop than with an unchanged jet. The correction term in the numerator expresses the change in the direct contribution of the jet to the lift.

2.4.2. Damping in heave. If the machine is moving downward with a velocity, $\dot{h}$, air must leave the base area and if the machine is moving with an upward velocity, air must flow into the base area. Damping forces arise because of changes in the over-all lift at any height which occur in either an underfed or an overfed regime. The mass flow leaving or entering the base area is determined by

$$m_l = \rho S \dot{h} \tag{24}$$

where m is now the mass flow.

For simplicity only the leveled condition is considered. Here the jet is uniform along the whole periphery.

2.4.2.1. Downward velocity. While losing altitude with a velocity $\dot{h} < 0$, the escaping air forms an additional jet with momentum J_{u2} over a unit length of the periphery, resulting in an underfed regime. Because of the leveled condition, $\beta = \beta_0$. Indicating the changes from the balanced condition we obtain from Equation 9

$$\frac{1}{2}(\bar{P}_{Bb} + \Delta\bar{P}_{Bu})\bar{h} = \eta_J\left[(\bar{J}_b + \Delta\bar{J}_u)(1 + \sin\beta_0) + \bar{J}_{u2}\right] \tag{25}$$

We get the pressure difference due to the escaping air if we subtract Equation 8 from Equation 25.

$$\frac{1}{2\eta_J}\,\Delta\bar{P}_{Bu}\,\bar{h} = \Delta\bar{J}_u\,(1+\sin\beta_o) + \bar{J}_{u2} \tag{26}$$

$$= \frac{d\bar{J}_b}{d\bar{P}_B}\,\Delta\bar{P}_{Bu}\,(1+\sin\beta_o) + \bar{J}_{u2}$$

The predominant term on the right hand side, $\bar{J}_{u2}$, indicates a pressure increase. $\Delta\bar{J}_u$ arises because the mass flow at the nozzle is a function of the base pressure. An increase in base pressure causes a decrease in mass flow, therefore $\Delta\bar{J}_u$ is a negative number. Solving Equation 26 for $\Delta\bar{P}_{Bu}$ we obtain,

$$\Delta\bar{P}_{Bu} = \frac{2\eta_J}{1 - \frac{2\eta_J}{\bar{h}}\,\frac{d\bar{J}_b}{d\bar{P}_B}\,(1+\sin\beta_o)}\;\frac{\bar{J}_{u2}}{\bar{h}} \tag{27}$$

$$= \frac{2\eta_J}{c_h}\,\frac{\bar{J}_{u2}}{\bar{h}}$$

where c_h is the same as defined in Equation 22.

Differentiating the specific lift, Equation 16, and using the base pressure change expressed by Equation 27, we obtain the following expression for the normalized damping force,

$$\overline{\Delta P}_{L_{dn}} = \left(2\eta_J \alpha \frac{d\overline{J}_B}{d\overline{P}_B} \cos\beta_o + \eta_L\right)\overline{\Delta P}_B \tag{28}$$

$$= 2\eta_L\eta_J \frac{C_b}{C_h} \frac{\overline{J}_{u2}}{\overline{h}}$$

where $\frac{C_b}{C_h}$ has been defined in Equation 22.

The additional momentum, $\overline{J}_{u2}$, can be determined from the mass flow, Equation 24, and Bernouilli's equation

$$J_{u2} \cong -\frac{S}{\ell}\sqrt{2\rho P_B}\,\dot{h} \qquad \dot{h} < 0 \tag{29}$$

In normalized form

$$\overline{J}_{u2} = -\frac{S}{\ell}\frac{1}{2tP_T}\sqrt{2\rho P_B}\,\dot{h} = -\frac{1}{a}\sqrt{\overline{P}_B}\,\frac{\dot{h}}{V_\infty} \tag{30}$$

where $V_\infty = \sqrt{\frac{2P_T}{\rho}}$ is the jet velocity out of ground effect.

Substituting into Equation 28

$$\overline{\Delta P}_{L_{dn}} \cong -\frac{2\eta_L\eta_J}{a}\frac{C_b}{C_h}\frac{1}{\overline{h}}\sqrt{\overline{P}_B}\,\frac{\dot{h}}{V_\infty} \tag{31}$$

2.4.2.2. Upward velocity. While gaining altitude with a velocity, $\dot{h} > 0$, air is being supplied by the jet into the base area, resulting in an overfed regime. For the leveled machine, $\beta = \beta_o$. Indicating the changes from the balanced condition, Equation 10 can be rewritten as follows:

$$\frac{1}{2}\left(\bar{P}_{Bb} + \Delta\bar{P}_{BO}\right)\bar{h} = \eta_J\left[\left(\bar{J}_b + \Delta\bar{J}_o\right)\sin\beta_o + \bar{J}_{o1} - \bar{J}_{o2}\right] \quad (32)$$

We get the pressure difference due to the flow into the base area if we subtract Equation 8 from Equation 32:

$$\frac{1}{2}\Delta\bar{P}_{BO}\bar{h} = \eta_J\left[\Delta\bar{J}_o\sin\beta_o - \left(\bar{J}_{b1} - \bar{J}_{o1}\right) - \bar{J}_{o2}\right] \quad (33)$$

We can arrive at a simple approximation to the right hand side as follows:

$$J_{b1} = m_o V_\infty \quad \text{where} \quad V_\infty = \sqrt{\frac{2P_T}{\rho}} \quad (34)$$

$$J_{o2} = m V_{o2} \quad \text{where} \quad V_{o2} = \sqrt{\frac{2(P_T - P_B)}{\rho}}$$

$$J_{o1} = (m_o + \Delta m_o - m)V_\infty \quad \text{where} \quad \Delta m_o V_\infty = \Delta J_{o1} \cong \Delta J_o$$

If we normalize by $J_\infty = m_\infty V_\infty$ where m_∞ is the mass flow at the nozzle out of ground effect we get

$$\bar{J}_{b1} - \bar{J}_{o1} = \frac{m}{m_\infty} - \frac{\Delta J_{o1}}{J_\infty} \cong \bar{m} - \Delta\bar{J}_o$$

and

$$\bar{J}_{o2} = \bar{m}\sqrt{1 - \bar{P}_B}$$

Using again $\bar{\Delta J} = \frac{d\bar{J}_b}{d\bar{P}_B}\bar{\Delta P}_B$, we find by substituting into Equation 33

$$\bar{\Delta P}_{BO} \cong -\frac{2\eta_J}{c_h \bar{h}}\,\bar{m}\left(1+\sqrt{1-\bar{P}_B}\right) \tag{35}$$

where c_h is the term as defined in Equation 27, and using the mass flow Equation 24

$$\bar{\Delta P}_{BO} = -\frac{2\eta_J}{c_h \bar{h}}\,\frac{1}{a}\left(1+\sqrt{1-\bar{P}_B}\right)\frac{\dot{h}}{V_\infty} \qquad \dot{h}>0 \tag{36}$$

The change in the specific lift describes the normalized damping

$$\bar{\Delta P}_{L_{up}} = c_b \eta_L \bar{\Delta P}_{BO} = -2\frac{\eta_L \eta_J}{a}\,\frac{c_b}{c_h}\,\frac{1}{\bar{h}}\left(1+\sqrt{1-\bar{P}_B}\right)\frac{\dot{h}}{V_\infty} \tag{37}$$

For determining a damping factor for comparison with experimental data we consider the average damping force acting over a complete cycle of oscillation.

$$\frac{1}{2}\left[|\bar{\Delta P}_{L_{dn}}| + |\bar{\Delta P}_{L_{up}}|\right] = \frac{\eta_L \eta_J c_b}{a\,\bar{h}\,c_h}\left(1+\sqrt{\bar{P}_B}+\sqrt{1-\bar{P}_B}\right)\frac{|\dot{h}|}{V_\infty} \tag{38}$$

We make an error of less than 4% for $0.1 < \bar{P}_B < 0.9$, i.e., for all practical values of $\bar{P}_B$, if we write

$$\frac{1}{2}\left[|\Delta\bar{P}_{L_{dn}}| + |\Delta\bar{P}_{L_{up}}|\right] = 2.33\ \frac{\eta_L \eta_J}{a}\ \frac{1}{\bar{h}}\ \frac{c_b}{c_h}\ \frac{|\dot{h}|}{N_\infty} \qquad (39)$$

This is an expression for the normalized average damping. We obtain the actual damping in terms of pressure if we multiply both sides by P_T

$$\frac{1}{2}\left[|\Delta P_{L_{dn}}| + |\Delta P_{L_{up}}|\right] = \qquad (40)$$

$$= 1.65\ \frac{\eta_L \eta_J}{a}\ \frac{c_b}{c_h}\ \frac{\sqrt{\rho P_T}}{\bar{h}}\ |\dot{h}|$$

2.4.3. Frequency and damping ratio of the heaving motion. The transformed differential equation describing the heaving motion with the coupling term neglected can be written as (See Equation 3):

$$\left(s^2 + \frac{g}{P_L}\ \frac{dP_L}{d\dot{h}}\ s - \frac{g}{P_L}\ \frac{dP_L}{dh}\right)\bar{h} = 0 \qquad (41)$$

Using Equations 19 and 22, the undamped natural frequency is,

$$\omega_H = \sqrt{\frac{g}{h}}\ \sqrt{\frac{\eta_L P_{Be} c_b}{P_L c_h}} \qquad (42)$$

$$= \sqrt{\frac{g/t}{\bar{h}}}\ \sqrt{\frac{\eta_L \bar{P}_B}{\bar{P}_L}\ \frac{c_b}{c_h}}$$

We can determine the relative damping ratio, ζ_H , from $2\zeta_H\omega_H = \frac{g}{P_L}\frac{\partial P_L}{\partial \dot{h}}$

Expressing $\frac{\partial P_L}{\partial \dot{h}}$ as the coefficient in Equation 40

$$\zeta_H = \frac{0.825}{a}\sqrt{\frac{\eta_t \eta_J^2 q t \rho}{P_L}}\sqrt{\frac{C_b}{C_n}}\frac{1}{\sqrt{\bar{P}_{Be}\bar{h}}} \qquad (43)$$

The influence of scaling is an increase of the damping ratio with the square root of the linear dimension. The volume of air which moves into or out of the base area increases proportionally with the base area, whereas the "nozzle" area through which this air moves increases proportionally with the length of the periphery.

The damping ratio also varies inversely with the square root of the specific load, P_L . The total pressure, P_T , must increase with P_L and the base pressure, P_B , is proportional to P_T . Therefore the variation of the velocity of the air moving into or out of the base area is reflected in the $1/\sqrt{P_L}$ factor.

2.5. Pitching motion.

2.5.1. Moments. The physical basis for the derivation of an expression for the moments acting on a ground effect machine as given below, is the same as the one adopted by Lin (Reference 18) and Webster (Reference 17). The following derivation is different, however, in the respect that a more general result is obtained so that the effects of different mechanisms and various assumptions can be discussed.

Consider that the machine is in equilibrium at some small attitude angle. The experimentally observed flow picture is similar to the one shown in the following Figure.

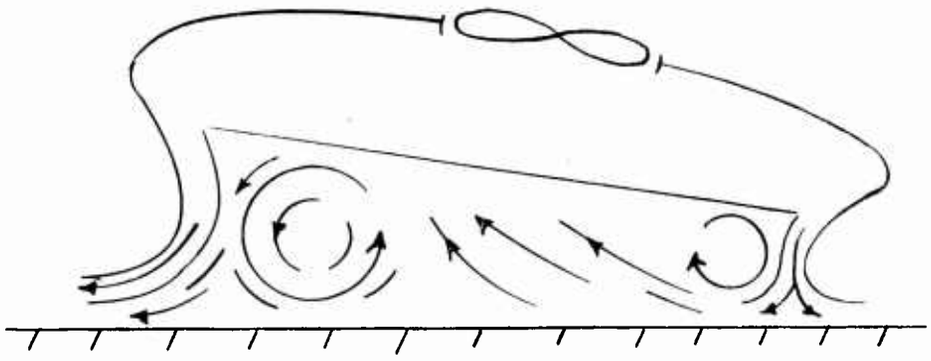

The cross flow is observed experimentally and can be explained by considering the balance of pressure and momentum forces. When the machine is tilted to the right, for instance, the force due to the base pressure has a component parallel to the ground. The machine must thus exert an equal and opposite force on the fluid mass under the base. In order for this fluid mass to remain in equilibrium, the pressure force must be balanced by a momentum change plus the frictional force at the ground. Since the skin friction force is quite small, the pressure must be balanced mainly by a momentum change which can only be brought about by part of the air from the low jet flowing toward the high jet.

The losses due to viscous effects including the pressure drops caused by the vortices are lumped into the lift efficiency factor, η_L . Differential pressure changes caused by the difference between the vortices at the two ends are considered. The result of the derivation will show that these assumptions are sufficient to explain the nature of the moment derivative.

The basic relationships will be derived for a two dimensional flow and the results will be later modified for application to a three dimensional machine.

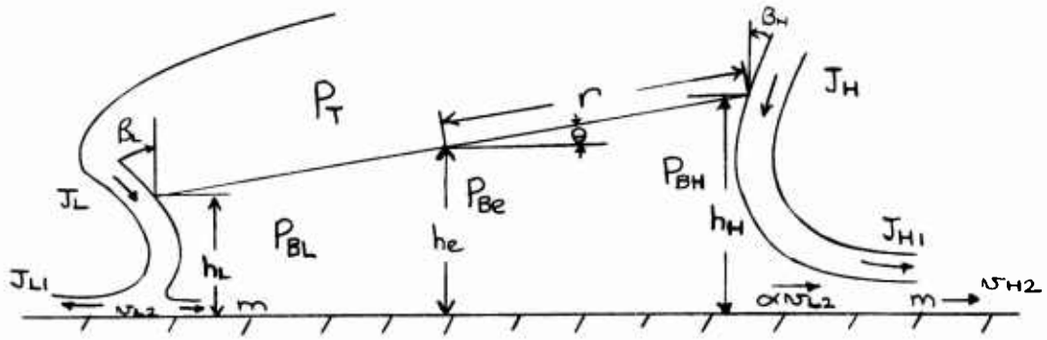

Let us take a section of the vehicle of unit width and denote the distance between the two jet sections by $2r$. If the base is inclined with respect to the ground at an angle, Θ , as illustrated in the above Figure, there is an underfed regime at the high end and an overfed regime at the low end. The mass flows into and out of the base area must be equal. Our unknowns are $\Delta P_{BL} = P_{BL} - P_{Be}$, $\Delta P_{BH} = P_{BH} - P_{Be}$, and the mass flow, m . We have two momentum balance equations for the two ends; the third equation is provided by writing the horizontal momentum balance equation for the total base area. Linear pressure distribution along the base will be assumed.

For the high end we can write, using Equation 5, and the notations of the above Figure.

$$\frac{1}{2} \bar{P}_{BH} \bar{h}_H = \eta_J \left[\bar{J}_H \left(1 + \mu \sin \beta_H \right) + \bar{J}_{H2} \right] \tag{44}$$

$$\frac{1}{2}(\bar{P}_{Be}+\Delta\bar{P}_{BH})(\bar{h}_e+\bar{r}\theta)-\eta_J\{(\bar{J}_b+\Delta\bar{J}_H)[1+\mu\sin(\beta_o-\theta)] + \bar{J}_{H2}+\bar{J}_b+\Delta\bar{J}_{H1}\} \quad (45)$$

We now make small angle approximations for Θ and neglect the second order terms

$$\bar{P}_{Be}\bar{h}_e+\bar{P}_{Be}\bar{r}\theta+\bar{h}_e\Delta\bar{P}_{BH}+\bar{r}\theta\Delta\bar{P}_{BH}= \quad (46)$$

$$=2\eta_J\left[(\bar{J}_b+\Delta\bar{J}_H)(1+\mu\sin\beta_o)-(\bar{J}_b+\Delta\bar{J}_H)\theta\cos\beta_o+\bar{J}_{H2}\right]$$

Subtracting the equilibrium equation for the leveled, balanced condition, $\bar{P}_{Be}\bar{h}_e = 2\eta_J\bar{J}_b(1+\mu\sin\beta_o)$ and substituting $\Delta\bar{J}_H=\frac{d\bar{J}_b}{d\bar{P}_B}\Delta\bar{P}_{BH}$ we get

$$(\bar{h}_e+\bar{r}'\theta)\Delta\bar{P}_{BH}= \quad (47)$$

$$=-\bar{P}_{Be}\bar{r}\theta+2\eta_J\left[\frac{d\bar{J}_b}{d\bar{P}_B}(1+\mu\sin\beta_o)\Delta\bar{P}_{BH}-\bar{J}_b\theta\cos\beta_o+\bar{J}_{H2}\right]$$

where $\bar{r}'=\bar{r}+2\eta_J\frac{d\bar{J}_b}{d\bar{P}_B}\cos\beta_o$

Rearranging and using C_h as defined in Equation 22 the differential momentum balance for the high end can be expressed as

$$(C_h\bar{h}_e+\bar{r}'\theta)\Delta\bar{P}_{BH}= \quad (48)$$

$$=-\bar{P}_{Be}\bar{r}\theta-2\eta_J\bar{J}_b\theta\cos\beta_o+2\eta_J\bar{m}(\bar{v}_{H2}-\alpha\bar{v}_{L2})$$

where $\bar{m}$ is the normalized cross flow and $\alpha \bar{v}_{L2}$ is the normalized velocity of the cross flow at the high end.

The left hand side of this equation expresses the pressure changes. The three terms on the right hand side indicate clearly the three major factors contributing to the pressure change. The first term is due to the increase of the nozzle-to-ground distance, the jet momentum can balance only a smaller pressure over a larger area. The second term is due to the change in jet incidence angle at the nozzle with respect to the ground, decreasing the horizontal component of the jet. The first two terms are of stabilizing nature, the third term which is due to the cross flow is a destabilizing term.

For the low end we can write, using Equation 10, and the notation of the Figure on page 32

$$\frac{1}{2} \bar{P}_{BL} \bar{h}_L = (\bar{J}_L \sin \beta_L + \bar{J}_{L1} - \bar{J}_{L2}) \eta_J$$

or

$$\frac{1}{2} (\bar{P}_{Be} + \Delta \bar{P}_{BL})(\bar{h}_e - \bar{r}\theta) = \tag{49}$$

$$= \eta_J \left[(\bar{J}_b + \Delta \bar{J}_L) \sin (\beta_o + \theta) + \bar{J}_{L1} - \bar{J}_{L2} \right]$$

We perform a sequence of steps similar to the manipulation of the equation for the high end, combined with the steps taken previously to express the conditions for the overfed regime.

$$(\bar{h}_e - \bar{r}'\theta)\Delta\bar{P}_{BL} = \tag{50}$$

$$= \bar{P}_{Be}\bar{r}\theta + 2\eta_J\left[\frac{d\bar{J}_b}{d\bar{P}_B}(1+\sin\beta_o)\Delta\bar{P}_{BL} + \bar{J}_b\theta\cos\beta_o - \bar{m} - \bar{J}_{L2}\right]$$

The final form is similar to Equation 37.

$$(c_h\bar{h}_e - \bar{r}'\theta)\Delta\bar{P}_{BL} = \tag{51}$$

$$= \bar{P}_{Be}\bar{r}\theta + 2\eta_J\bar{J}_b\theta\cos\beta_o - 2\eta_J\bar{m}(1+\bar{\nu}_{L2})$$

The physical meaning of the terms has been described following Equation 48.

The third equation expresses the horizontal momentum balance over the whole base area. All losses in the base area including the pressure drops due to vortices are averaged and included in the lift efficiency factor η_L. Assuming a linear pressure distribution under the base and neglecting the friction forces due to the cross flow, we can write for small θ

$$\frac{\eta_L}{2}\left[\bar{P}_{Be} + \frac{1}{2}(\Delta\bar{P}_{BH} + \Delta\bar{P}_{BL})\right]2\bar{r}\theta = \tag{52}$$

$$= \eta_J\left[\bar{J}_H\sin\beta_H - \bar{J}_L\sin\beta_L + J_{H1} + J_{H2} - J_{L1}\right]$$

and making similar steps as before

$$= \eta_J \left[(\bar{J}_b + \Delta\bar{J}_H)(\sin\beta_o - \theta\cos\beta) - (\bar{J}_b + \Delta\bar{J}_L)(\sin\beta_o + \theta\cos\beta_o) \right.$$

$$\left. + \bar{J}_{H1} + \bar{J}_{H2} - \bar{J}_{L1} \right]$$

$$= \eta_J \left[-2\bar{J}_b \theta\cos\beta_o + \frac{d\bar{J}_b}{d\bar{P}_B} (\Delta\bar{P}_{BH} - \Delta\bar{P}_{BL}) \sin\beta_o \right.$$

$$- \frac{d\bar{J}_b}{d\bar{P}_B} \theta\cos\beta_o \, (\Delta P_{BH} + \Delta P_{BL}) + \bar{J}_B + \Delta\bar{J}_H$$

$$\left. + \bar{J}_{H2} - \bar{J}_{L1} \right]$$

Substituting $\bar{J}_b - \bar{J}_{L1} = \bar{m} - \Delta\bar{J}_L$; $\bar{J}_{H2} = \bar{m}\bar{N}_{H2}$;

and $2 \frac{d\bar{J}_b}{d\bar{P}_B} (1 + \sin\beta_o) = \bar{h}_e (1 - c_h)$

We arrive at the following final form of our third equation

$$\left[\eta_L \bar{r}'\theta - (1 - c_h)\bar{h}_e\right]\Delta\bar{P}_{BH} + \left[\eta_L \bar{r}'\theta + (1 - c_h)\bar{h}_e\right]\Delta\bar{P}_{BL} \quad (53)$$

$$= -2\eta_L \bar{P}_{Be} \bar{r}\,\theta - 4\eta_J \bar{J}_b \theta\cos\beta_o + 2\eta_J \bar{m}(1 + \bar{N}_{H2})$$

Since the moment will be proportional to $\Delta\bar{P}_{BH} - \Delta\bar{P}_{BL}$ it is advantageous for the calculation to choose this as one of the variables. Multiplying Equations 48 and 51 by η_L and writing their difference and their sum we arrive at the following set of equations.

$$\eta_L \bar{r}'\theta\,(\Delta\bar{P}_{BH} + \Delta\bar{P}_{BL}) - (1-c_h)\bar{h}_e\,(\Delta\bar{P}_{BH} - \Delta\bar{P}_{BL})$$
$$- 2\eta_J(1+\bar{N}_{H2})\bar{m} = -2\left(\eta_L \bar{P}_{Be}\bar{r} + 2\eta_J \bar{J}_b \cos\beta_o\right)\theta$$

$$\eta_L c_h \bar{h}_e\,(\Delta\bar{P}_{BH} + \Delta\bar{P}_{BL}) + \eta_L \bar{r}'\theta\,(\Delta\bar{P}_{BH} - \Delta\bar{P}_{BL}) \qquad (54)$$
$$+2\eta_J\eta_L\bar{m}\,(1 + \bar{N}_{L2} - \bar{N}_{H2} + \alpha N_{L2}) = 0$$

$$\eta_L \bar{r}'\theta\,(\Delta\bar{P}_{BH} + \Delta\bar{P}_{BL}) + \eta_L c_h \bar{h}_e\,(\Delta\bar{P}_{BH} - \Delta\bar{P}_{BL})$$
$$-2\eta_L\eta_J\bar{m}\,(1+\bar{N}_{L2} + \bar{N}_{H2} - \alpha\bar{N}_{L2}) =$$
$$= -2\left(\eta_L \bar{P}_{Be}\bar{r} + 2\eta_L\eta_J \bar{J}_b \cos\beta_o\right)\theta$$

The solution for $\Delta\bar{P}_{BH} - \Delta\bar{P}_{BL}$ can be expressed in the following form:

$$\Delta\bar{P}_{BH} - \Delta\bar{P}_{BL} = \frac{c_1\theta + c_2\theta^2}{c_3 + c_4\theta + c_5\theta^2} \tag{55}$$

We wish to determine the moment derivative $\frac{dM}{d\theta}$ at $\theta = 0$. This restriction is justified because experiments indicate that $\frac{dM}{d\theta}$ is fairly constant in the vicinity of zero degree. Therefore we need to determine only

$$\frac{d}{d\theta}\left(\Delta\bar{P}_{BH} - \Delta\bar{P}_{BL}\right)\Big|_{\theta=0} = \frac{c_1}{c_3} = \tag{56}$$

$$= \frac{2\left[\left(\eta_L \bar{P}_{Be}\bar{r} + 2\eta_J \bar{J}_b \cos\beta_o\right) N_{L2}(1-\alpha) - (1-\eta_L)\bar{P}_{Bo}\bar{r}(1+N_{H2})\right]}{\bar{h}_e\left[1 + N_{H2} + (1-c_h)N_{L2}(1-\alpha)\right]}$$

The moment acting on a segment of unit width is easily derived as follows

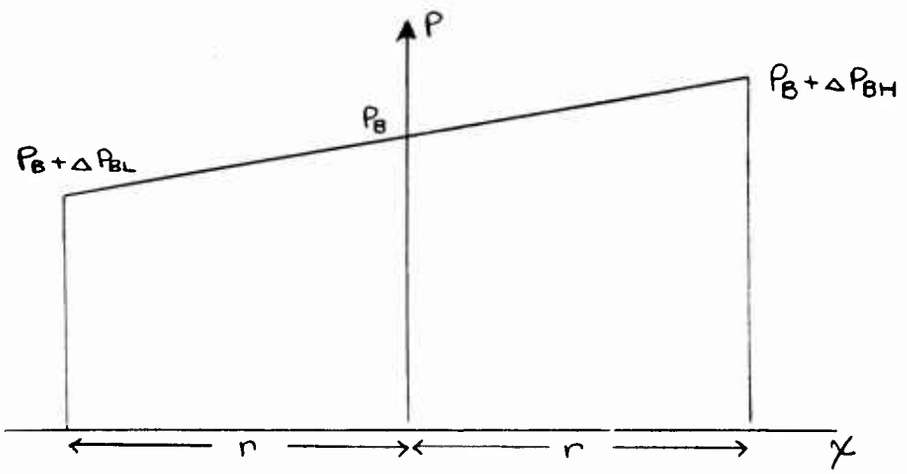

Assuming linear pressure distribution,

$$\Delta P_B = \frac{(\Delta P_{BH} - \Delta P_{BL})}{2r} \chi$$

$$dM = \Delta P_B \chi \, d\chi$$

Integrating this gives*,

$$M = 2\int_0^r \Delta P_B \chi \, d\chi = \frac{1}{3}(\Delta P_{BH} - \Delta P_{BL}) r^2 \tag{57}$$

We normalize by $2Lr = 4P_L r^2$ where L is the lift acting on the segment and the area is $S = 2r$. The moment coefficient of our two dimensional segment is

$$C_M = \frac{M}{2Lr} = \frac{1}{12 P_L}(\Delta P_{BH} - \Delta P_{BL}) = \frac{1}{12\bar{P}_L}(\Delta \bar{P}_{BH} - \Delta \bar{P}_{BL}) \tag{58}$$

The moment derivative at $\Theta = 0$ is

$$\frac{dC_M}{d\Theta} = \frac{1}{12\bar{P}_L} \frac{d}{d\Theta}(\Delta \bar{P}_{BH} - \Delta \bar{P}_{BL}) = \tag{59}$$

$$= \frac{1}{6\bar{P}_L} \frac{\bar{r}}{h_e} \frac{(\eta_L \bar{P}_{Be} + 2\eta_J \bar{J}_D \frac{1}{F} C_M \beta_0) N_{L2}(1-\alpha) - (1-\eta_L)\bar{P}_{Be}(1-N_{H2})}{1 + N_{H2} + (1-C_h) N_{L2}(1-\alpha)}$$

*There is an additional moment, the change in jet momenta multiplied by their moment arms. It can be shown that this moment is negligible as long as $r/t \gg 1$

Recognizing that in $\bar{P}_L = 2\bar{J}_b \eta_J \alpha \cos\beta_o + \eta_L \bar{P}_{Be}$ and that for our segment $\alpha = \frac{2t}{2r} = \frac{1}{\bar{r}}$, we can write the moment derivative in the following form:

$$\frac{dC_M}{d\theta} = \tag{60}$$

$$= \frac{1}{6}\frac{\bar{r}}{\bar{h}e} \frac{\frac{\bar{v}_{L2}(1-\alpha)}{1+\bar{v}_{H2}} - (1-\eta_L)\frac{\bar{P}_{Be}}{\bar{P}_L}}{1 + \frac{2}{\bar{h}e}\frac{d\bar{J}_b}{d\bar{P}_B}\frac{\bar{v}_{L2}(1-\alpha)}{1+\bar{v}_{H2}}(1+\sin\beta_o)}$$

This result clearly indicates some of the influences of different physical parameters and assumptions on the moment derivative. The two terms in the numerator of the coefficient of $\bar{r}/6\bar{h}e$ are of distinctly different origins. The positive term $\frac{\bar{v}_{L2}(1-\alpha)}{1+\bar{v}_{H2}}$ could be called a cross flow variable. The parameter $\bar{v}_{L2}$ is the normalized velocity of the inward flowing jet at the low end, and it can be approximated by $\bar{v}_{L2} = \sqrt{1-\bar{P}_{Be}}$ since this jet is flowing into an area where the average pressure is P_B. As to $\bar{v}_{H2}$ the picture is not so clear. We know that the mass flow must be the same as that of the inward flow at the low end and, therefore, the change in jet momentum at the high end is determined by the change in velocity of the outflowing jet. Because of dissipation, the cross flow will not have the velocity v_{L2} when it reaches the high side. We designate the velocity of the cross flow when it reaches the high side by αv_{L2}

where α is a parameter which can have any value between zero and one. Using Bernouilli's equation, we then find that the normalized velocity of the cross flow outside the base area $\bar{v}_{H2}$ is:

$$\bar{v}_{H2} = \sqrt{\bar{P}_B + \alpha^2 (1 - \bar{P}_B)}$$

When there is complete dissipation, $\alpha = 0$ and we obtain the minimum estimate for $\bar{v}_{H2}$

$$\bar{v}_{H2} = \sqrt{\bar{P}_B}$$

If there were no dissipation α would be equal to one and this would correspond to expansion from the total pressure to the ambient pressure and would give

$$\bar{v}_{H2} = 1$$

The quantitative effect of different values of α will be shown later.

The positive "cross flow term" is destabilizing. If the other numerator term were zero, this term alone would make the ground effect machine statically unstable at all heights.

The second and stabilizing term could be called a "base efficiency term." The $(1 - \eta_L)$ factor indicates that this term would vanish if there were no losses under the base. We have incorporated in η_L all losses resulting in a pressure loss, including the averaged pressure drop due to the vortices. Therefore, we can state that, in an indirect way, the vortices provide the source of a stabilizing mechanism.

We have not considered any differential effects of the vortices; but such effects can be expected to be of secondary importance if our assumptions lead to a good quantitative agreement with experiments. That this is the case will be shown later.

As to the denominator the consistently negative sign of the $\frac{d\bar{J}_B}{d\bar{P}_B}$ factor makes the sum in the denominator always less than one. $\frac{\bar{v}_{L2}(1-\alpha)}{1+\bar{v}_{H2}}$ decreases as $\bar{h}_e$ decreases, so that their ratio is not expected to vary by any large amount. However, at very low heights $\frac{d\bar{J}_b}{d\bar{P}_B}$ can be expected to increase, thereby causing a decrease of the denominator and an increase in the absolute value of the moment derivative. The physical meaning of the $\frac{d\bar{J}_b}{d\bar{P}_B}$ factor is that it expresses the contribution of the changes in jet momentum to the moment.

It is interesting to notice that both the stabilizing and the destabilizing terms in the moment derivative have their physical origin in the losses occurring in the base area, according to the momentum theory. If the lift efficiency factor, η_L, were unity there would be no stabilizing moment. If the cross flow were not dissipated at all ($\alpha = 1$), there would be no destabilizing moment. Consequently, if no losses occurred in the base area the moment at $\theta = 0$ as well as the moment derivative would be zero at any height.

2.5.2. Three dimensional corrections. We now have to make an estimate of the correction to be used for the application of our moment derivative result to three dimensional machines.

We shall normalize the moment of the three dimensional machine by dividing the total amount by $2LR_2 = 2P_L S R_2$ where L is the total lift, S is the total base area and R_2 is the maximum half-length (half-width) of the machine. As an approximation in the following derivation we shall neglect

the $\bar{J}_b$ term in the moment derivative. This term, which represents the direct contribution of the jet momentum to the total moment, is small at practical heights. Using the notation of the Figure shown below and referring to the derivation of Equation 59, we can write

$$\left.\frac{dC_M}{d\theta}\right|_{3D} = \frac{1}{2\bar{P}_L S R_2} \int_{-R_1}^{R_1} \left.\frac{dM}{d\theta}\right|_{2D} dr_1$$

$$= \frac{1}{6\bar{P}_L S R_2} \int_{-R_1}^{R_1} \frac{d\left(\Delta P_{BH} - \Delta P_{BL}\right)}{d\theta} r_2^2 \, dr_1$$

$$\cong \frac{1}{6\bar{P}_L S R_2} \int_{-R_1}^{R_1} \frac{\bar{r}_2}{\bar{h}_e} \frac{2\left[\eta_L \bar{P}_{Be} \frac{\bar{v}_{L2}(1-\alpha)}{1+\bar{v}_{H2}} - (1-\eta_L)\bar{P}_{Be}\right]}{1 + \frac{2}{\bar{h}_e}\frac{d\bar{J}_b}{d\bar{P}_B}(1+\Delta\eta\beta_0)\frac{\bar{v}_{L2}(1-\alpha)}{1+\bar{v}_{H2}}} r_2^2 \, dr_1$$

$$= \left[\frac{1}{6\bar{P}_L} \frac{\bar{R}_2}{\bar{h}_e} \frac{\eta_L \bar{P}_{Be} \frac{\bar{v}_{L2}(1-\alpha)}{1+\bar{v}_{H2}} - (1-\eta_L)\bar{P}_{Be}}{1 + \frac{2}{\bar{h}_e}\frac{d\bar{J}_b}{d\bar{P}_B}(1+\Delta\eta\beta_0)\frac{\bar{v}_{L2}(1-\alpha)}{1+\bar{v}_{H2}}}\right] \left[\frac{1}{2} \frac{4R_1R_2}{S} \int_{-R_1}^{R_1} \left(\frac{r_2}{R_2}\right)^3 d\left(\frac{r_1}{R_1}\right)\right]$$

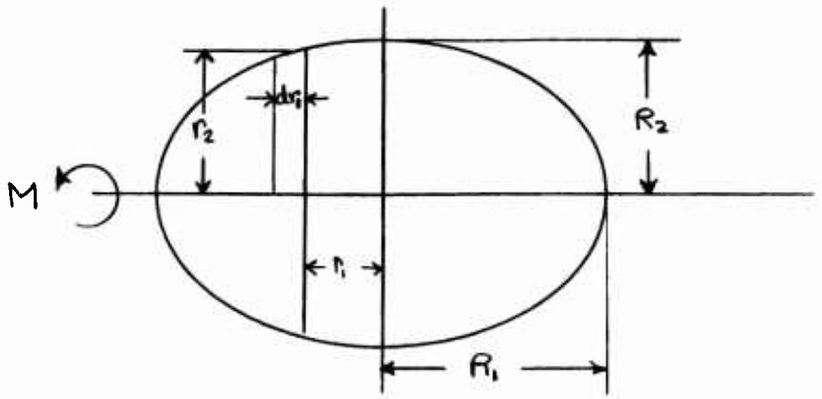

Comparing this result with Equation 59, the first bracket can be recognized as the two dimensional moment derivative, except for the omitted $\bar{J}_b$ term. The second bracket is the correction factor. Applying this result to the entire moment derivative, including the $\bar{J}_b$ term, we can write

$$\left.\frac{dC_M}{d\theta}\right|_{3D} = \Gamma \left.\frac{dC_M}{d\theta}\right|_{2D} \qquad (62)$$

where

$$\Gamma = \frac{1}{2} \frac{4R_1R_2}{S} \int_{-R_1}^{R_1} \left(\frac{r_2}{R_2}\right)^3 d\left(\frac{r_1}{R_1}\right)$$

This correction factor is essentially the same as that obtained by Webster (Reference 17) who made somewhat different assumptions. The factor $\frac{4R_1R_2}{S}$ is the ratio of the rectangle enclosing the periphery to the base area. The integral represents the effect of the shape of the machine on the correction factor. For a rectangular machine $\Gamma = 1$, for a circular machine $\Gamma = .75$.

It should be considered that there is no practical need for a greater accuracy in estimating the moments. Therefore, our approximation to the correction factor by simply using the area ratio can be considered adequate for our purposes.

2.6. Determination of base pressure and jet momentum.

In all of the expressions given previously for frequency and damping of the heave motion and for the pitching (or rolling) moment, it is necessary to know the base pressure, P_B, and the jet momentum, J_B, as a function of the height, h, and the physical parameters of the machine. A number of different expressions can be obtained for P_B and J_B depending on the assumptions made about the flow pattern or the jet momentum. We will briefly review three methods of obtaining these expressions which have been given in the literature.

1. Thin jet theory (Chaplin, Reference 7)

The balance between pressure forces and momentum change for a level GEM can be expressed as,

$$P_B(h\ell) = J(1 + \sin\beta_o) \tag{63}$$

where ℓ is the length of the jet. If the jet thickness, t, is small compared to the height, h, we can assume the momentum, J, is constant and equal to its value out of ground effect. Then,

$$J = 2\ell t\left(\tfrac{1}{2}\rho V_J^2\right) = 2\ell t P_t \tag{64}$$

where V_J is the velocity of the jet. Therefore,

$$\bar{P}_B = \frac{P_B}{P_T} = \frac{2(1+\sin\beta)}{\bar{h}} = 2\chi \tag{65}$$

which defines χ.

Obviously, this theory cannot be expected to yield good results near and within the height range where it gives $\bar{P}_B > 1$ and this range is within our range of interest.

2. Exponential theory. (Stanton-Jones, Reference 12)

In this approach we assume that Equation 63 is satisfied for a differential element of the jet, i.e.,

$$h\,dP = T\,(1 + \mu n \beta) \tag{66}$$

where

$$T = \rho V^2\,dt$$

and V is the jet velocity at the element under consideration.

From Bernouilli's equation,

$$\frac{1}{2}\rho V^2 = P_T - P \tag{67}$$

Combining these equations and integrating across the jet gives,

$$\bar{P}_B = 1 - e^{-2\chi} \tag{68}$$

Substituting the Taylor series for the exponential, we note that this approaches the value given by Equation 65 for small χ.

$$\bar{P}_B = 2\chi - \frac{(2\chi)^2}{2!} + \frac{(2\chi)^3}{3!} - \cdots\cdots$$

3. Uniform jet theory. (Fuller, Reference 9; and Rethorst, Reference 11)

If we assume that the jet near the machine has approximately constant thickness, then the balance of pressure and centrifugal force in the jet gives

$$\frac{dP}{dr} = \frac{\rho V^2}{r} \tag{69}$$

Using Bernoulli's equation and integrating gives,

$$\bar{P}_B = 1 - \frac{r_o^2}{r_i^2} \tag{70}$$

where r_o is the radius of curvature of the outside of the jet and r_i that of the inside. Expressing these in terms of height, h, jet thickness, t, and jet inclination angle β_o and defining

$$\Phi = \frac{\frac{h}{t} - 1}{\frac{h}{t} + \sin\beta_o} = \frac{\bar{h} - 1}{\bar{h} + \sin\beta_o}$$

gives,

$$\bar{P}_B = 1 - \Phi^2 \tag{71}$$

In the thin jet theory it was assumed that the jet momentum, J_b, was constant. In the last two theories we can easily obtain the following expression for $\bar{J}_b$ (i.e., J_b divided by J_b out of ground effect)

$$\bar{J}_b = \frac{1}{2\pi}\left(1 - e^{-2\pi}\right) \tag{72}$$

for the exponential theory and

$$\bar{J}_b = \Phi \tag{73}$$

for the uniform jet theory.

These three theories are compared graphically in Figure 1. It will be noticed that the last two theories agree quite well, and that the thin jet theory differs appreciably only for small height, $\bar{h}$. The last two theories also follow very closely the exact, inviscid, incompressible solution given by Strand (Reference 28).

The exponential theory is believed to be superior to the other two approximate approaches at very low heights. The uniform jet theory leads to zero jet strengths at $\bar{h} = 1$. The derivatives of the normalized momentum with respect to the normalized pressure, $\frac{d \bar{J}_B}{d \bar{P}_B}$, which appears in the denominators of some of the stability parameters we have investigated can be found to be $-\frac{1}{2\Phi}$ with this theory. These expressions then tend to infinity as $\bar{h}$ tends to one.

In the sample calculations which will be given later and compared with experimental results, we shall use the exponential theory. The term, $\frac{d \bar{J}_B}{d \bar{P}_B}$ is easily shown to be,

$$\frac{d \bar{J}_B}{d \bar{P}_B} = \frac{1}{4} \left[\frac{1 - e^{2\chi}}{\chi^2} + \frac{2}{\chi} \right] \tag{74}$$

For very small χ $(\bar{h} \gg 1)$

$$\frac{d \bar{J}_b}{d \bar{P}_B} \simeq -\frac{1}{2} - \frac{1}{3} \chi \tag{75}$$

3. DISCUSSION OF THE THEORETICAL AND EXPERIMENTAL RESULTS

In the preceding section theoretical expressions were obtained for several of the important stability derivatives for the hovering GEM. The variation of these derivatives with changes in the important physical parameters are shown by means of a number of plots given at the end of the report. These results are discussed in the following section along with results obtained from a series of experiments with an eight foot diameter GEM model. The experimental set up and the procedure used for obtaining the data is discussed in detail in Appendix B.

It was shown previously that, for a vehicle initially trimmed parallel to the ground, the heave and pitch motion can be considered uncoupled. We thus divide the discussion into two sections: heaving motion and pitching motion.

3.1. Heaving motion.

We previously obtained expressions for the variation of the lift force with height and rate of change of height and used these results to find expressions for the frequency and damping ratio of the heaving motion. Figures 4 and 5 are plots of the undamped natural frequency of the heave motion times the square root of the jet thickness (in feet) $\omega_H \sqrt{t}$ (see Equation 42), as functions of jet inclination, β_o ; nozzle to base area ratio, α ; lift efficiency factor, η_L . The general character of these curves is similar to the curve obtained by thin jet theory except for low heights. In the thin jet theory, the base pressure becomes infinite as the normalized height $\bar{h}$ (hereafter called simply the height) tends to zero which results in an infinitely stiff spring as height tends to zero. Actually the base pressure cannot exceed

the total pressure, P_T . We see from Figure 1 that the two thick jet theories satisfy this condition. The base pressure also approaches the total pressure in such a way that the spring stiffness falls to zero as the height approaches zero. The spring stiffness for small height depends to a considerable extent on the derivative of the normalized momentum with respect to the normalized base pressure $\frac{d\bar{J}_b}{d\bar{P}_b}$, which, as shown in Figure 1, tends to become very large and differs considerably for the two thick jet theories. For this reason, even the result for thick jet theory can not be relied upon for very small values of the height (e.g. $\bar{h}$ less than 1.5). We see from these Figures that the lift efficiency factor, η_L , has very little effect on the value of the natural frequency, ω_H , and that this frequency is decreased as the nozzle to base area ratio, a , is increased. Comparing Figure 4 with Figure 5, shows that the heave frequency, ω_H , is decreased for small height and increased for large height when the jet inclination angle, β_o , is changed from 0 to 45 degrees. The nozzle to base area ratio, a , cannot vary over too great a range due to consideration of lift efficiency. (i.e., for efficiency the vehicle should operate at small values of height to diameter ratio, $\frac{h}{D}$,where D is an equivalent diameter for non-circular GEMs, and when this ratio is small the optimum nozzle to base area ratio is small.)

The values obtained experimentally (experimental procedure described in Appendix B) are shown in Figure 6. Also included in this Figure are the appropriate theoretical curves ($a = \frac{1}{25}$, $\beta_o = 45°$, $t = 1"$) and the thin jet theory expression $\sqrt{\frac{g}{h}}$ (g is the acceleration of gravity).

The theoretical expression for the damping ratio (43) has been plotted in Figure 7. It has been normalized in the form $\zeta_H \sqrt{\frac{p_L}{t}}$ (where p_L is the specific lift or weight per unit base area and t is the jet thickness). The nozzle width, t, represents the effect of scaling since $\zeta_H \sqrt{\frac{p_L}{t}}$ is only a function of the acceleration of gravity, g, the air density, ρ, and non-dimensional parameters. Thus, increasing the specific lift (i.e., $p_L = \frac{W}{S}$) decreases the damping ratio, ζ_H, but has no effect if the size of the machine is increased proportionally. We note from this Figure that the effect of the jet to base area ratio, a, is considerably greater than that of, β_o, and, η_L. This dependence on a is physically reasonable. The experimental values obtained on the eight foot model are shown for different values of specific lift, p_L, in Figures 8, 9 and 10. The comparison with the theoretical curves is fairly good. The magnitude is appreciably correct and there is no noticeable dependence on height, $\bar{h}$. Figure 11 shows how the damping ratio, ζ_H, varies, for constant RPM, with specific lift, p_L, as a parameter along the curve.

Finally, in Figure 12 we have plotted a number of calculated and experimental values of the roots of the heave stability equation. The variation with the height, $\bar{h}$, is shown for several values of specific lift, p_L.

3.2. Pitching motion.

In an earlier section of this report momentum considerations were utilized to obtain an estimate of the moments acting on a GEM. In particular, an expression was obtained for the slope of the moment versus attitude curve for a machine trimmed parallel to the ground. Referring to this expression (Equation 60), we note that the two terms in the numerator depend on $(1-\alpha)$ and $(1-\eta_L)$ respectively, so that if both the cross flow dissipation factor, α, and the lift efficiency factor, η_L, are equal to one, the moment derivative is identically zero. The behavior of the moment curve slope as a function of these parameters will be compared with the experimental results obtained on the eight foot model.

Recall that Equation 60 for the moment coefficient derivative, $\frac{dC_M}{d\theta}$, shows that when $\alpha = 1$ (i.e., no dissipation of cross flow) this derivative is always negative. Thus, the momentum theory predicts that in the absence of jet dissipation, the GEM would be stable at all altitudes. We also see from the same expression that if the lift efficiency factor, η_L, were equal to one (i.e., if the lift were actually as predicted by the momentum theory) then the GEM would be unstable at all altitudes. Experience has shown that typical values of the lift efficiency factor, η_L, are in the range 0.7 to 0.8. (Reference 27, for example, suggests a value 0.8 for well designed machines.) Since all machines tested to date are stable at a very low altitude and become unstable as the altitude is increased, the cross flow dissipation factor, α, must be less than one for the moment slope to give results which correspond with experiment. Figures 13 and 14 show how curves of the moment coefficient derivative, $\frac{dC_M}{d\theta}$ versus height are affected by changes in the cross flow dissipation factor, α. Larger values of α are not included since they result in unreasonably high stability crossover points (i.e., values of height, $\bar{h}$, where the vehicle becomes neutrally stable). We see that the curves differ considerably even for small changes in α. Increasing α, decreases the maximum of the moment coefficient derivative and increases the crossover point. Figure 14 which is plotted for a larger value of the lift efficiency factor, η_L, shows the same general behavior with respect to the cross flow dissipation factor, α, although the crossover point does not increase as rapidly. Figure 17 in which the jet inclination angle, β_o, is zero, also shows the same behavior as a function of the cross flow dissipation factor.

The behavior of the curves for different values of the lift efficiency factor, η_L , is shown in Figures 18 and 19. These two sets of curves are drawn only for the cross flow dissipation factor $\alpha = 0$. The general character of the curves, however, is the same for all values of this factor. We note that the behavior of the moment coefficient derivative, $\frac{dC_M}{d\theta}$ with varying height is quite different for the different values of the lift efficiency factor, η_L . As was pointed out previously, η_L represents the fact that the actual lift produced by the base pressure falls short of that computed on the basis of a uniform base pressure. There are probably a number of phenomena not included in our simplified approach which could account for this decrease in lift. Probably the most significant of these is the vortices. Smoke studies of the flow under the base show that there are vortices near the jets under the base which reduce the pressure on the base below the pressure which acts near the center of the base.

When the lift efficiency factor, $\eta_L = 1$ the GEM is unstable for all values of height, $\bar{h}$. For smaller values of the lift efficiency factor, η_L , the machine becomes stable for some heights, but the cross over height and the maximum unstable value of the moment coefficient derivative, $\frac{dC_M}{d\theta}$ varies considerably for different values of the lift efficiency factor, η_L . On comparing Figures 18 and 19 we see that, for a particular value of the left efficiency factor, the machine becomes stable only at a much lower height, $\bar{h}$, when the jet inclination angle, β_o, equals zero and that the maximum unstable moment slope for this case is also considerably greater.

Figure 16 shows how the moment coefficient derivative $\frac{dC_M}{d\theta}$ varies for fixed values of lift efficiency η_L and jet to base area ratio, a, as the jet inclination angle, β_o, varies from zero degrees to 60 degrees. We see that the GEM becomes increasingly stable as this angle increases. From Figure 15 we see that the jet to base area ratio, a, also has some influence on the value of the moment coefficient derivative $\frac{dC_M}{d\theta}$. This influence, however, is much less than the influence of other parameters.

We now consider the experimental results. Static moments were measured for different values of pitch (or roll) angle, θ, at a number of height and power settings throughout the range available in the experimental set up. Some typical curves obtained in this manner are shown in Figure 21. For the lower heights the moment curve is very nearly a straight line and has a stable slope. As the height is increased, the moments reach a maximum at some angle and then drop off. The angle at which this maximum occurs becomes larger as the height is increased. The moment curves were, however, nearly linear near zero angle for all heights.

It will be noticed that in most of the curves zero moment does not occur exactly at zero angle. This can be assumed to be due to slight asymmetries in the flow field of the model. The slopes of the moment curves at zero incidence are plotted as a function of height, $\bar{h}$, in Figure 20 along with the appropriate theoretical curves. A number of curves were computed to determine which combination of the cross flow dissipation factor, α, and the lift efficiency factor, η_L, would give the best match to the experimental data. It was found that the closest matches were obtained for η_L between 0.7 and 0.8 and for α between 0 and 0.2. All of the theoretical curves have a maximum for

a height, $\bar{h}$, of the order of 10, whereas the experimental points seem to be increasing with height even at $\bar{h}$ equal to 11. We should note here, however, that one of the conditions for the theory to be valid is that the height to diameter ratio, $\frac{h}{D}$, not be too large, since for sufficiently large $\frac{h}{D}$ the jets on the right and left of the two dimensional model may come together. In this case, the moment behavior may be quite different from that shown by the present theory.

For small values of the height, $\bar{h}$, the theoretical curves drop off much more rapidly than the experimental curve. This is probably due to the fact that one of the assumptions of the analysis becomes weak when the height becomes sufficiently small. This is the assumption that the total pressure in the chamber, P_T, could be considered constant. Also, the derivative of the normalized jet momentum with respect to the normalized base pressure, $\frac{d\bar{J}_b}{d\bar{P}_B}$, as shown in Figure 1, becomes very large at very small height, $\bar{h}$, which is probably unrealistic. These results seem to indicate that the theory is satisfactory for estimating the magnitude of the slope of the moment curve, as well as its behavior with height changes and changes in the various physical parameters of the vehicle. Accurate values of the moment slope can not be determined, however, due to the sensitivity of the results to the lift efficiency, η_L, and the dissipation factor α. Although these parameters can be estimated, they can not be easily determined accurately. Also, to improve the accuracy of the results for small height, $\bar{h}$, it would probably be necessary to refine the theory and include the effects of changes in total pressure and vortices.

Using the present theoretical approach it was not possible to find a satisfactory explanation for damping in the pitching motion. Experiments seemed to indicate, however, that there was a considerable amount of damping in this mode of motion. Results of these experiments are shown in Figure 22. These curves indicate that the damping decreases quite rapidly as height, $\bar{h}$, is increased. The damping itself, however was relatively high in all of the tests.

These results indicate that, for all but the very lowest heights tested, the characteristic roots of the pitching mode are both real, one lying to the left of the imaginary axis and one to the right. If there had been no damping in the system the two roots would have been placed symmetrically with respect to the imaginary axis. The damping moves both roots to the left. In Figure 23 we see how these roots move along the real axis as the altitude is varied. The abscissa of the curve shown represents the position of the two roots along the real axis for a given height. As the height, $\bar{h}$, decreases, the divergent root moves toward the origin, passing through the value zero at $\bar{h} = 3.3$, while the convergent root at first moves away and then starts back toward the origin at about the same height, $\bar{h}$ at which the divergent root passes through the value zero. The two roots come together at a position -7.3 on the real axis for $\bar{h}$ equal to 1.4. For heights lower than this the roots would represent a damped oscillation. This last point is the result of extrapolation.

4. FORWARD FLIGHT CONSIDERATIONS

In considering the hovering GEM we were able to present a theory which predicted the most important dynamic characteristics of the machine's behavior. We were also able to present experimental results with which to check these predictions. For the GEM in forward flight the situation is considerably more difficult. No adequate theory is available and the small amount of experimental results available are for fairly high free stream velocities (greater than 30 feet per second). For this reason, the discussion given here will be confined to summarizing what is known about the forward flight regime and to making a few observations as to how this might effect the dynamic characteristics of the GEM in low speed flight.

The character of the flow around the GEM changes considerably as the free stream velocity is increased. Depending on the dynamic pressure, the flow field will be similar to one of forms illustrated as A and B below.

A Low Velocity B High Velocity

If the freestream velocity is zero there is no cross flow when the GEM is parallel to the ground. When the free stream velocity is not zero, the static pressure in front of the jet will be increased. The difference between the base pressure and the ambient pressure becomes less so that, if the height remains constant, the forward jet need not be as strong. Thus, part of the jet will pass under the GEM as shown in A above. As the dynamic pressure increases, the strength of the

cross flow will increase until finally all of the jet passes under the base as shown in B above. The velocity at which the flow pattern A changes to pattern B will be approximately determined by equating the free stream dynamic pressure to the base pressure,

$$\frac{1}{2}\rho V^2 \cong P_B \cong P_L = \frac{W}{S} \tag{76}$$

for small $\bar{h}$. This will be only a very rough estimate since the vortex ahead of the jet (shown in A) will influence the pressure there. We neglect this effect. Observe that the velocity at which the flow change occurs will increase with increasing specific load. Smoke studies described in Reference 29 seem to indicate that the jet turns back under the base at a dynamic pressure somewhat lower than the one corresponding to the base pressure. If, however, the specific load, P_L , is very low, flow pattern B might be reached before the dynamic pressure is high enough to make control surfaces effective. We shall consider here only forward flight at low speeds where control surfaces are not effective. The speed at which the control surface becomes useable would depend on the particular design under consideration.

In hovering we could, with sufficient accuracy, consider the motion to have only two degrees of freedom (i.e., forces introduced by horizontal motion about the zero velocity condition could be neglected), we now have three degrees of freedom. For low speed flight of a level GEM, however, the heave degree of freedom is nearly uncoupled from the pitch and forward velocity degrees of freedom. There is a small coupling because there is some lift change with either a change in forward velocity or a change in attitude. The former lift change should be small if the forward velocity is sufficiently small, and the latter lift change should be zero (or nearly so) if the aircraft is initially

trimmed in a level attitude. Thus, in order to keep the analysis simple, we neglect the heave degree of freedom in forward flight and consider only the attitude and translational degrees of freedom. This does not imply that the variation of vertical force with changes in the steady state velocity will be small. However, such variation should introduce no severe dynamic problems.

The perturbation equations describing the GEM in forward flight will thus be,

$$I\ddot{\theta} + \frac{\partial M}{\partial \dot{\theta}}\dot{\theta} + \frac{\partial M}{\partial \theta}\theta + \frac{\partial M}{\partial V}V = \frac{\partial M}{\partial \delta}\delta \qquad (77)$$

$$\frac{\partial X}{\partial \theta}\theta + m\dot{V} + \frac{\partial X}{\partial V}V = \frac{\partial X}{\partial \delta_t}\delta_t$$

The rate term, $\frac{\partial X}{\partial \dot{\theta}}\dot{\theta}$, which arises in conventional aircraft primarily because of a change in the angle of attack of the horizontal tail, can be neglected at low velocities. We then need to estimate $\frac{\partial M}{\partial V}$, the pitching moment change with forward velocity; $\frac{\partial X}{\partial \theta}$, the horizontal force change with pitch angle; $\frac{\partial X}{\partial V}$, the horizontal force change with velocity; $\frac{\partial M}{\partial \theta}$, the moment due to attitude change; and $\frac{\partial M}{\partial \dot{\theta}}$, the damping moment. We would like to know how these derivatives change with changes in the height, $\bar{h}$, and the forward velocity, V .

The forces acting on the GEM in the horizontal direction are:

a. the thrust from auxiliary propulsion

b. the component of lift vector in horizontal direction

c. the momentum drag

d. the parasite drag (skin friction and form drag)

e. the interference thrust (momentum recovery).

Additional drag will be encountered in flight over water; however, this effect will not be considered here. For a more complete discussion of drag forces acting on GEMs, see Reference 21 (Andu and Miyashita).

Thus, (with the X-axis parallel to the ground) the horizontal force can be expressed:

$$X = T\cos\theta - L\sin\theta - \mu V - \tfrac{1}{2}\rho V^2 C_{Dp} + T_{int} \qquad (78)$$

where T = propulsion thrust

L = lift

μ = mass flow

C_{Dp} = parasite drag coefficient

T_{int} = interference thrust

We shall assume that the thrust is constant and that

θ = 0 in equilibrium; thus $\tan\theta \cong \theta$

$L \cong W$ (machine weight)

C_{Dp} is approximately independent of both V and θ

Thus we obtain,

$$\frac{\partial X}{\partial V} = -\mu - \rho V C_{Dp} + \frac{\partial T_{int}}{\partial V}$$

$$\frac{\partial X}{\partial \theta} = -W + \frac{\partial T_{int}}{\partial \theta} \qquad (79)$$

Little is known about the interference thrust T_{int}. The following experimental curves from Reference 26 (Sweeney and Nixon), however, show that it is strongly dependent on velocity.

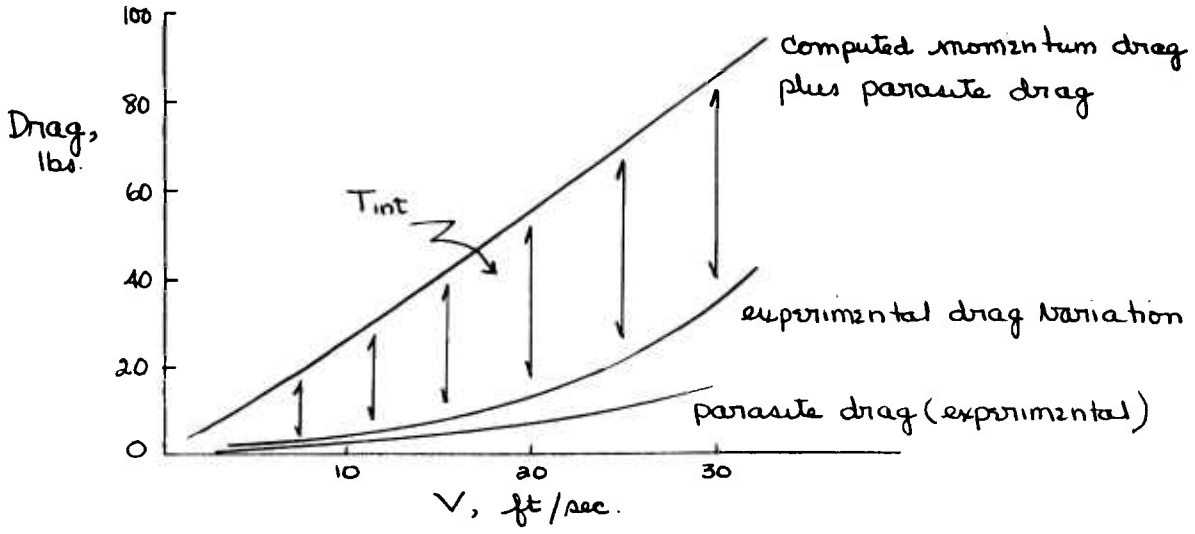

Andu and Miyashita (Reference 21) have suggested the following mechanisms for this term,

a. the disappearance of dead air at the air intake and nozzle exit (which was present in power-off parasite drag experiments), and the reduction of friction drag on the base, reduce the parasite drag in a power-on condition;

b. the ingested and ejected air bring about a favorable effect on the external flow;

c. the ejected air has energy in the form of total pressure, some part of which is converted to propulsive work in the process of expansion.

Because of the present lack of understanding, the derivatives of this term will have to be estimated from experimental data. From the curve shown above, it appears that the interference thrust decreases with increasing velocity. No data is, however, available to estimate its behavior with pitch angle.

There will be moments acting on the machine for the following reasons:

a. change in the base pressure distribution

b. change in pressure distribution over the exterior of the machine

c. change in jet strength at the front and back of the machine.

As soon as the GEM starts to move forward, the pressure distribution over the upper surface and around the exterior of the jet will change. One would at first think that the increased pressure at the front of the machine would cause the base pressure just inside of the front jet to increase and hence give a positive nose-up pitching moment. Experiments, however, have shown that, for low velocities (corresponding to condition A above), this is not the case (see Reference 19). This effect would appear to be attributable to the presence of the large vortex at the front of the machine. Measurements of the base pressure distribution given in Reference 19 show that the pressure is lowest at the front of the machine and increases monotonically (although not always linearly) to the rear of the machine. This results in a negative pitching moment. Because of the presence of the forward vortex and the fact that air is being drawn into the top of the machine, it would be very difficult to make any general statements about the pressure distribution over the upper surface of the machine. It will certainly be considerably different from the pressure distribution of an unpowered machine and it will probably depend strongly upon the particular exterior shape of the GEM.

Moments arising directly from the change in jet strength will be small as long as the jet area is small compared to the base area. If we neglect this contribution of the jets we can then express the moment as follows:

$$M = M_{EXT} + \frac{K}{3} r^2 \Delta P \qquad (80)$$

where

M_{EXT} = moment due to the pressure changes on the upper surface of the machine

ΔP = difference between the base pressure at the front and the back of the machine

r = equivalent radius of the machine

K = a factor which accounts for the three dimensional character of the machine, as well as for differences between the actual and a linear pressure distribution.

We are mainly interested in estimating the moment change with change of attitude angle, $\frac{\partial M}{\partial \theta}$, and the moment change due to change in forward velocity $\frac{\partial M}{\partial V}$. We can express these as follows:

$$\frac{\partial M}{\partial \theta} = \frac{\partial M_{EXT}}{\partial \theta} + \frac{K}{3} r^2 \frac{\partial \Delta P}{\partial \theta}$$

$$\frac{\partial M}{\partial V} = \frac{\partial M_{EXT}}{\partial V} + \frac{K}{3} r^2 \frac{\partial \Delta P}{\partial V} \qquad (81)$$

The damping in pitch, $\frac{\partial M}{\partial \dot{\theta}}$, will probably not be much effected by the small forward velocities and will be considered to be approximately the same as for a hovering GEM.

Because of the complexity of the flow under the base and across the surface of the GEM, the two derivatives $\frac{\partial M}{\partial \theta}$ and $\frac{\partial M}{\partial V}$ must be determined for any specific machine by experimental means. Using the results of some wind tunnel tests which have been made, however, we can make some general qualitative observations concerning the manner in which these two derivatives can be expected to behave.

Consider first the moment change due to velocity, $\frac{\partial M}{\partial V}$. We can obtain some feeling for the behavior of this derivative from the results of Reference 19. The curves below show the qualitative behavior of the moment coefficient, C_M , with changes in velocity for different heights. (The notation is ours and not that of the Reference cited).

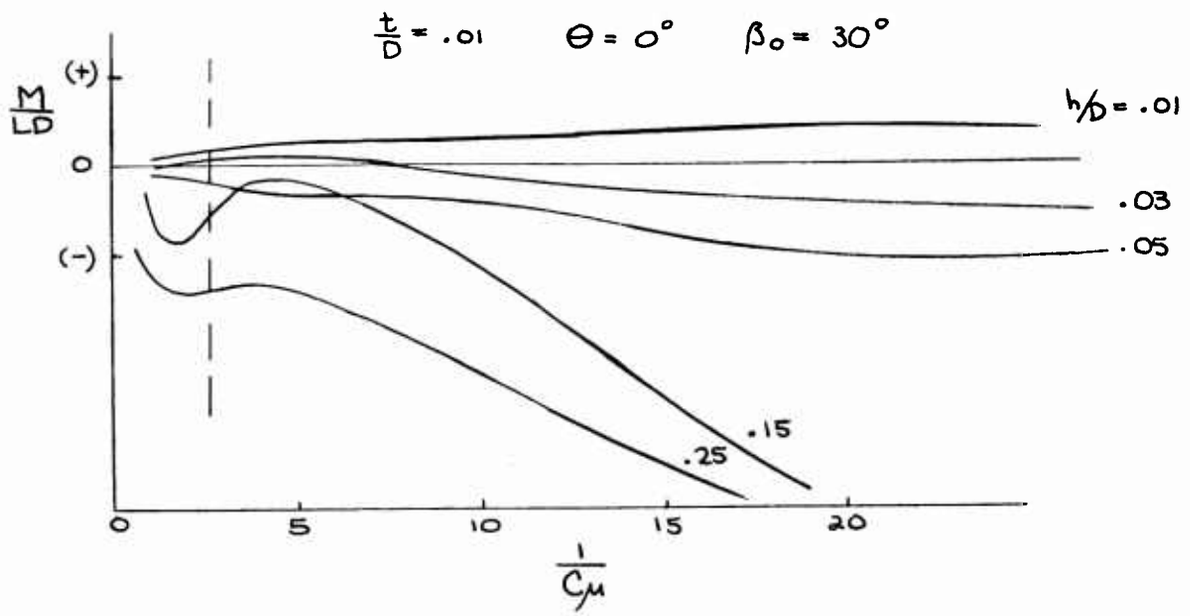

The parameter C_μ is defined to be:

$$C_\mu = \frac{J\ell}{\frac{1}{2}\rho V^2 S}$$

where J is jet strength per unit length; ℓ is the circumference; and S is the base area of the GEM.

If we equate the dynamic pressure to the base pressure and use the above definition of C_μ we find that,

$$\frac{1}{C_\mu} \simeq \frac{1 + \sin\beta_0}{4\ h/D} \qquad (82)$$

In the curves shown above, the sharp changes occur at a value of $\frac{1}{C_\mu}$ approximately equal to the one given in this Equation. Thus, the region of interest to us in these curves is only that small portion lying to the left of the sharp slope changes (i.e., to the left of the dotted line in the Figure).

We note from the curves that, for very small height to diameter ratio, h/D, the derivative $\frac{\partial M}{\partial V}$ is positive and that, for the larger values of h/D, it is negative for small forward velocities and changes sign rapidly at some velocities. As h/D increases the magnitude of the slope, $\frac{\partial M}{\partial V}$, becomes greater. This would seem to indicate that an accelerating GEM would experience rapid changes in dynamic characteristics if it were operating at sufficiently large value of h/D.

We now consider the derivative $\frac{\partial M}{\partial \theta}$. Almost no information is available concerning the effect of forward velocity on this derivative in the region in which we are interested (i.e., $\frac{1}{2}\rho V^2 < P_B$). This is because of the fact that all moment information which is available comes from wind tunnel tests which cannot be conducted with accuracy at less than about 30 feet per second. In order to conduct experiments at lower velocities a facility such as the Princeton University Forward Flight Facility would be required. Although some ground effect experiments have been conducted in this Facility with a four foot model, none have yet included pitching moment measurements.

Sweeney and Nixon (Reference 30) have stated that the Princeton 20-foot GEM (P-GEM) becomes statically stable in forward flight, although it is quite unstable in hover (at full power with stabilizing slots closed). They remark, however, that this might be associated with the fact that the P-GEM achieves forward propulsion by tilting the nose down, and that the stability increase could be associated either with the slight height loss in this attitude or to the attitude itself. Further tests with a leveled machine will probably be required to determine whether the note of optimism in these results is justified. However, one might conclude from these results that the effect of low forward velocities will at least not decrease the static stability.

5. PRELIMINARY CONTROL SYNTHESIS*

5.1. Stability augmentation

General experience with ground effect machines, as well as the theoretical results presented in the first part of this report, indicate consistently that a peripheral jet machine exhibits static instability in attitude well within the height range where it's performance is still economical. Stabilization by aerodynamic means, such as slots, has to be paid for in performance. Artificial stability augmentation by means of automatic feedback control suggests itself as a powerful and convenient alternative.

The development of the ideas concerning artificial stability augmentation consists of three steps:

a. description of the uncontrolled system

b. establishing design principles for the controlled system

c. conclusions to be drawn from (a) and (b) as to the design of a controller, as well as consideration of the limitations of its use.

In the following we shall consider first pitch stabilization in hover, and then discuss the effect of forward velocity on this proposed stabilization.

5.1.1. Description of the uncontrolled system. In the initial approach we are going to consider only the attitude degree of freedom (pitch or roll). In the previous discussion of the equations of motion, the attitude degree of freedom has been singled out as causing the most significant stability problems. Tests and theory have shown that the aerodynamic "spring" of this second order system varies from positive (stabilizing) to negative (destabilizing) values. With increased hovering height the negative "spring constant" reaches a rather flat maximum absolute value. The practically useful performance range of the GEM reaches into the region of this maximum.

*Methods used below are discussed in servomechanism texts (e.g. Reference 31)

The transfer function for one degree of freedom in attitude can be written in the following form:

$$G_\theta = \frac{\theta}{\delta_\theta} = \frac{A_c/I}{(s-s_1)(s-s_2)} \tag{83}$$

where

$$s_1 = \omega_p \left(-\zeta + \sqrt{1+\zeta^2}\right)$$

$$s_2 = \omega_p \left(-\zeta - \sqrt{1+\zeta^2}\right)$$

$$\omega_p^2 = \frac{\partial M/\partial\theta}{I}$$

With no damping, $\zeta = 0$, $s_1 = -s_2 = \omega_p$. The effect of the damping on the location of the roots of a second order system with a negative spring is shown in Figure 25. Our test results (see Figures 22 and 23) have shown the existence of fairly high damping throughout the useful height range, although no theoretical explanation for this phenomenon could be found.

It seems reasonable to assume that the general behavior of the roots (s_1 and s_2) would be similar to the behavior indicated in Figure 23, and that this would be independent of the size of the machine.

The effect of scaling on the "undamped natural frequency", ω_p , is the following:

$$\omega_p^2 = \frac{\partial M/\partial\theta}{I} = \frac{a L r (r/t)\left(\frac{1}{r}\frac{\partial C_M}{\partial\theta}\right)}{M r_g^2} \tag{84}$$

where r_g is the radius of gyration and $\frac{1}{r}\frac{\partial C_M}{\partial\theta}$ is the form in which the moment derivatives are plotted (Figures 13 through 20). With $M = \frac{W}{g}$ and $W = L$ we obtain

$$\omega_p^2 = 2 \frac{g}{t} \left(\frac{r}{r_g}\right)^2 \left(\frac{1}{r} \frac{\partial C_M}{\partial \theta}\right) \qquad (85)$$

This expression indicates a decrease in the natural frequency, ω_p, inversely proportional to the square root of the size of the machine, represented in this equation by the nozzle width, t. It should be noted that the explicit dimension, t, in this expression reflects the size of the machine; the effect of the nozzle width on the moment derivative has been indicated in Figure 15 in terms of the nozzle area to base area ratio.

In the damped case a change in the natural frequency, ω_p, means a proportional change in the distance, $\omega_p \sqrt{1+\zeta^2}$, of the roots from their arithmetic mean, $-\omega_p \zeta$. The effect of a change in the damping ratio on the arithmetic mean is also proportional. Its effect on the distance between the roots is, however, less than proportional.

Because of the simplifying assumptions made in the derivation of the moment derivative, and because of the lack of knowledge about the damping, we cannot expect highly accurate theoretical results. The use of the theoretical results together with the experimental results, however, yields sufficient information for an approximate model to be used in a preliminary control system synthesis. We observe (see Figure 23) that the root on the left hand side does not change much throughout the useful range of heights. For practical purposes this root can be assumed to be constant. It is suggested that its value could be determined by assuming a certain damping ratio, ζ_m, at the height where $\frac{\partial C_M}{\partial \theta}$ is maximum: $s_{1m} = \omega_{p\,max} \left(-\zeta_m - \sqrt{1+\zeta_m^2}\right)$. The other root would be determined from the fact that the product of the roots is $s_1 s_2 = \omega_p^2$. Either theoretical or experimental moment derivatives

could be used to determine the natural frequency, ω_p . In order to approximate the mean value of the root, S_1 , a correction factor should be used, $S_{1m}' \cong 1.2\, S_{1m}$. Assuming $\zeta_m = 1$ and using the theoretical curve (Figure 20) for the values $\eta_L = .75$, $\alpha = 0$ we obtain: $\omega_{p\,max} = 4.6$ at $\bar{h} \cong 8$ and $S_{1m}' = 13.3$. This value and the curve calculated for S_2 are shown as dashed lines in Figure 23. The effect of deviations from our somewhat arbitrary approximations will be discussed later.

We return now to the expression (Equation 83) for the transfer function describing the uncoupled attitude response to a control input, δ_θ . The gain, A_c , is actually an approximation to the transfer function which would accurately express the relationship between the control moment and the control input. This relationship varies with the height and generally may involve some dynamics. For example, if throttling of a portion of the jet, or inclination of the jet, is used in order to produce control moments, a part of the moment develops immediately in proportion to the change in jet momentum. Another part of the control moment, however, will develop only after the flow pattern under the base has changed. At the present time, no information is available on the magnitude and the lag of this part of the control moment which must depend largely upon the height above the ground as well as size of the machine. This is one reason why a considerable margin must be introduced in the design criteria.

5.1.2. Design principles for the controlled system. Establishing reasonable and realistic performance criteria for the feedback control of a vehicle so vaguely understood as the ground effect machine, is perhaps the most intricate step in the entire synthesis procedure. The following discussion is actually not restricted to ground effect machines but is of broader validity.

Our design criteria must be based on criteria for controllability by a pilot. In recent years considerable progress has been made toward a technically meaningful

formulation of the requirements which have to be met in order to permit a human pilot to perform satisfactory control. (See References 22, 23 and 24.) This approach is based on the fact that the human pilot is actually an element in a feedback loop closed around the controlled airframe or vehicle.

Extensive experiments have shown that the response of a human operator in a feedback loop can be considered to be made up of two parts. One part is linearly correlated with the pilot's input; the remainder, usually called the remnant, cannot be linearly correlated with the input. The latter part is presumably attributable to nonlinearities in the pilot's action, to noise introduced by the pilot, and to the pilot's response to inputs other than the ones considered in the experiment. The following basic ideas have emerged for describing the human operator.

a. In order to obtain the linearly correlated part of the pilot's response, the pilot can be replaced by a transfer function of the form (see Reference 24):

$$G_p = \frac{A_p e^{-\tau s}}{1 + T_N s} \cdot \frac{1 + T_L s}{1 + T_I s}$$

where

τ = reaction time delay } basically not adjustable

T_N = neuromuscular lag } by the pilot

$\frac{1 + T_L s}{1 + T_I s}$ = the pilot's equalization characteristic

A_p = the pilot's gain

This transfer function is a good approximation for a wide variety of control tasks.

b. The human pilot is highly adaptive. He is able to change his gain, A_p, his lead time constant, T_L, and his lag time constant, T_I, over a wide range.

Numerous experiments indicate that his efforts are aimed at providing a sufficient phase margin (40-80 degrees) for the open loop transfer function so as to assure satisfactory closed loop control.

c. The pilot's opinion of the handling qualities of the machine is strongly correlated with the gain as well as the lead and lag time constants he must use in order to achieve a satisfactory degree of stability. This opinion deteriorates rapidly when he reaches the limits of his capabilities.

Some important deductions from the correlation between the pilot's opinion and the transfer function of the human operator are the following:

a. The human pilot seems to have the best opinion of tasks in which only a pure gain and no lead or lag has to be applied on his part.

b. There is a rather flat range of optimum values for the gain, A_ρ , of the pilot. A considerable range (e.g., 1:8 in Reference 23) is acceptable. Too low or too high a gain are respectively described as a too sluggish response or a too sensitive control.

c. The pilot's opinion is degraded if an increasing amount of equalization, especially lead, is necessary. Also the remnant (i.e., uncorrelated part of the pilot's response) is relatively small if little equalization is needed, and it increases with an increasing effort on the part of the pilot to provide "good" control.

d. The bandwidth of the closed loop determines the disturbance (gust) bandwidth for which the vehicle can be kept well under control. Therefore, the pilot will tend to adjust his gain and compensation so that he can meet this requirement under given gust conditions.

These extremely simple and reasonable principles have been chosen by the authors as a guide in determining design criteria for the feedback stabilization

of the GEM. No particular quantitative pilot transfer function can be identified because only extensive flight experiments with ground effect machines involving the evaluation of pilots' opinions of the handling qualities could justify such a choice. We can, however, utilize the principles which have been outlined without being specific about the pilot's transfer function. This will be shown later.

It is important to appreciate that the approximations involved in the description of the dynamics of the GEM leave a considerable amount of uncertainty in the synthesis of feedback stabilization. There are two possible choices in dealing with this problem. The difference in the principle of these two approaches is of the utmost practical importance. The nature of each possible choice is discussed below.

a. Adaptive control: We may specify some dynamic performance criterion for the vehicle which is to be controlled by the pilot. This leads to the application of the adaptive control principle. In this case, we make up our mind about a feasible optimum vehicle performance and keep checking the responses of the vehicle to its inputs. These are then continuously compared with the performance criterion. Adjustments are automatically made to the gains of an inner feedback loop closed around the vehicle, as well as possibly in an equalizing network between the pilot and the inner loop.

Applying the adaptive control principle relieves us of the burden of finding how significant stability derivatives vary. The price we have to pay is in the increased complexity of the feedback system. Also, we must face some possibly severe problems in connection with the dynamic stability of a fast acting adaptive loop closed around an inherently unstable vehicle.

b. Nonlinear compensation: If we know how the significant stability derivatives vary, we can make the adjustments in the feedback loop on the basis of

measuring or estimating the parameters which affect the derivatives. If the parameters are very weakly or not at all coupled dynamically to the controlled variable, we have a nonlinear compensation which can be mechanized in a relatively simple way. These means do not ordinarily involve severe stability problems.* In the weakly coupled case, the success of a design depends heavily upon our knowledge concerning the relationships between stability derivatives and the parameters which change them.

After sketching these two different approaches (adaptive control and nonlinear compensation) let us return to our concept of the human pilot and see how the principles outlined earlier are involved in the choice of a design approach.

The most significant aspect of the human operator is his adaptability. This property enables him to control a system with widely varying parameters. Our problem with the peripheral jet ground effect machine is that the range of stability derivative variations exceeds the range of human adaptability.

If we knew nothing about the variations of the stability derivatives, our only choice would be adaptive control. If we knew everything about them, nonlinear compensation would solve the problem perfectly. We are, however, in a state between these two extremes. The actual criterion for the choice can be presented in the following question:

Do we have sufficient information about the variation of the stability derivatives so that the use of nonlinear compensation and feedback results in a system not exceeding the range of adaptability of the pilot for satisfactory control?

*Stability problems may arise if a parameter is dynamically coupled to the controlled variable so strongly that an adjustment of the feedback loop based on this parameter must be considered as a nonlinear feedback rather than as a compensation.

The most important point in this question is that we wish to make use of the adaptability of the human operator. If the answer to the above question is "yes", then there is no need to go into the design of a more complex adaptive feedback system. The answer is "yes." Material presented in this report provides sufficient information for the preliminary design of a nonlinear compensation for attitude stability augmentation by means of feedback control.

The basic design principle is now the following: We endeavor to design a feedback loop to be adjusted at any height in such a way that the pilot is always confronted with a vehicle which is easy to control. We cannot achieve this goal perfectly for three reasons:

a. We cannot predict very accurately the magnitudes of the stability derivatives.

b. We do not know exactly what an optimum GEM configuration would be like from the point of view of handling qualities.

c. We have made numerous approximations in order to simplify the system to a form suitable for mathematical synthesis.

These three points may seem discouraging but we have two strong points to make in order to balance all the uncertainties.

a. The range of adaptability of the pilot can absorb the uncertainties of points (a) and (c) above.

b. Since we cannot expect to hit the center of the test pilot's range of adaptability, provisions may be made for adjustments of the feedback gains during test flights. Results from these test flights can then easily be incorporated into the automatic compensation scheme.

5.2. Preliminary design of a feedback system for attitude stability augmentation.

Up to this point, our effort has been concentrated on simplifying the system while keeping the most significant stability problems in the simplified model,

and in establishing reasonable and practical design principles for the feedback system.

According to our previous discussion we are not going to consider any lead or lag contributed by the pilot, but rather leave his ability to provide such contributions as a safety margin which can be expected to absorb inaccuracies in the feedback synthesis. It is important to keep in mind that the primary goal of the pilot is to steady the attitude. The use of attitude control for maneuvering is not very efficient. Therefore, the task of fighting disturbance moments is strongly emphasized. Such moments are caused by any change of the center of pressure under the base. Experience indicates that small changes of a random nature always occur. At heights where the machine is statically unstable, this is sufficient to initiate an exponential divergence. Additional disturbance moments are caused by gusts.

At this point we can consider three basic feedback configurations. The configuration to be found most advantageous will be investigated in further detail. The three configurations to be considered are the following:

a. a lead-lag circuit to be inserted between the pilot and the vehicle, no internal control loop (see Figure 26A);

b. internal loop with rate feedback only (see Figure 26B);

c. internal loop with combined attitude and rate feedback (see Figure 26C).

Configuration A is actually an open loop compensation, and the response to a disturbance moment develops uninhibited. Among the three configurations this makes the task of the pilot the most difficult.

In configuration B the effect of the rate feedback is to slow down the divergence. With increased damping provided by the rate feedback, the unstable root moves toward the origin. However, even infinite inner loop gain cannot move this root into the region of stability for unattended operation.

It should be mentioned that, if there were no additional lag in the control, we could count on the pilot to provide lead sufficient to pull the right hand side root over into the region of stability. However, as pointed out earlier, we must expect a lag in the development of a part of the control moment. Considering this additional effect, we would be left with only a narrow range of pilot gain for stability, if any. This approach would be likely to lead to a highly critical design and would leave no margin for absorbing the inaccuracies to be expected in the design information.

Configuration C is more advantageous. The zero of the transfer function of the inner loop can be placed on the left hand side of the real axis without any contribution from the pilot. This is the combined effect of attitude and rate feedback. Then the vehicle which confronts the pilot can be made stable in attitude. The nature of the control which he exercises changes from moment control to attitude control. Using this approach, we count on the pilot's adaptability only in order to counteract the effects of the presently unknown additional lag and inaccuracies in the design information.

A single vertical gyroscope can provide attitude signals for both the pitch and the roll control feedback loops. This is a very reasonable price for the advantage of Configuration C. Therefore this is chosen as the suggested basic feedback configuration for the attitude stability augmentation of the ground effect machine.

The transfer function of a feedback path (Figure 26C) which consists of an attitude gyro and a rate gyro, can be expressed as:

$$G_F = A_F (1 + s T_F) \qquad \text{where} \quad T_F = \frac{A_R}{A_F}$$

This indicates that the location of the zero ($s = -\frac{1}{T_F}$) can be changed by adjusting only the rate feedback gain, A_R . For an adjustment of the loop

gain, either A_C can be changed, or else the attitude feedback gain, A_F, and the rate feedback gain, A_R, must be changed in the same proportion. One objective of the design is that the product, $A_C A_F$ be as large as possible. This is because the response to disturbance moments is diminished almost in proportion, without any contribution from the pilot.

It has been shown previously that the left hand side pole, S_1, of the attitude transfer function, G_θ, (Equation 83) does not change much throughout the useful height range. This suggests that the feedback time constant, $T_F = A_R / A_F$, can be kept constant so as to approximately cancel S_1 at all heights: $T_F = -\left(\frac{1}{S_1}\right)$

The inner loop gain and the control system bandwidth depends to a large extent on the additional control lag time constant, T_C. We can arrive at an estimate of the inner loop gain from the following considerations. In order to obtain a simple picture, let us assume that we have managed to cancel the root, S_1, and, therefore, we are left with two transfer function poles: the unstable right hand side GEM pole, S_2, and the control lag pole $S_C = -1/T_C$. As a criterion for the gain of the simplified inner loop we suggest a damping ratio, $\zeta_{CL} = \frac{1}{\sqrt{2}}$, as a convenient and reasonable compromise. Much higher damping is not easy to use because near critical damping ($\zeta_{CL} = 1.0$) the roots move relative rapidly with any change in gain. We are not able to be exact in specifying the gain. A much lower damping would not provide a sufficient margin of stability. Although, according to experience, it might be expected that the pilot could probably handle a smaller margin of stability, we wish to stress again that we do not suggest basing the design criteria on the limits of the pilot's capability.

Using our simplifying assumptions, and writing $A_C/(1+sT_C) = -A_C S_C/(s-S_C)$ we arrive at the following block diagram for the inner loop:

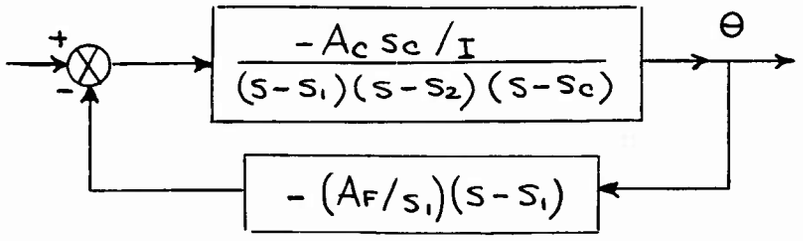

The characteristic equation of the closed loop is

$$S^2 - (S_2 + S_c)S + S_2 S_c + \frac{A_c A_F}{I} \frac{S_c}{S_1} = 0$$

Since the roots corresponding to a damping of $\frac{1}{\sqrt{2}}$ must be on the lines enclosing an angle of 45° with the negative real axis, we can find the inner loop gain for this damping by substituting $S = -\sigma + j\omega = -\sigma + j\sigma$ in the characteristic equation. We eliminate σ from the two equations obtained for the real and imaginary parts, both of which must become zero for the same σ . We then obtain:

$$A_c A_F = \frac{I}{2} S_1 S_c \left[1 + \left(\frac{S_2}{S_c}\right)^2\right] \qquad (86)$$

A measure of the bandwidth of the inner loop is $|\sigma| = \frac{|S_2 + S_c|}{2}$ (rad/sec). These results indicate how strongly the control lag pole, S_c , influences the adjustment of the inner loop gain. Examining Equation 86, we find that if $|S_c| > 2\,|S_2|_{max}$, the influence of the change of S_2 (i.e., of the moment derivative) on the desired inner loop gain is fairly small (less than 25%). This means that if the ratio of the control gain and the control lag root $-A_c/S_c = A_c T_c$, were to remain constant throughout the height range, our choice of feedback configuration and dynamic performance criteria would probably

satisfy all practical purposes with a fixed feedback gain, A_F, and a fixed rate feedback, A_R. However, the fact that the desired feedback gain, A_F, is inversely proportional to $A_c T_c$ indicates that we should provide a variable gain.

Since the variations of the control parameters influence the controllability even if no feedback is used, it would seem advantageous to provide for changes so that A_c would remain nearly constant. That is to say, the moment versus stick displacement relationship should not vary appreciably throughout the height range. Considering the very close relationship between height and throttle setting for a particular configuration it seems feasible that this "automatic" gain adjustment could be provided purely mechanically by changing a linkage-arm ratio by means of the throttle. It is then conceivable that fixed feedback gains could be used to provide satisfactory dynamic characteristics. Another advantage of this approach is that the gain adjustment would be an open loop adjustment. This eliminates the problems of measuring height and obviates any problem of dynamic coupling between the attitude and heave modes through the automatic control. It may, however, be necessary to provide for some adjustment in the gain control to compensate for large variations of the load.

It may also be pointed out that, if necessary, an additional lead-lag compensation could be used in the inner loop in order to increase its bandwidth and make it "tighter" by applying higher loop gain. Unfortunately this is not immediately possible in the absence of information available about the variation of the control system parameters, A_c and T_c. In the present state of the art, therefore, "tuning" of an experimental autopilot throughout the height range in hovering is necessary in order to find out about the effect of the height dependence of the control parameters. Since the proposed inner loop

provides stability in attitude by itself, such tests can easily be carried out by checking moment-pulse responses. These can be measured by recording the attitude gyro output.

The previous discussion has been based on several assumptions and simplifications. It is appropriate to discuss the effects of inaccuracies in these assumptions on our conclusions.

In our simplified approach we considered three real roots: the two roots S_1 and S_2 of the GEM attitude freedom and a control lag root, S_c. We have arbitrarily chosen S_1 to be approximately cancelled by the feedback zero because this choice offered the possibility of a fixed rate gyro gain. If S_c should turn out to be nearly constant throughout the height range, it could be cancelled instead. It is definitely advantageous, however, to cancel the root nearest the origin. It should be kept in mind that the GEM roots S_1 and S_2 would be much closer to the origin in the case of any practical full scale design than they are for the eight foot model. The relative radius of gyration of a practical machine would be larger than that of our model. In our case $r/r_g = 2.5$ (r_g = radius of gyration), whereas in a practical design $r/r_g < 2.0$ seems more realistic. With the value $r/r_g = 2.0$ and a diameter of 40 feet instead of eight feet, the GEM attitude roots would be 2.8 times closer to the origin than the roots of our test model (if the relative nozzle area is kept the same). It would be difficult to decide whether S_1 or S_c would be closer to the origin. The control lag can be expected to increase with size but to decrease if the total head pressure is increased.

The following practical procedure for optimizing the location of the feedback zone can be suggested. As a first approximation locate the zero, (i.e., adjust the rate gyro gain) with the assumption that the relative damping ratio

does not change with size, i.e., use a root locus plot similar to Figure 23 but with the scale changed according to the size and the r/r_g ratio. Adjust the feedback gain, A_F, according to Equation 86 and check the pulse response at several heights. Readjust, A_F, for approximately critical damping. Now change the rate feedback (i.e., the zero location) and check for uniformity of the response over the height range. Check also whether a higher feedback gain can be applied for the same damping. Change the rate feedback in the other direction and repeat. A relatively short test should lead to an optimum location of the feedback zero. Now keeping this zero constant, one can establish experimentally the way in which the feedback gain should be changed in order to compensate for the change in the control parameters by adjusting for approximately the same damping at all heights. Since the height is very closely related to the throttle setting and since high accuracy is not a requirement, the gain change could be most easily instrumented by gearing appropriate nonlinear gain potentiometers for the pitch and roll feedback to the throttle.

We should like to emphasize again the important role of the control lag. We can conclude that, if this lag can be avoided, a significantly tighter inner loop with a considerably larger bandwidth could be obtained or, if such improvement is not needed, the elimination of the attitude feedback and the application of rate feedback alone could be considered. It may be that the vehicle designer can exercise some control over this feature of the machine.

We have, in addition, neglected some singulatities of the inner loop. We assumed that the servo motor transfer function poles are far enough removed so that their effect on the dynamics of the controlled vehicle in the critical area is negligible. We have shown that for practical machines the dominant poles

are much closer to the origin than those of our eight foot test model, so that this assumption is certainly justified. We have further neglected any effect of dead zone or backlash in the controls. This would be very difficult to consider, unless a specific design was analyzed. We have also, however, neglected one somewhat favorable singularity. This is the zero which appears because, presumably, only part of the control moment is lagging. If we write the control transfer function in the form

$$G_c = A_{c1} + \frac{A_{c2}}{1+sT_c} = \frac{A_{c1} + A_{c2} + sA_{c1}T_c}{1+sT_c} = A_c \frac{1+s(A_{c1}/A_c)T_c}{1+sT_c}$$

where $A_c = A_{c1} + A_{c2}$ is the total static control gain, we can see that the control zero is A_c/A_{c1} times as far from the origin as the control pole. It can be expected that the lagging part will be larger if the largest part of the weight is supported by the base pressure and pressure differentials are responsible for the largest part of the moment. The control zero can, therefore, be expected to come closer to the control pole with increases in height, but it could reach it only if the full control moment was to develop without delay. Only near the upper limit of the useful height range could favorable effect of this zero be expected to be noticeable. This should actually have no influence on the design.

We have considered the control of the GEM in the vicinity of zero attitude angle, and we have shown that, in this case, the coupling between the attitude and the heave degrees of freedom can be neglected. These assumptions are quite valid for hovering. Up to now, we have discussed the synthesis of the control system for hovering only; we now have to discuss the performance we can expect of our system in forward flight, together with changes or additions, which seem

necessary. Since there is little information available, at the present time, concerning the stability derivatives in forward flight, we shall not be able to make quantitative predictions as in hovering. We wish to emphasize that we are concerned here only with the control of a GEM at low speeds. The use of more or less conventional aerodynamic surfaces for control is not considered because of the wide variety of possibilities and because of the existence of already well established methods for the analysis of such situations.

Let us first consider forward flight with the machine in a level attitude. This situation has been discussed in the section concerning forward flight. From the point of view of our control system we have to consider two distinct problems.

The first problem arises because, as the velocity is increased, an increasing moment is acting on the GEM. Rather than to put the burden of counteracting this moment on the control system described so far, it is advantageous to counteract at least a large part of this moment independently of the automatic control system. This could be achieved, for example, by allowing for a moment arm for the auxiliary thrust vector, or, alternatively, by gradually shutting off the jet at the front edge with increasing velocity. The latter solution seems more desirable because it tends to eliminate the moment rather than fighting it. Also, some additional lift may be gained by adding some of the mass flow saved in the front to the rear edge. The disadvantage of this approach is the more complicated control system.

After the problem of trimming the steady state moment has been solved, we still face a second problem: the changes in stability and control derivatives with velocity. Because of the scarcity of quantitative information, an empirical approach with an experimental autopilot is suggested. This is feasible with the

proposed feedback system since pulse responses can be used for the tests. Once the desired static control gain versus velocity characteristics are established, we can use an approach to the mechanization similar to the one already employed for the changes in height. The steady state velocity is closely related to the throttle setting of the auxiliary thrust source, therefore as a first approach, the gain adjusting potentiometers could be simply geared to this throttle. However, it can be expected that for fast accelerations and decelerations the throttle setting could lead the velocity too much to provide smooth control during the acceleration. If this is the case a lag should be inserted between the throttle and the control gain potentiometers.

Concerning the effect on the controlled system of the coupling between the attitude and the translational freedom, the following argument can be made. Since we have a rather tight attitude control only small deviations from the zero attitude angle are to be expected, and corrections in attitude will occur fast enough so that no appreciable change in velocity can occur. In other words, the forces coupling the translational freedom to the attitude mode are kept small by the feedback control. We can say the same thing, however, about the moments occurring due to velocity changes and gusts; these must be considered as disturbance inputs to the attitude control. The coupling, however, can be considered to be practically unilateral, and no additional stability problems are to be expected.

There are two practical situations in which deviation from zero attutide angle must be desired. One is banking in a turn, the other is enhancing deceleration and acceleration by tilting the vehicle in pitch. Since we assume that the height at which the GEM flies is determined by the obstacle to be cleared, tilting can be used only if reserve power is available so that the

lowest edge remains at the reference height. It is obvious that only small angles can be achieved in practice. Because of the attitude feedback the equilibrium angle can be commanded by the control stick input. It may be expected that, for the practical small angles, the stability derivatives do not change appreciably. The coupling between the heave and the attitude mode is small with small angles, and, since the heave mode is inherently stable and damped, no severe stability problems are expected in connection with small tilt angles.

In summary, the relatively simple autopilot devised on the basis of a fairly detailed analysis of the hovering case can be expected to also work satisfactorily in forward flight, after it has been provided with suitable automatic gain adjustments. In the present state of the art, the gain adjustment functions have to be established experimentally. Once these functions have been established they can be permanently set, and there is apparently no need for adaptive control. Great precision in the synthesis of closed loop system dynamics is not required since we can count on the pilot's ability to handle a considerable range of vehicle characteristics.

6. CONCLUSIONS

As is usually the case when one attempts to synthesize a feedback control system, the large part of the effort is this investigation went into the analysis of the system to be controlled. In the course of an effort to isolate the most significant problems, the stabilization of the ground effect machine in attitude was singled out. In the theoretical approach the principle of the balance of momentum changes and forces was used. Derivations of expressions for the undamped natural frequency and the damping in heave as well as for the static attitude moment yielded results which reveal the basic mechanisms influencing these parameters and which are in good agreement with experimental results. This agreement established a certain amount of confidence in the theoretical results so that they could be used in the preliminary design of a feedback control system. A discussion indicated the influence of different physical parameters as well as the influence of scaling on the theoretical results.

Especially interesting is the form of the result for the attitude moment derivative which indicates the sources of both the stabilizing and the destabilizing static moments. Both of these moments can be attributed to losses in the base area: the stabilizing moment to a loss in base pressure (due to vortices and other possible causes), the destabilizing moment to the loss of momentum of the crossflow in the base area (primarily due to dissipation). The change of the balance of these moments against each other causes the crossover from static stability to instability. This result has been obtained by way of some rather crude approximations; nevertheless, it seems to provide a frame into which more refined analysis of the future can be expected to fit.

Experiments were carried out with an eight foot diameter model to yield information about the static and the dynamic stability derivatives in a hover condition. In general, satisfactory agreement with the theoretical results was obtained. However, from the measurement of attitude damping, unexpected results were obtained for which no theoretical explanation could be given. These tests indicated the presence of a degree of damping sufficiently large to influence considerably the preliminary design procedure of the feedback system. This influence seems significant enough to suggest exploration of the effect of scaling on attitude damping. It was not explored in the present study.

In the course of determining design principles for the automatic stability augmentation, it was decided that the adaptability of the human pilot could be effectively employed. This, and the consideration of disturbance moments, leads to the selection of a combined attitude and rate feedback control system with open loop gain adjustments to take care of the significant effects of flight condition variations.

The preliminary synthesis brings out the significance of the moment control lag and the variation of the moment control effectiveness with height. Because of the significant role of these parameters the study of the attitude control dynamics of practical GEM control systems can be suggested as a worthwhile subject for future investigations. A series of arguments leads to the conclusion that the suggested feedback control configuration could be expected to perform satisfactorily in hovering and in forward flight, up to speeds where aerodynamic control surfaces become effective. This is the case even though very little information is available, at this time, concerning the variation of stability parameters in

forward flight. Therefore, the installation of an experimental autopilot built according to the preliminary design described in this report, and installed in a piloted flying model, is suggested as the next important step in the study of automatic stability augmentation.

It should be kept in mind that this report is concerned only with the overland characteristics of the ground effect machine. Experimental over-water studies have indicated a different behavior of the stability derivatives. The suggested feedback control configuration, however, is able to cover such a wide range of characteristics that a different gain adjustment program can be expected to provide satisfactory stability augmentation over-water also. Switching from one set to another set of gain adjusting potentiometers on the part of the pilot would probably be preferred to an automatic adaptive control system because of the faster adaptation. The application of adaptive control principles might be needed to replace the human adaptivity if remote control of ground effect machines were contemplated.

REFERENCES

1. Feng Isum-Ying; "Hovering and Longitudinal Dynamics of the Ground Effect Machine with Derivations of the Stability Derivatives for Vertical Motion", Proceedings of the National Specialists Meeting on Guidance of Aerospace Vehicles, IAS, May 1960.

2. "Progress Report of U.S. Navy Contract Number NONR-317 3/001 GEM Stability Control Study", A Research Manfacturing Division; The Garrett Corporation Report No. AP-5018-R June 21, 1960; Second Progress Report No. AP-5025-R, November 11, 1960.

3. Eames, Michael C.; "Fundamentals of the Stability of Peripheral Jet Vehicles", Volume's I, II, III, Pneumodynamics Corporation, Bethesda, Maryland, November 1960.

4. Helgesen, J.O.; "Some Dynamic Stability Characteristics of a Hovering Peripheral Jet Ground Environment Machine - Motion in Heave Only", Grumman Aircraft Engineering Corporation, Research Memorandum RM - 184, February 1961.

5. Higgins, H.C. and Martin, L.W.; "Effects of Surface Geometry and Vehicle Motion on Forces Produced by a Ground Pressure Element", Symposium on Ground Effect Phenomena, Princeton University, October 1959.

6. van Glahn, V.H.; "Exploratory Study of Ground Proximity Effects on Thrust of Angular and Circular Nozzles", NACA TN 3982, April 1957.

7. Chaplin, H.R.; "Theory of the Angular Nozzle in Proximity to the Ground", David Taylor Model Basin Aeronautical Report No. 923, July 1957.

8. Chaplin, H.R.; "Effect of Jet Mixing on the Angular Jet", David Taylor Model Basin Aeronautical Report No. 953, February 1959.

9. Fuller, F.L.; "An Approximate Theory for the Ground Effect Vehicle Employing A Thin Sheet Jet", Grumman Aircraft Research Note RN-109.

10. Boehler, G.D. and Spindler, R.J.; "Aerodynamic Theory of the Annular Jet", Aerophysics Company, Inc., Washington D.C., Report No. AR 581-R, December 1958.

11. Rethorst, S. and Royce, W.W.; "Lifting Systems for VTOL Vehicles", Institute of the Aeronautical Sciences Paper No. 59-123, June 16-19.

12. Stanton-Jones, R.; "The Development of the Saunders - Roe Hovercraft", "SRNI" Saunders-Roe Limited Publication No. TP 414.

13. Nixon, W.B. and Sweeney, T.E.; "Some Qualitative Characteristics of A Two-Dimensional Peripheral Jet", Princeton University Department of Aeronautical Engineering, Report No. 484, September 1959.

14. "Symposium on Ground Effect Phenomena - a compilation of papers presented", Princeton University Department of Aeronautical Engineering, October 1959.

15. Shen, Shan-Tu; "Effects of Cushion Vortices on Peripheral Jet Vehicles", Appendix to Reference (3).

16. Magnus, R.J.; "Use of Vortices in Calculation of Bottom Pressures of Annular Jet Ground Effect Machines", Convair Engineering Research, Report No. ERR-SD-061, March 1961.

17. Webster, W.C.; "The Static Stability of Ground Effect Vehicles - Thin Jet Theory", Hydronautics, Inc., Technical Report No. 011-1, December 1960.

18. Lin, J.D., "Static Stability of Ground Effect Machines - Thick Jet Theory", Hydronautics, Inc., Technical Report 011-2, June 1, 1961.

19. Foltz, C.A.; "Ground Effect Machine Investigations at the University of Wichita, Final Report Summarizing the Test Program and Data Obtained", University of Wichita Engineering Research Report No. 352-6, May 1961.

20. Greif, R.K.; Kelly, M.W.; Tolhurst, W.H. Jr.; "Wind-Tunnel Tests Of A Circular Wing With An Annular Nozzle in Proximity to The Ground", NASA TN D-317, May 1960.

21. Ando, S. and Migashita, J.; "Aerodynamic Drag of Ground Effect Machines", Aerospace Engineering Volume 20, No. 11, November 1961.

22. Ashkenas, L. and McRuer, T.; "The Determination of Lateral Handling Quality Requirements from Airframe-Human Pilot System Studies", WADC Technical Report 59-135, June 1959.

23. McRuer, T.; Ashkenas, L. and Guerre, C.L.; "A System Analysis View Of Longitudinal Flying Qualities". WADD Technical Report 60-43, January 1960.

24. Ashkenas, L. and McRuer T.; "A Theory of Handling Qualities Derived from Pilot Vehicle System Considerations", Aerospace Engineering Volume 21, Number 2, (February 1962) PP 60.

25. Tulin, P.; "On The Vertical Motions of Edge Jet Vehicles", Symposium on Ground Effect Phenomena, Princeton, October 1959.

26. Nixon, W.B. and Sweeney, T.E.; "Preliminary Flight Experiments With The Princeton University Twenty-Foot Ground Effect Machine", Princeton University, Department of Aeronautical Engineering, Report No. 506, January 1960.

27. Chaplin, R.; "Ground Cushion Research At The David Taylor Model Basin - A Brief Summary of Progress to Date", Proceedings, Part II of Decennial Symposium, Institute of Aerophysics, October 1959.

28. Strand, T.; "Inviscid-Incompressible-Flow Theory of Static Peripheral Jets in Proximity to the Ground", Journal of Aerospace Sciences Volume 28, Number 1, January 1961.

29. Knowlton, M.P. and Wojciechowicz, A.F., Jr.; "Model Studies of the Forward Flight Characteristics of the P-GEM", Princeton University, Department of Aeronautical Engineering, Report No. 581, December 1961.

30. Sweeney, T.E. and Nixon, W.B.; "Some Notes on the P-GEM", Princeton University, Department of Aeronautical Engineering, Report No. 537, January 1961.

31. Truxal, John G.; "Automatic Feedback Control System Synthesis", McGraw-Hill Book Company, 1955.

APPENDIX A

EFFECT OF GYROSCOPIC COUPLING

In order to be able to estimate the effect of gyroscopic coupling, let us investigate the following case. Let us assume that a sinusoidal oscillation takes place around the roll axis, with some frequency ω_{xo}, which cannot be easily controlled by the pilot. Let the amplitude of this oscillation be A_x. A sinusoidal gyroscopic moment around the pitch axis induces an oscillation of the same frequency with an amplitude A_y. The amplitude ratio A_y/A_x can be considered as a practical measure of the significance of the gyroscopic coupling. It can be easily shown that

$$\frac{A_y}{A_x} = \frac{J_z}{J_y} \frac{\Omega_z}{\omega_{xo}} \qquad \text{(A-1)}$$

where J_z is the moment of inertia of the propeller and shaft aligned with the z axis, Ω_z is the angular velocity of the propeller and J_y is the moment of inertia of the machine around the y axis. If we choose $\omega_{xo} = 2\pi$/sec as the "input" frequency, Equation A-1 can be written as

$$\frac{A_y}{A_x} = \frac{J_z}{J_y} f_z \qquad \text{(A-1-a)}$$

where f_z is the propeller speed in revolutions per second. If we substitute in this expression the measured values of the tested eight foot model, $J_z = .07$ (ft. lb. sec.^{2}); $J_y = 13.4$ (ft. lb. sec.^{2}) we find with the maximum propeller speed (4350 RPM) $A_y/A_x = 0.38$. This amplitude ratio is not negligible.

The following discussion indicates the effect of scaling on the gyroscopic coupling. For two machines of similar shape and weight distribution, but different in size, the moments of inertia differ by an approximate ratio

$$\frac{J_{y2}}{J_{y1}} = \frac{W_2 D_2^2}{W_1 D_1^2} = \frac{P_{L2}}{P_{L1}} \frac{D_2^4}{D_1^4} \qquad \text{(A-2)}$$

where P_{L1} and P_{L2} are the specific loads in lb/ft.^{2}. If the index 2 marks the larger machine, the moment of inertia ratio increases by more than the fourth power of the diameter ratio if the larger machine also has a larger specific loac P_L .

In order to make an estimate of the increase in the moment of inertia of the propeller, the horsepower requirement must be considered. The horsepower required is proportional (indicated by $\sim$) to the product of the mass flow and the square of the jet velocity,

$$HP \sim \frac{1}{2} m_{TOT} v_J^2 \sim S_N P_T^{3/2} \qquad \text{(A-3)}$$

where S_N is the nozzle area, P_T the total pressure, v_J is the jet velocity and m_{TOT} is the total mass flow of the jet. By definition the lift is $L=W= A J_{TOT}$ (where A is the augmentation factor and J_{TOT} is the total jet momentum). From this expression we obtain $P_L S \sim A S_N P_T$ by using $P_L = \frac{W}{S}$ and the fact that $J \sim S_N P_T$. We can use this relationship to eliminate P_T from the horsepower relationship giving,

$$HP \sim \left(\frac{P_L}{A}\right)^{3/2} \left(\frac{S}{S_N}\right)^{1/2} S \qquad \text{(A-4)}$$

The propeller horsepower can be scaled approximately as $HP \sim R_{prop}^2 V_{tip}^3$ or as

$$HP_{prop} \sim R_{prop}^2 \tag{A-5}$$

if the tip speed is unchanged. Comparing the last two relationships we find that the propeller diameter should be proportional to the GEM diameter in the case of a circular machine, if the scaling is made for the same augmentation and specific load. We assume that the mass of the propeller increases only approximately with the square of the diameter because relatively less structural strength is needed because of smaller RPM of the larger propeller. Then

$$\frac{J_{z2}}{J_{z1}} \sim \left(\frac{A_1}{A_2}\right)^2 \left(\frac{D_2}{D_1}\right)^4 \left(\frac{P_{L2}}{P_{L1}}\right)^3 \tag{A-6}$$

Applying the formulas A-6 and A-2 to A-1-a

$$\frac{A_{y2}/A_{x2}}{A_{y1}/A_{x1}} \sim \left(\frac{A_1}{A_2}\right)^2 \left(\frac{P_{L2}}{P_{L1}}\right)^2 \frac{f_{z2}}{f_{z1}} = \left(\frac{A_1}{A_2}\right)^2 \left(\frac{P_{L2}}{P_{L1}}\right)^2 \frac{D_1}{D_2} \tag{A-7}$$

Using this formula with $A_1/A_2 = 1$ the gyroscopic coupling of the Princeton twenty foot model could be characterized from the data of the eight foot model with

$$A_{y2}/A_{x2} \cong 0.3$$

Actually, however, the propeller diameter is larger by a factor of only two and the necessary horsepower is obtained by means of a larger tipspeed. This leads to a corrected estimate of $A_{y2}/A_{x2} \cong 0.18$. Considering that our fixed frequency $\omega_{x0} = 2\pi$/sec. is rather fast for an attitude oscillation,

this A_{yz}/A_{xz} ratio indicates a comparatively small effect of the gyroscopic coupling. This is confirmed by the pilot's opinion. According to Equation A-7 this situation can be expected to remain unchanged as long as the increase of the specific load is not larger than the square root of the increase in diameter.

This discussion leads to the following general conclusions:

a. The significance of gyroscopic coupling in practical machines can be considered practically negligible except for single rotor ground effect machines with very large specific loads.

b. The scaling of the gyroscopic coupling must be considered if the dynamics of a single propeller ground effect machine are to be investigated on a scaled model.

c. In the case of large specific loads, gyroscopic coupling can and should be practically eliminated by using a number of contrarotating propellers.

APPENDIX B

EXPERIMENTAL INVESTIGATION

The discussion which follows describes the model used for the tests, the testing procedure and the results of the tests. Because of limitations in the length of time available, no tests were made in forward flight.

Model and Test Setup: The model on which the experiments were carried out is a circular, annular jet ground effect machine with a diameter of 8 feet and a weight of 170 pounds. The jet is one inch thick and is inclined inward at an angle of 45 degrees. Power is supplied by a four-blade propeller driven by a three-phase, 115 volt electric motor. The propeller is 24 inches in diameter. Power to the motor is controlled by means of a Variac located at the control station.

The model is attached to a rig, as shown in Figure 28, so that it has two degrees of freedom. The bearings supporting the model are located on an axis passing through the center of gravity. This allows freedom in pitch about this axis only. The bearings, in turn, are supported by the yoke shown in Figure 27. A vertical shaft from the yoke extends through a sleeve in the main rig. This allows freedom of motion in the heave mode. The model can be locked in either heave or pitch by means of notched shafts extending from the yoke in the case of the pitch lock, and from the main rig in the case of the heave lock (see Figure 27). The notches are made at intervals of one degree in pitch and one inch in heave. A pneumatic release system effects the release of the model in either pitch or heave or both with power on. (Springs which can be seen in the Figure pull the notched shafts free when released.)

Heave and pitch motion are read by means of potentiometers. Referring to Figure 27, the pitch pot may be seen, with its linkage, at the base of the yoke. The pot is rigidly attached to the yoke while its wiper arm is free

to move with the model. The heave pot may be seen in Figure 27 just above the yoke at the apex of the linkage connecting the main rig and the yoke. This pot is rigidly attached to the main rig while its wiper arm is free to move with the yoke. The wiper voltages are fed into a Sanborn recorder at the control station and also into meters for direct reading.

The weight of the machine can be increased by attaching copper weights to the structure and can be decreased by means of a spring attached to a hoist above the model. The spring is sufficiently soft so that it has only a small effect on the period of the transient oscillations in heave. Corrections are made to account for the fact that the mass does not decrease when the spring is used to reduce the weight.

Static moments are measured by means of a strain guage which is bonded to a beam attached to the model at one end and to a cable which is suspended fromabove at the other end. Weights are added to this end of the model so that all moment readings are positive. The signal is read on the output of a Sanborn amplifier at the control station.

Testing Procedure: Measurements were made to show the variation of the lift force with height for various constant values of the motor RPM. Weight was both added to and subtracted from the basic weigh in 20 pound increments. For each weight, the resulting hovering height was recorded at three specific values of the motor RPM. The results of these measurements are shown in Figure 2. The curves of Figure 3 show the effect of small attitude changes on the lift.

A series of experiments was conducted to determine the dynamic behavior of the model in heave. To accomplish this, the model was locked in pitch so that it had only vertical freedom. Because of the presence of some flexibility

in the supporting structure the model tended to exhibit some attitude change with variations in the power supplied to the propeller; however, these changes were usually small and were accounted for whenever possible.

The tests were conducted as follows: The model was raised to a certain height, the attitude locked at a certain angle and the model weight set by either adding weights or increasing the spring force. The propeller was then brought up to an RPM which corresponded to an equilibrium height either somewhat greater or somewhat less than the one at which the model was set. The model was then released and the resulting transient was recorded. The frequency and damping ratio were then determined from the recorded trace. Systematic variations were made in the model weight, pitch angle, equilibrium height and also in the size of the input. It was found that inputs of about plus or minus 1.5 inches were a good compromise. (Smaller inputs did not give a sufficient number of readable overshoots for determining the frequency and damping, and larger inputs would run the risk of causing nonlinear behavior). The results of the tests are shown in Figure 6 and in Figures 9 to 12.

Pitch Freedom Tests: The desired information in the pitch degree of freedom was somewhat more difficult to obtain because of the fact that the model was unstable in pitch at all but the very lowest heights. Essentially two measurements were made at each height. The variation of pitching moment with pitch angle was recorded, and the variation of pitch damping was determined separately. In each case the model was rigidly fastened at a given height from the ground. To determine the effect of variation of the machine weight, each test was made at three different values of the motor RPM. This was equivalent to varying the weight of the machine since it had no vertical freedom.

As described previously, the moment measurements were made using a strain gauge which was bonded to a beam at the edge of the machine. The machine was set at the desired height, the cable adjusted to give the desired pitch angle and then the propeller was brought up to speed. Moment readings were taken at each of three previously determined RPM readings. The results of these tests are shown in Figure 21. In all of the moment measurements there was a considerable amount of fluctuation present and each of the readings represents an average taken over several seconds of the motion of the needle indicating the strain gauge output. The fluctuations appeared to be due to the unsteadiness of the flow beneath the model.

Pitch damping was determined by a test in which a fixed moment was applied to the model at different height and RPM settings. The time history of the pitch angle was recorded until the model struck the ground. The moment was applied in such a manner as to insure that the pitch angle varied through the linear portion of the moment curve. Assuming that this motion could be described by a second-order differential equation in which the inertia and spring force (negative) were known, curves showing the pitch angle response to a step input as a function of damping ratio were plotted. From these curves the damping ratio corresponding to the measured pitch angle could be found. The variation of the damping ratio with height is shown if Figure 22.

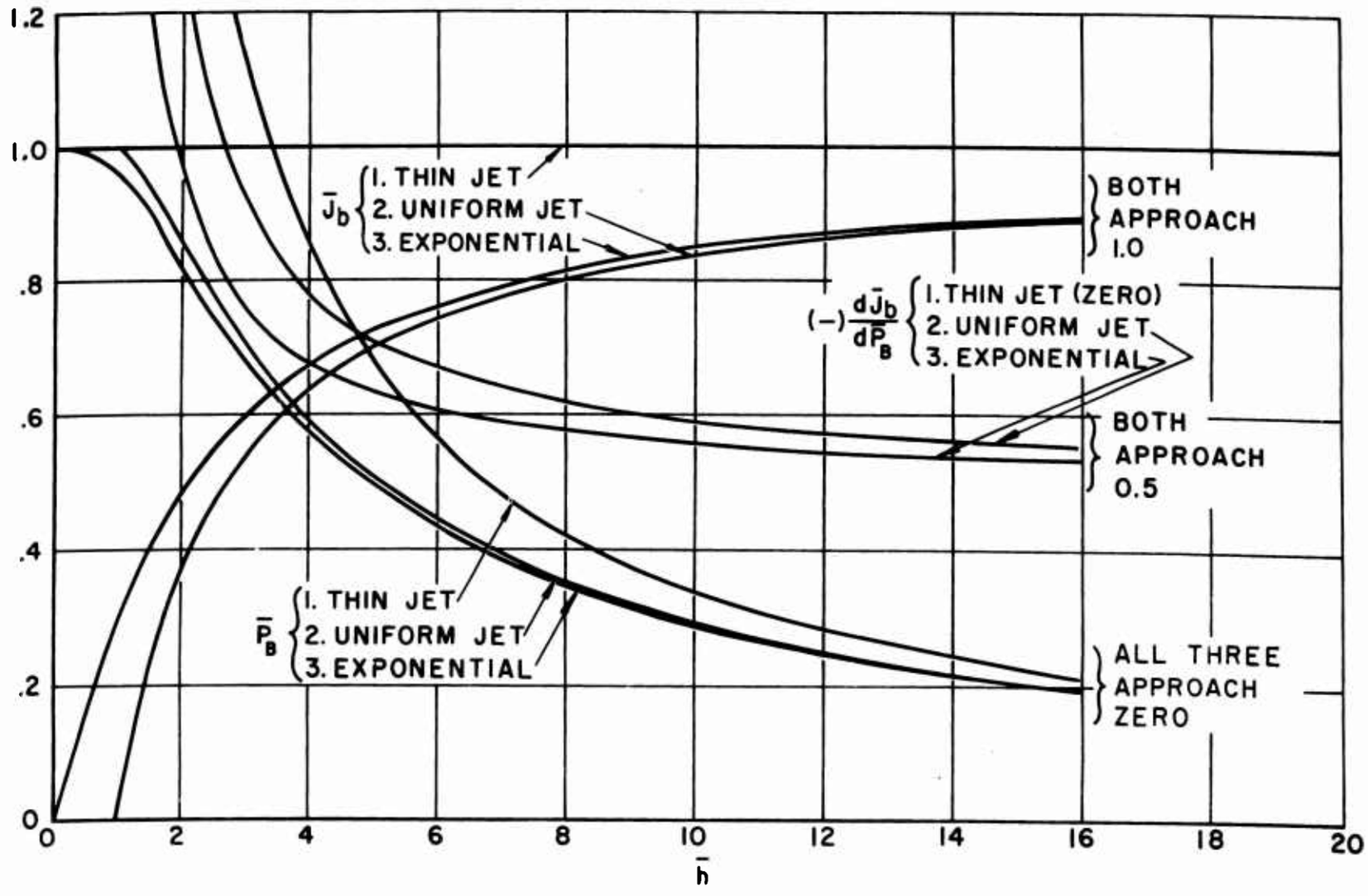

FIGURE 1 COMPARISON OF JET THEORIES

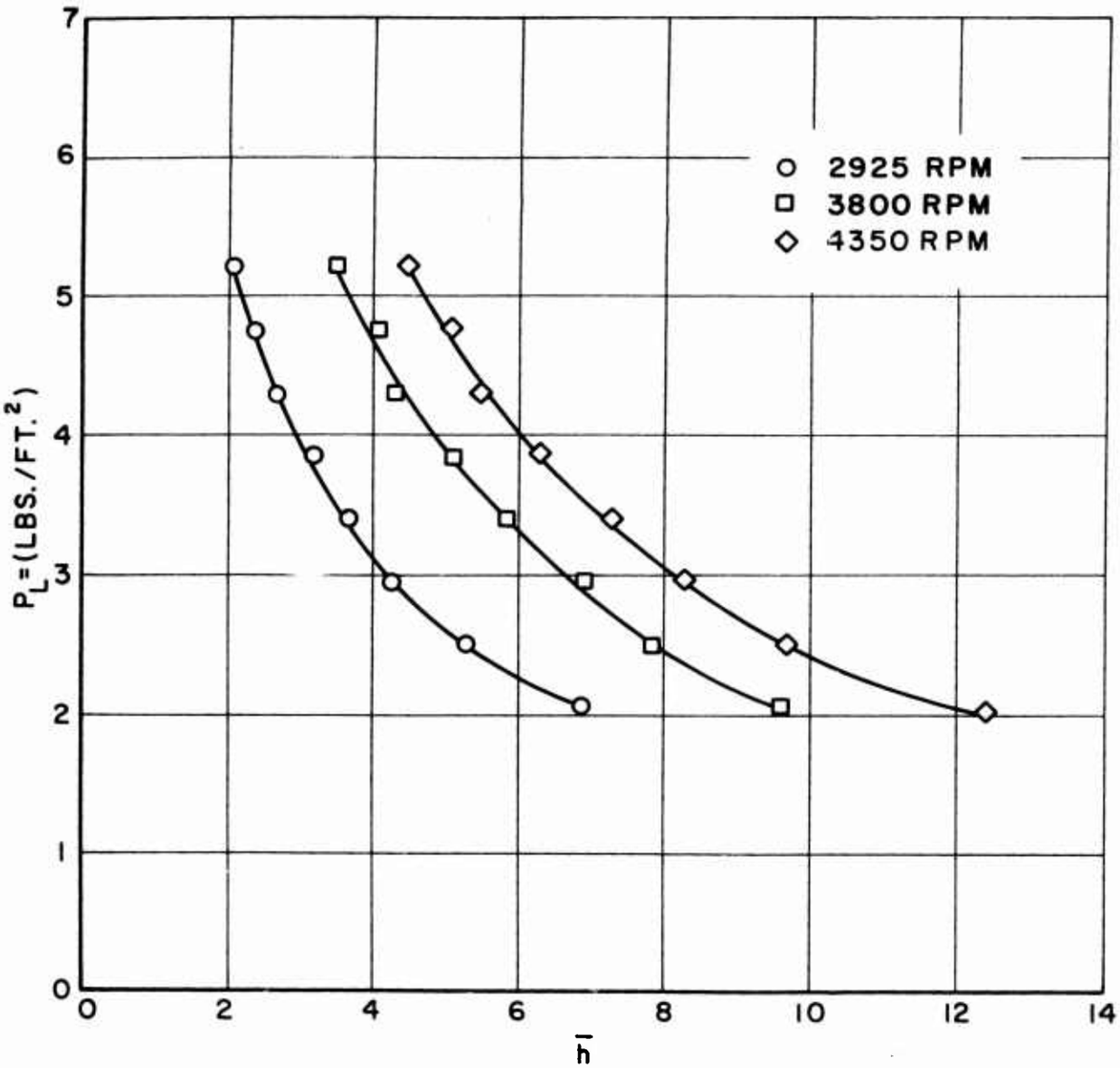

FIGURE 2 LIFT VS. HEIGHT

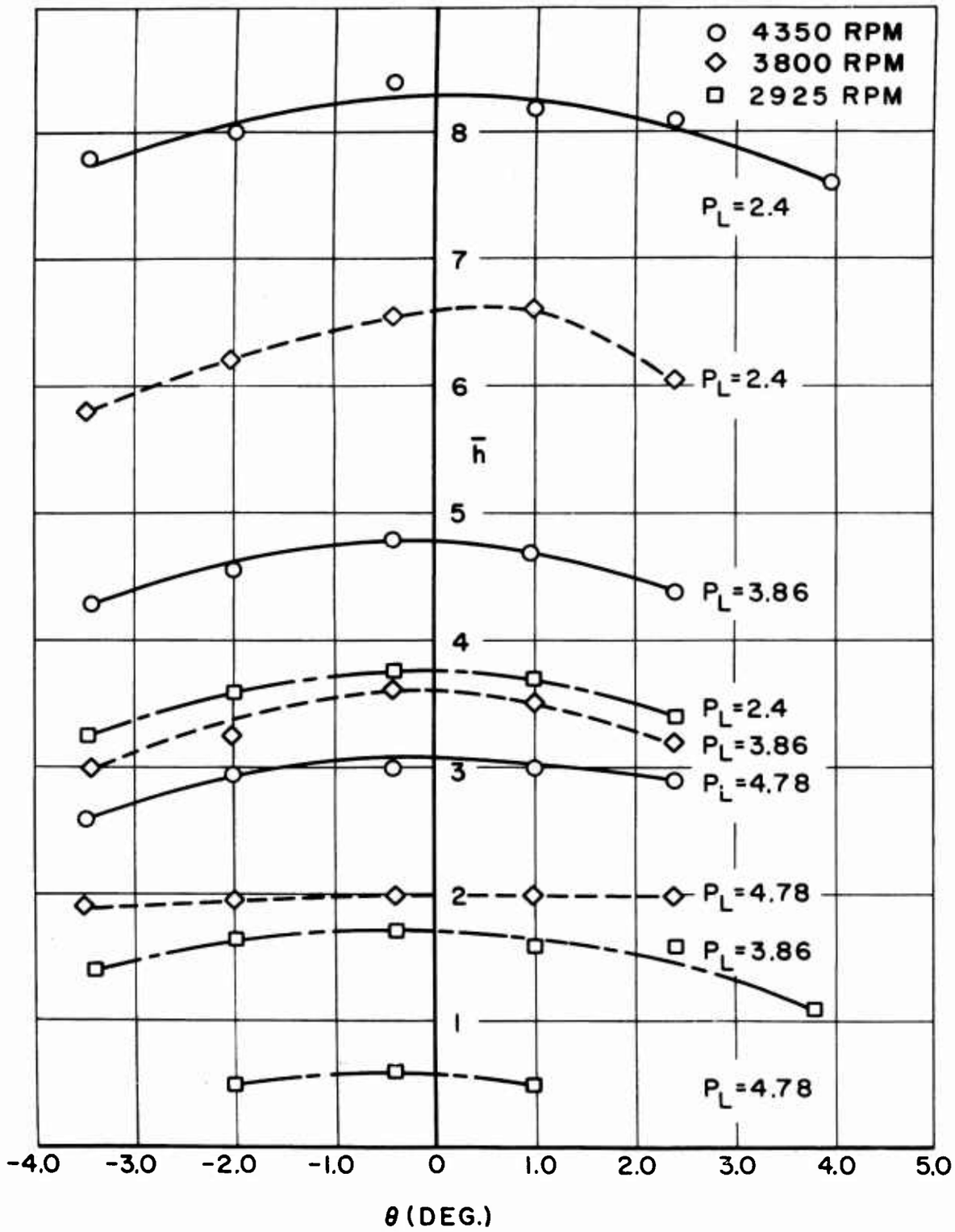

FIGURE 3 EQUILIBRIUM HEIGHT VS. ATTITUDE ANGLE

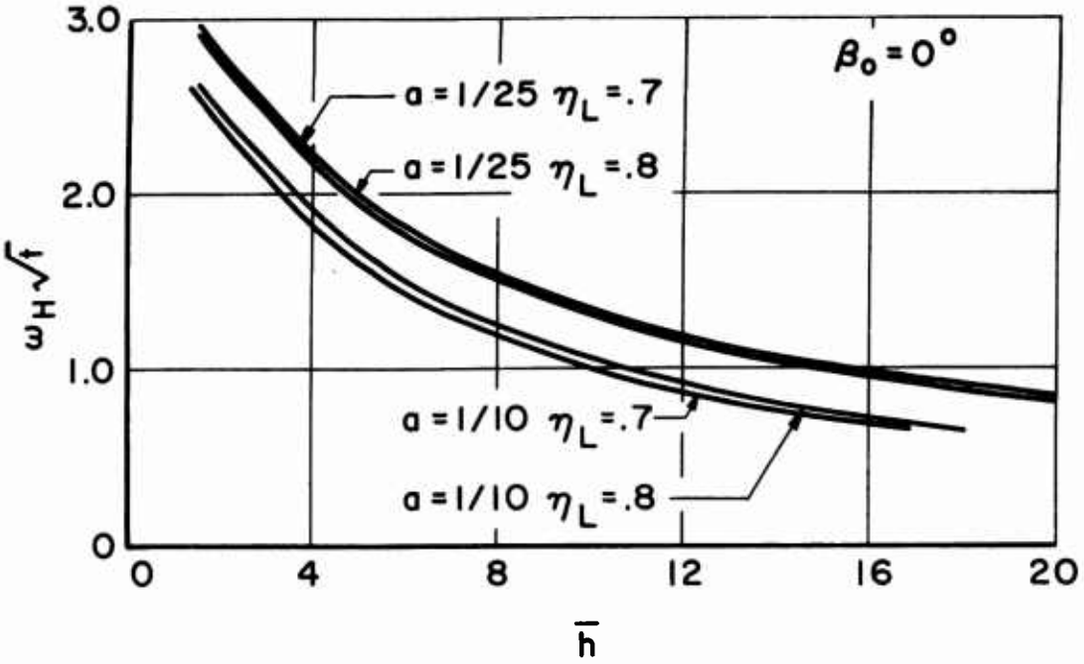

FIGURE 4 HEAVE FREQUENCY, 0° JET INCLINATION

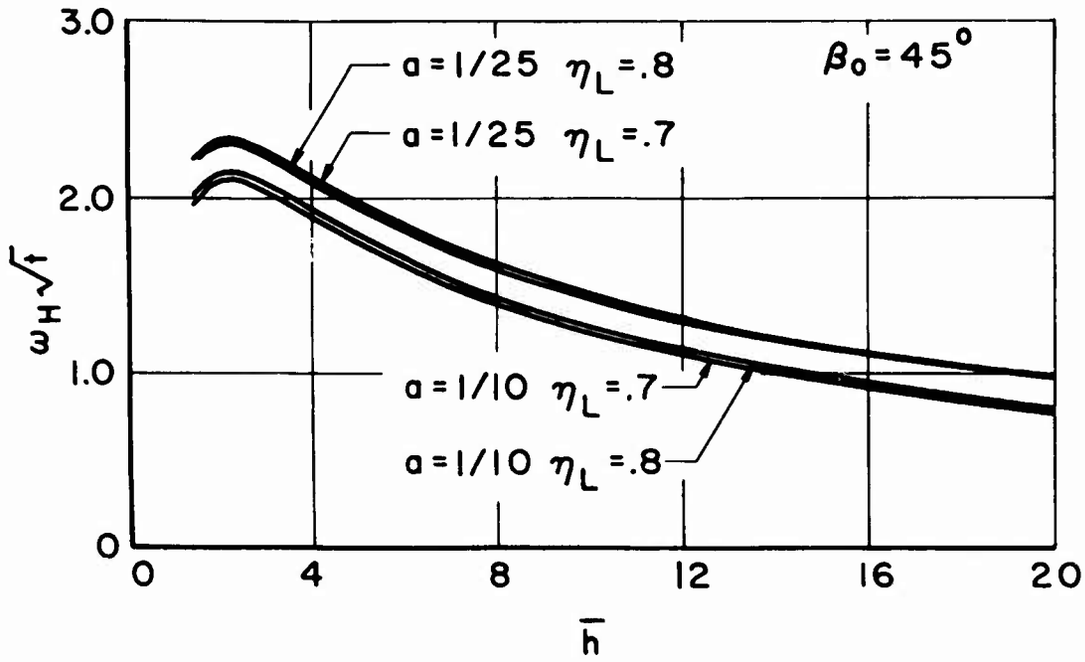

FIGURE 5 HEAVE FREQUENCY, 45° JET INCLINATION

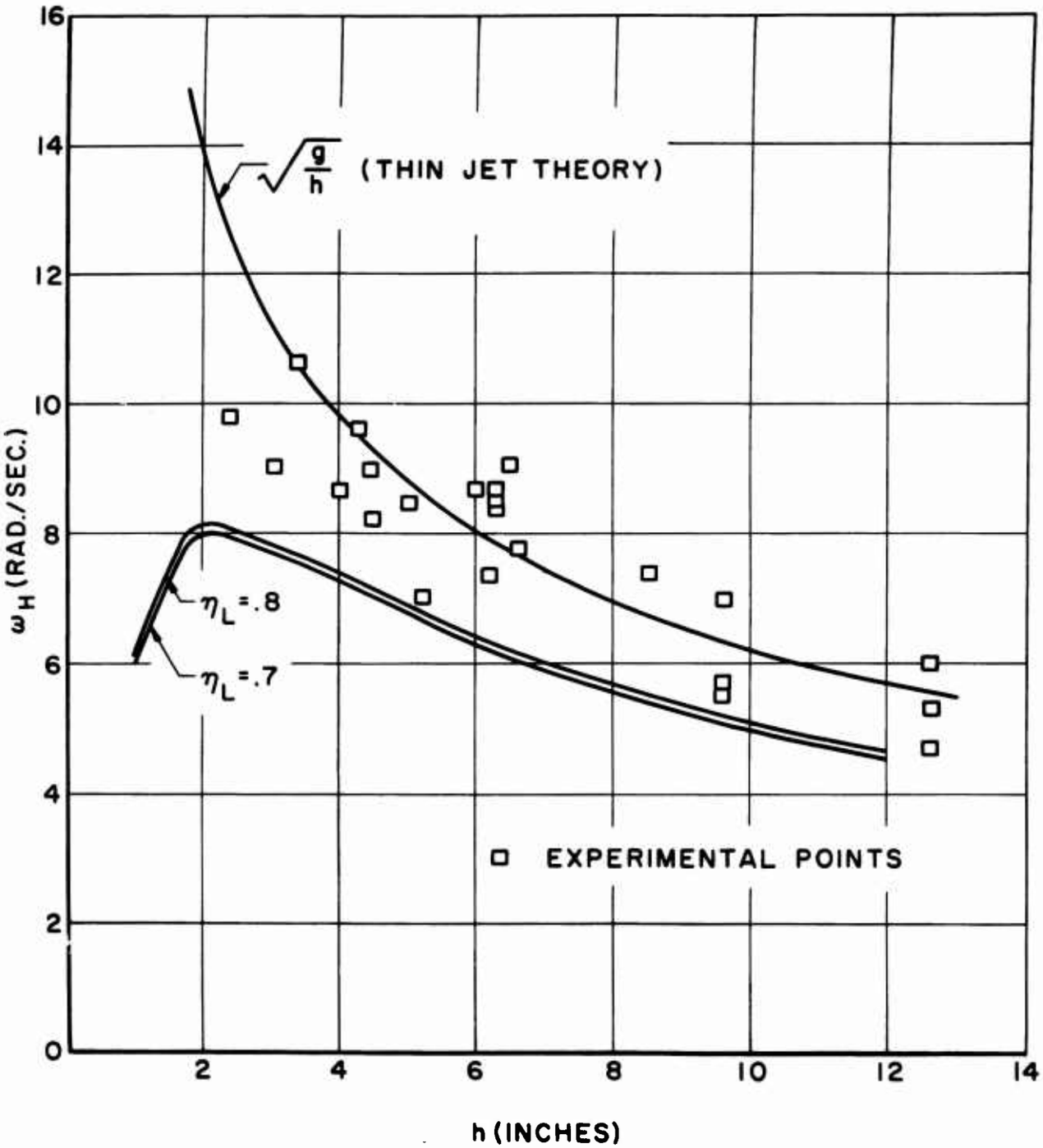

FIGURE 6 EXPERIMENTAL HEAVE FREQUENCY

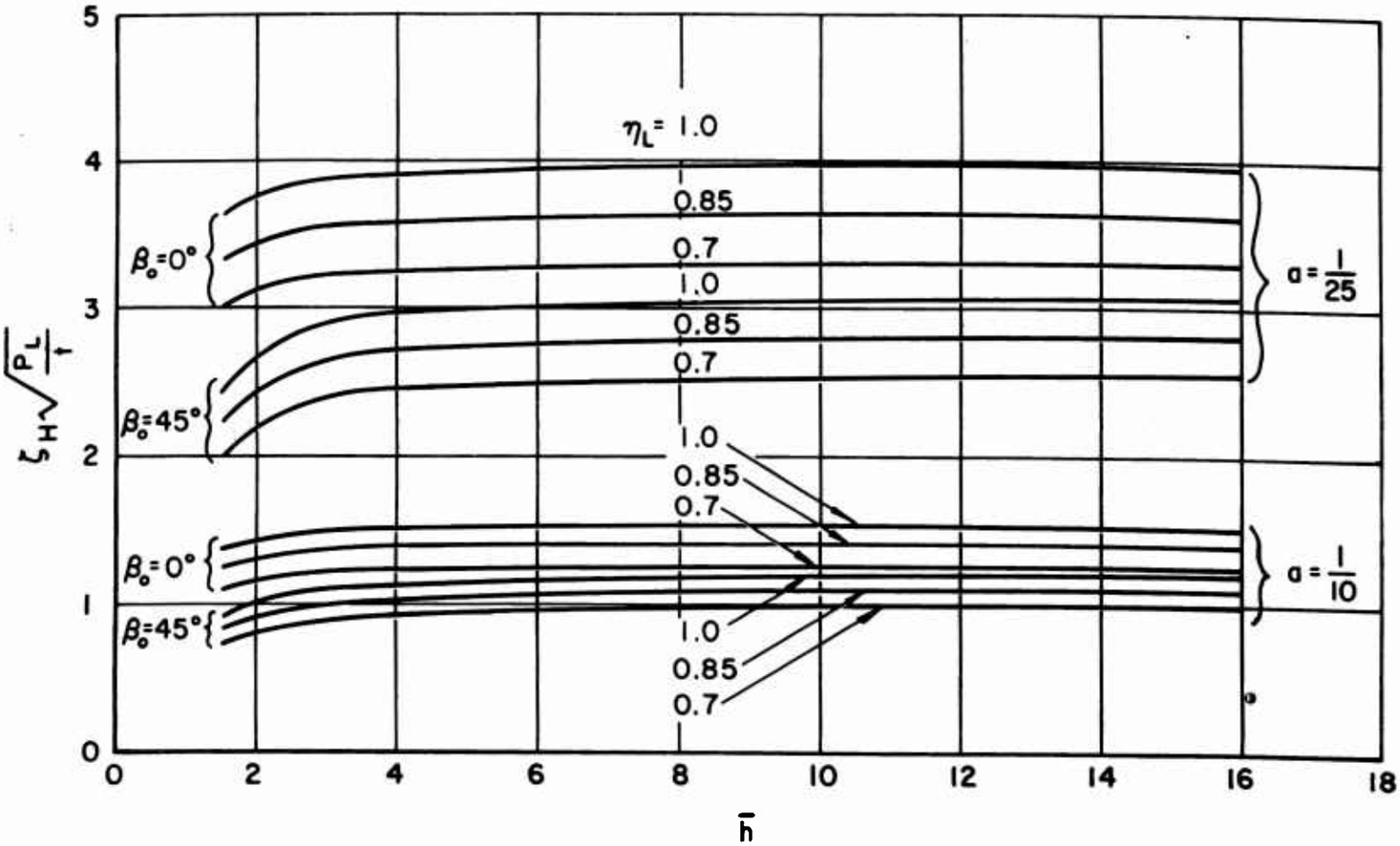

FIGURE 7 HEAVE DAMPING

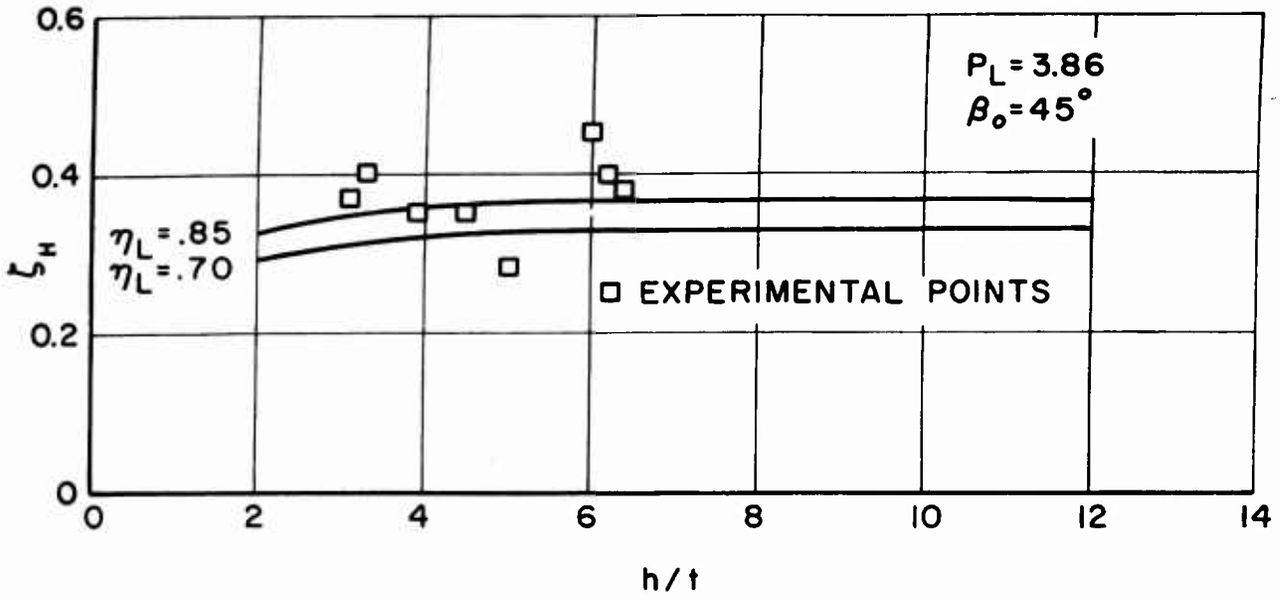

FIGURE 8 EXPERIMENTAL HEAVE DAMPING

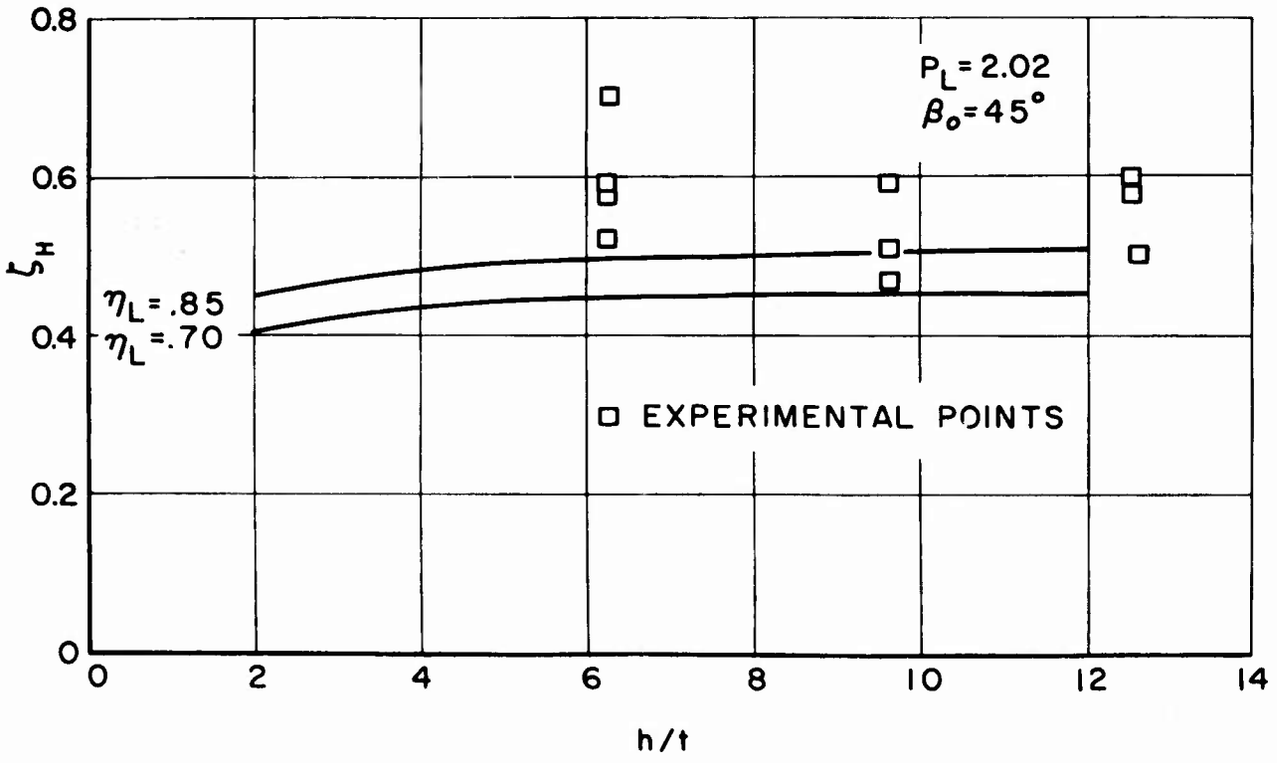

FIGURE 9 EXPERIMENTAL HEAVE DAMPING

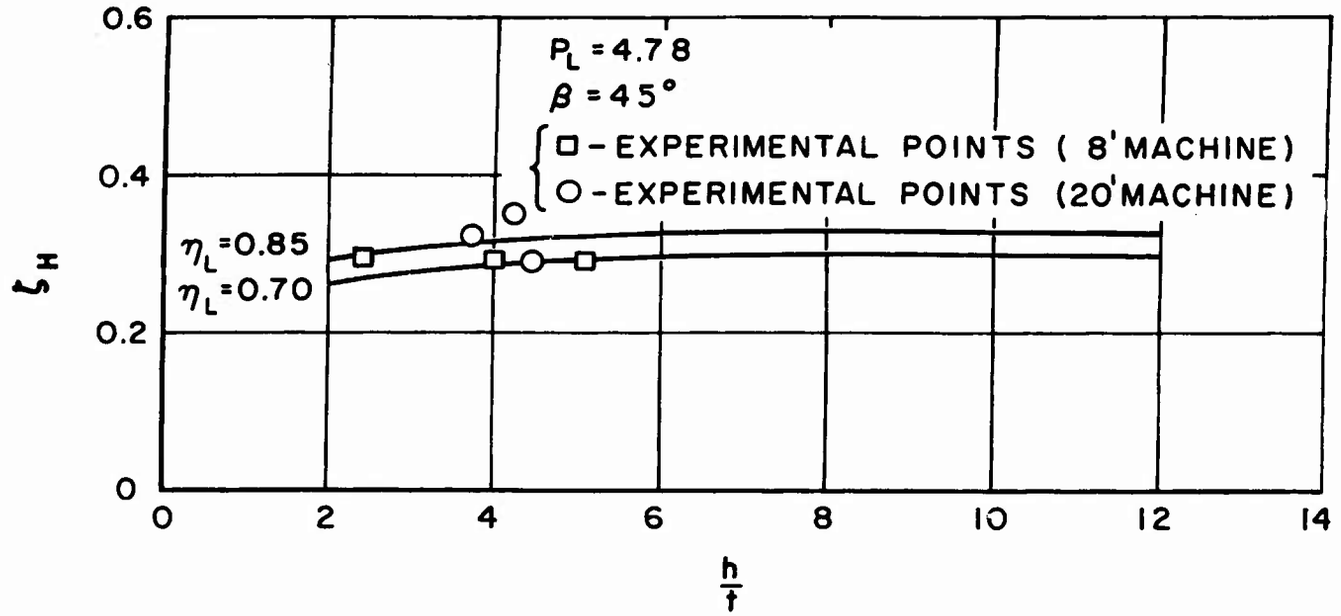

FIGURE 10 EXPERIMENTAL HEAVE DAMPING

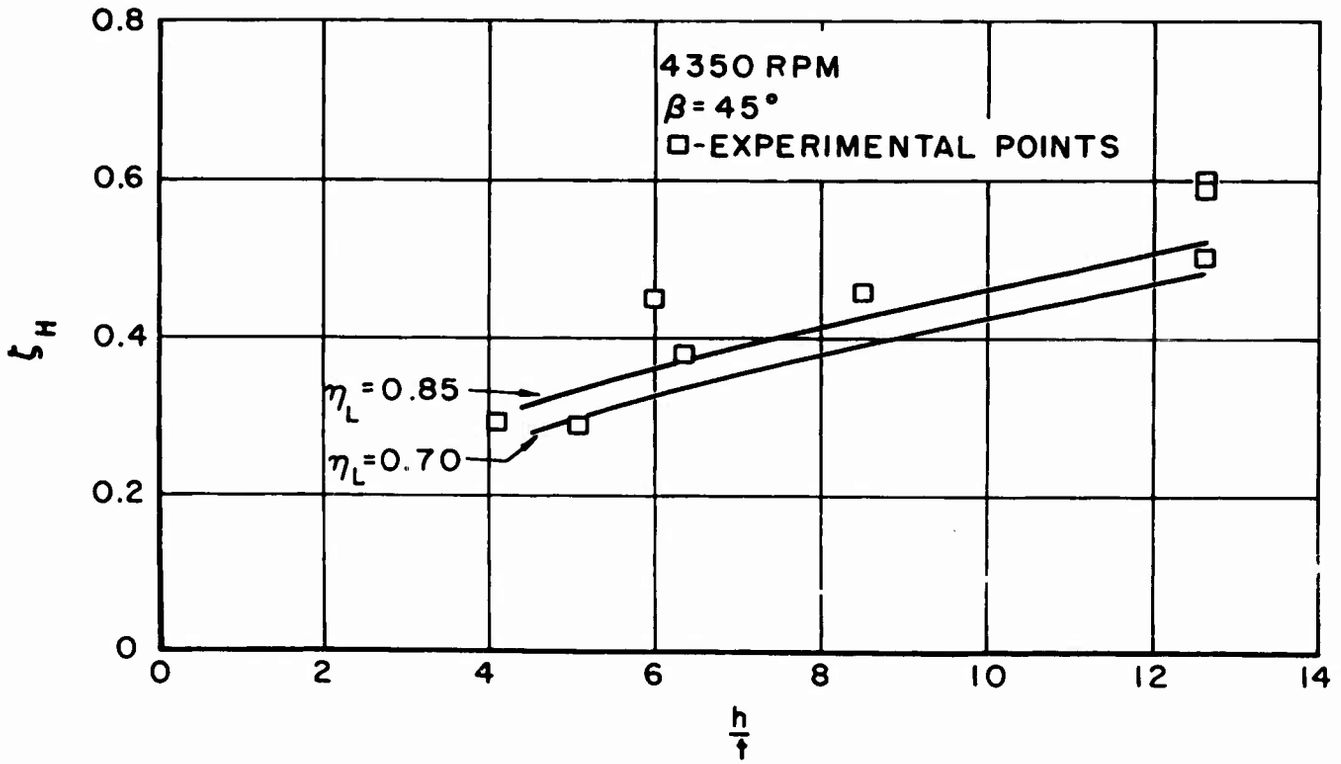

FIGURE 11 EXPERIMENTAL HEAVE DAMPING

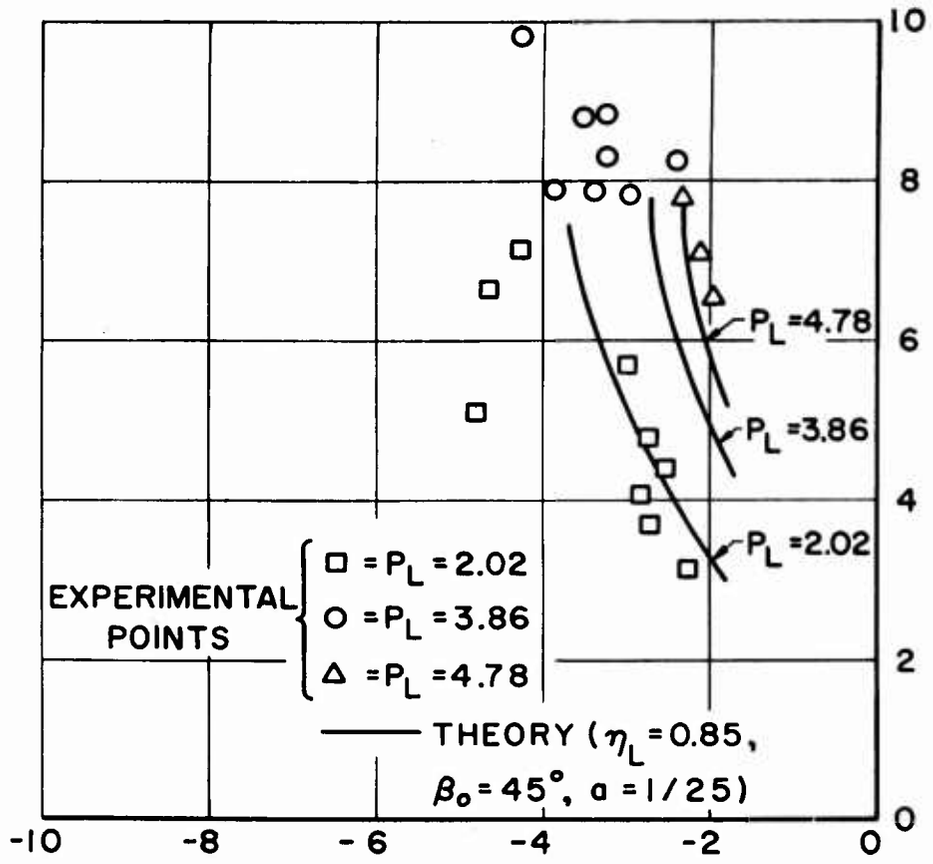

FIGURE 12 HEAVE MODE ROOT LOCUS

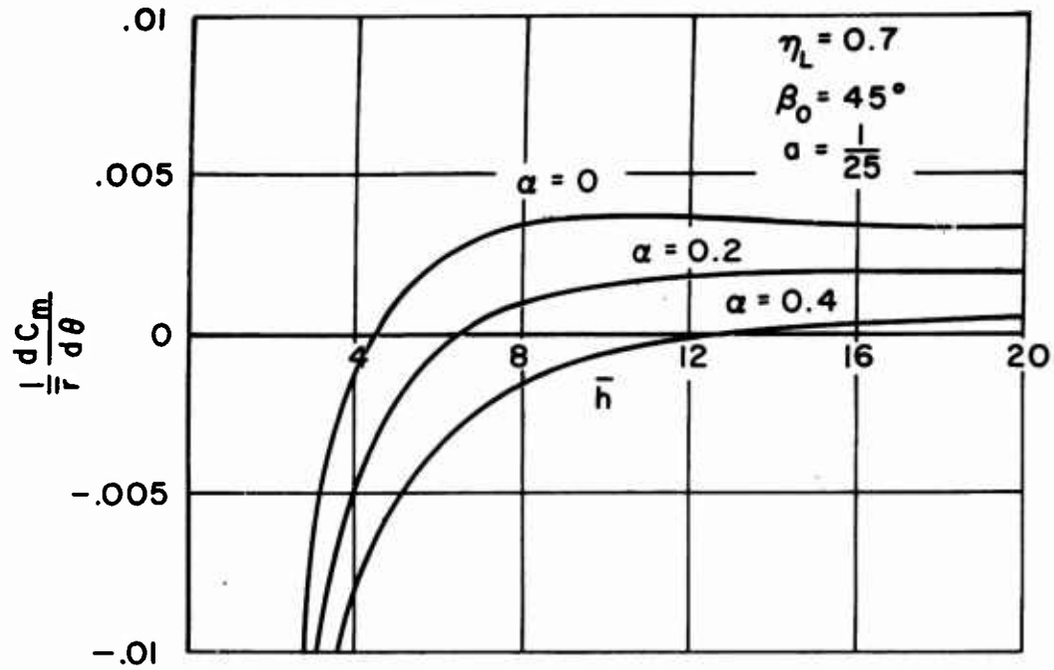

FIGURE 13 EFFECT OF CROSS FLOW DISSIPATION FACTOR ON $\frac{1}{\bar{r}}\frac{dC_m}{d\theta}$

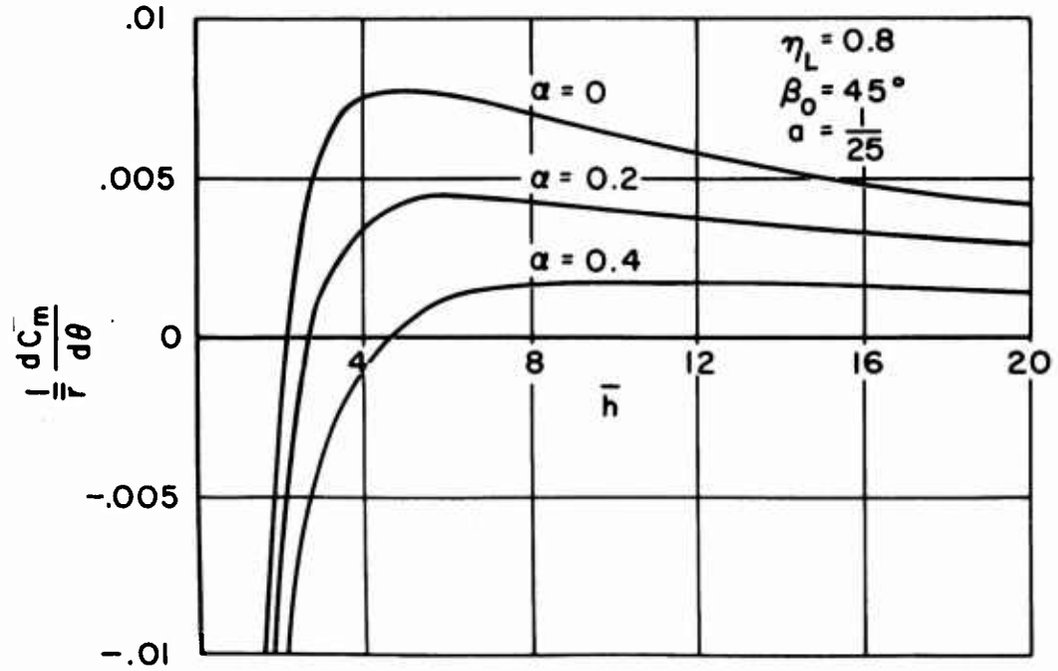

FIGURE 14 EFFECT OF CROSS FLOW DISSIPATION FACTOR ON $\frac{1}{\bar{r}}\frac{dC_m}{d\theta}$

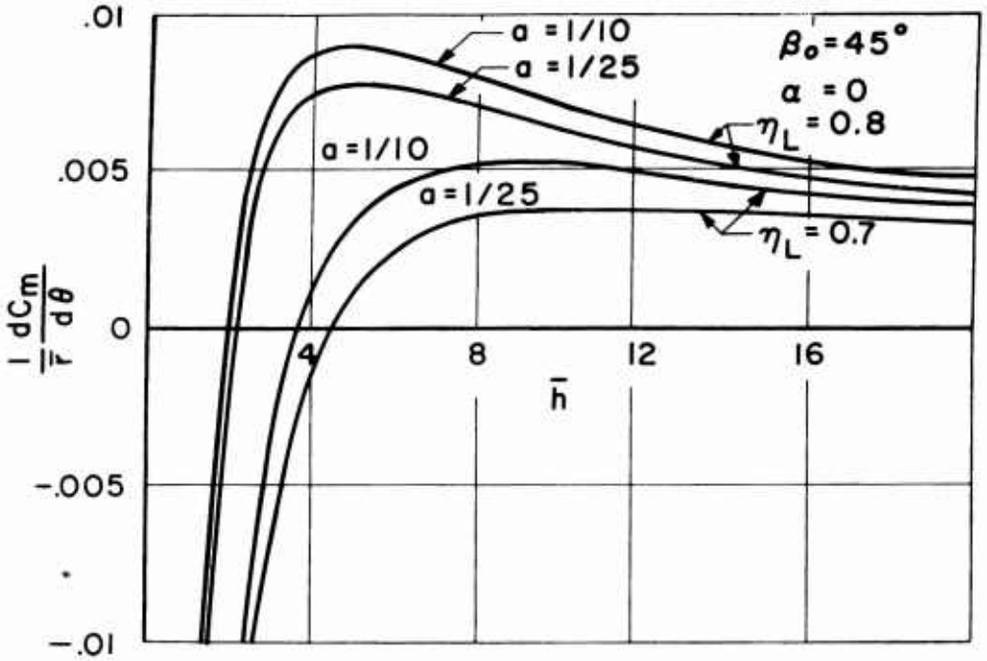

FIGURE 15 EFFECT OF NOZZLE TO BASE AREA ROTOR ON $\frac{1}{\bar{r}}\frac{dC_m}{d\theta}$

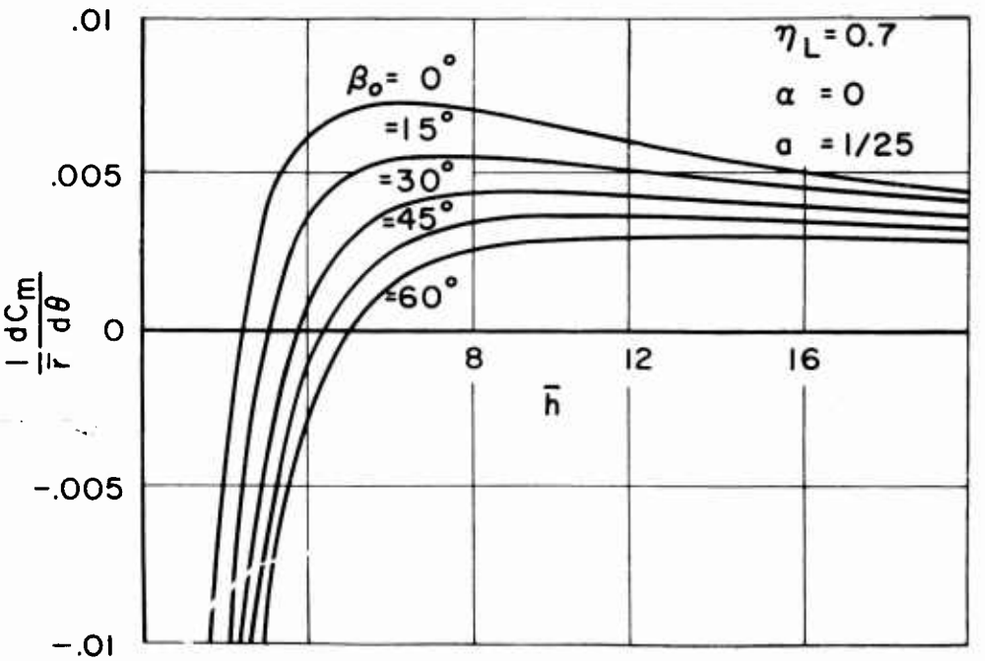

FIGURE 16 EFFECT OF JET INCLINATION ANGLE ON $\frac{1}{\bar{r}}\frac{dC_m}{d\theta}$

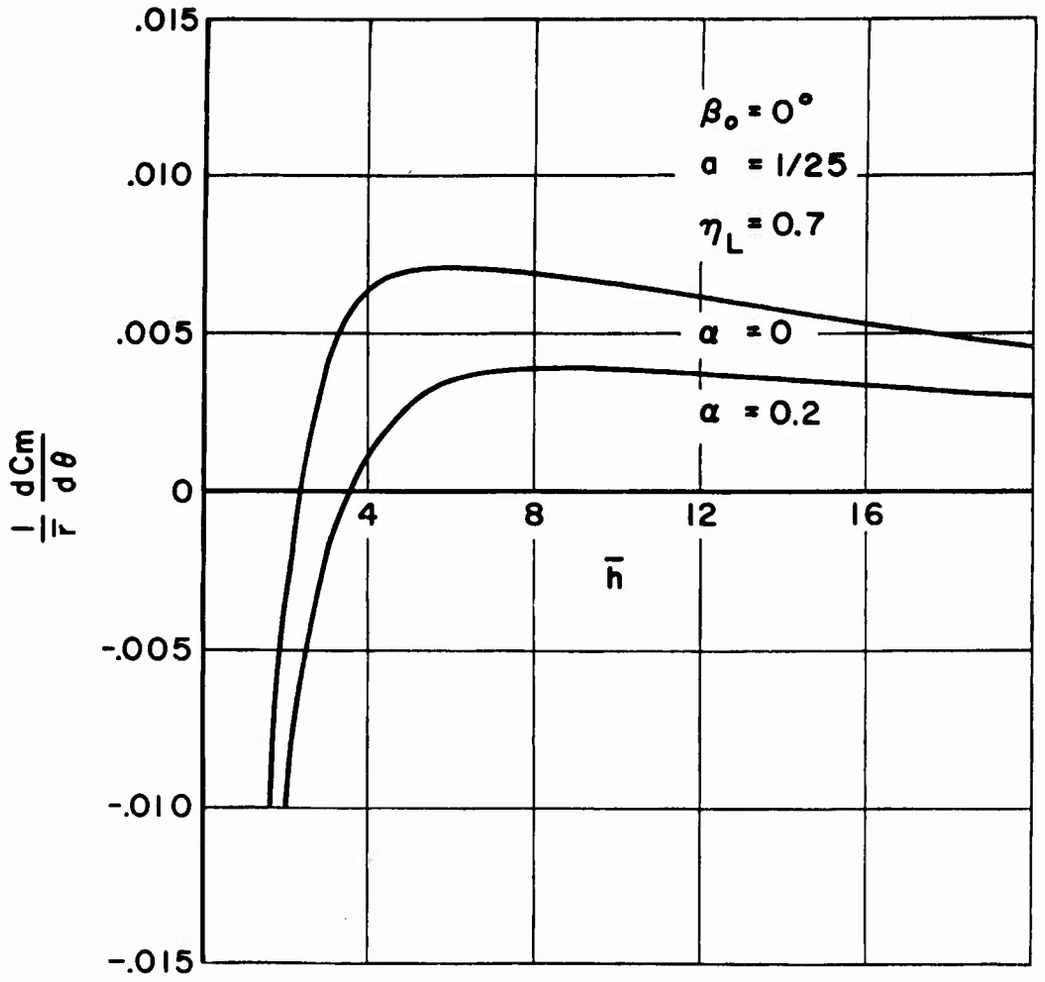

FIGURE 17 EFFECT OF CROSS FLOW

DISSIPATION FACTOR ON $\frac{1}{\bar{r}}\frac{dCm}{d\theta}$

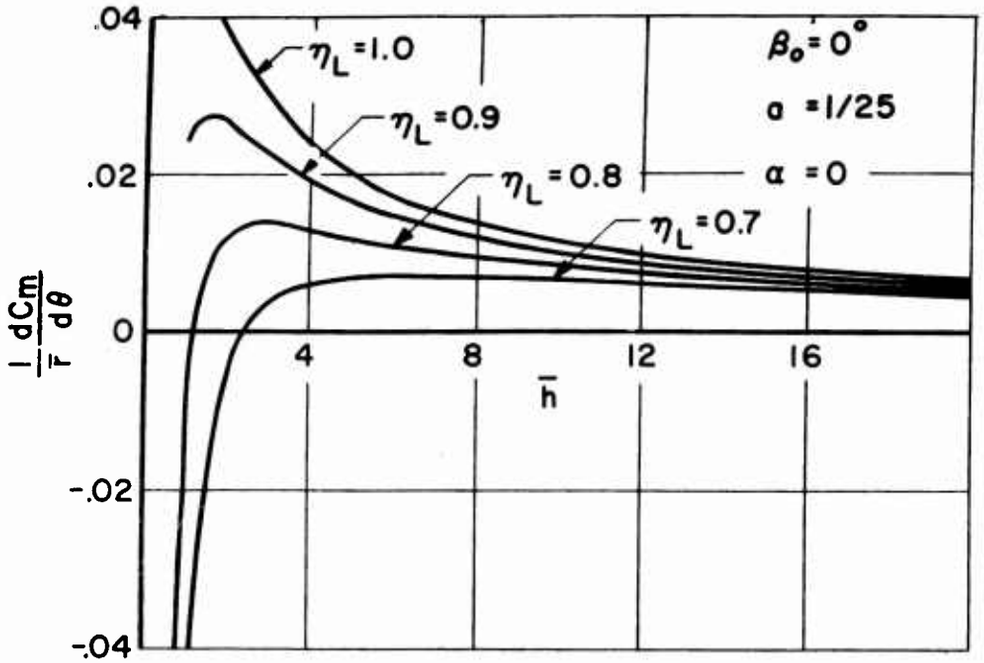

FIGURE 18 EFFECT OF LIFT EFFICIENCY FACTOR ON $\frac{1}{\bar{r}}\frac{dC_m}{d\theta}$

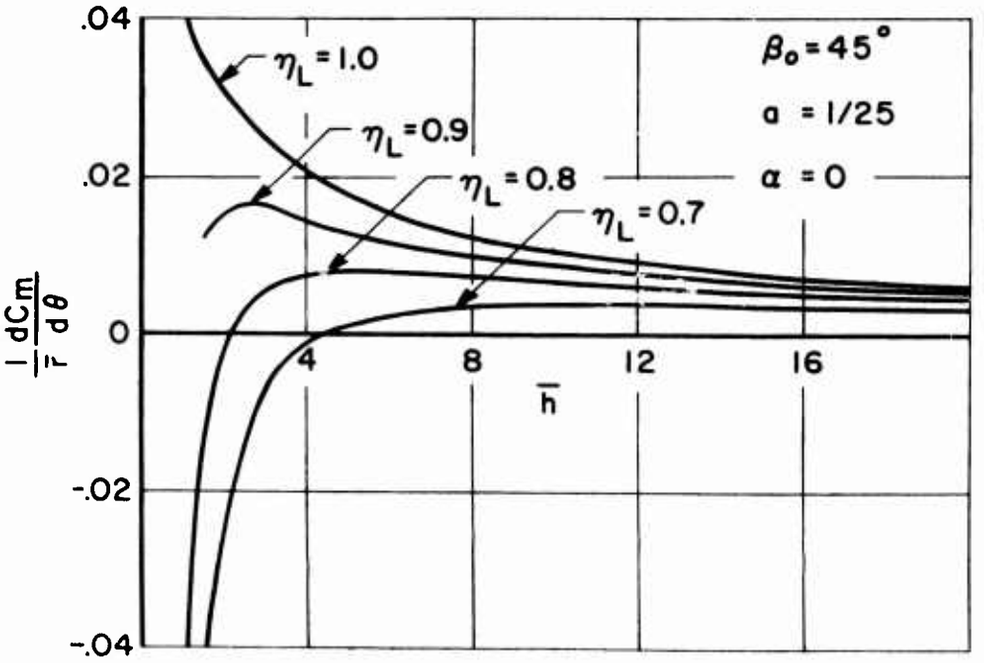

FIGURE 19 EFFECT OF LIFT EFFICIENCY FACTOR ON $\frac{1}{\bar{r}}\frac{dC_m}{d\theta}$

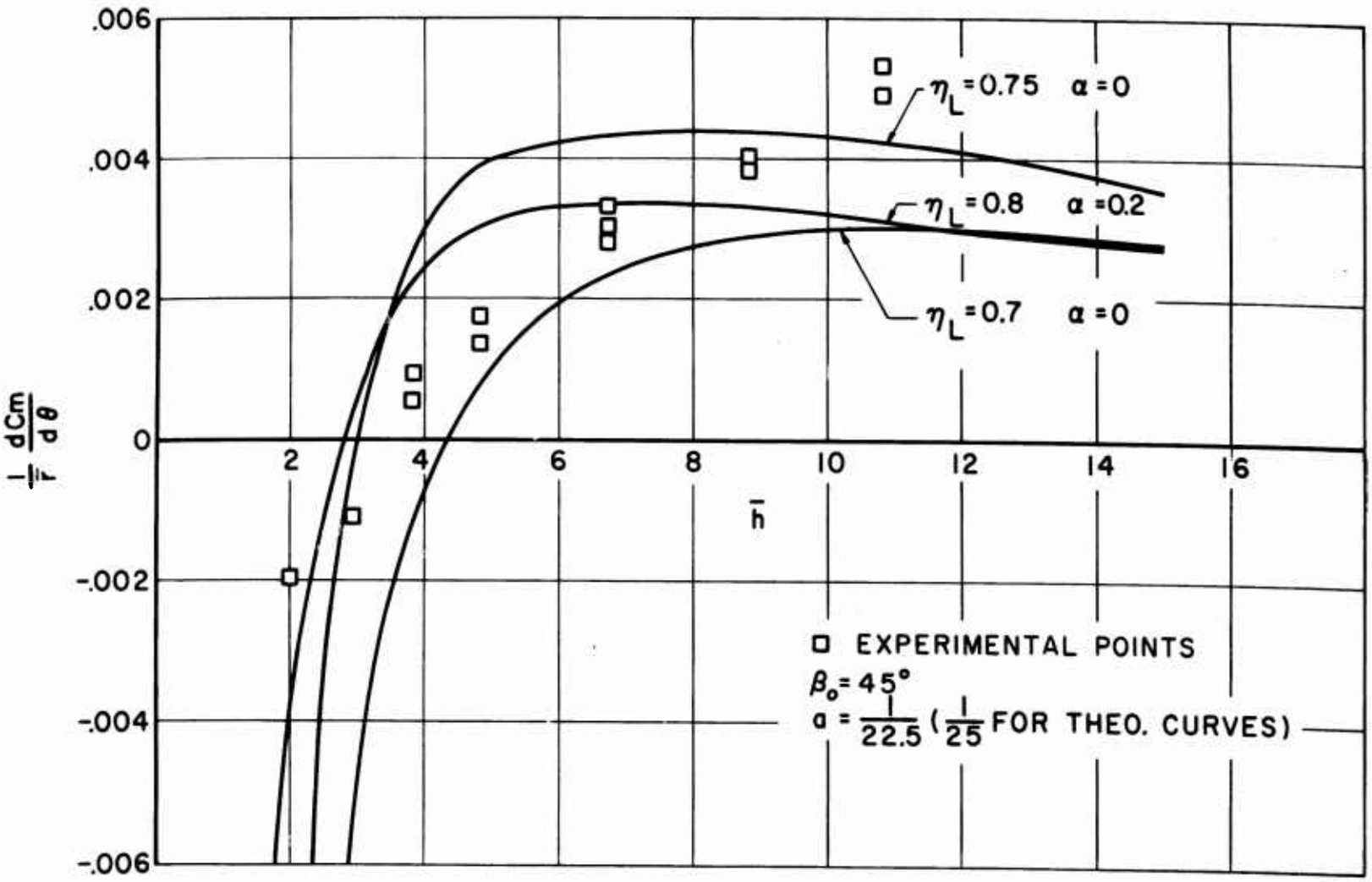

FIGURE 20 EXPERIMENTAL VALUES FOR $\frac{1}{\bar{r}}\frac{dC_m}{d\theta}$

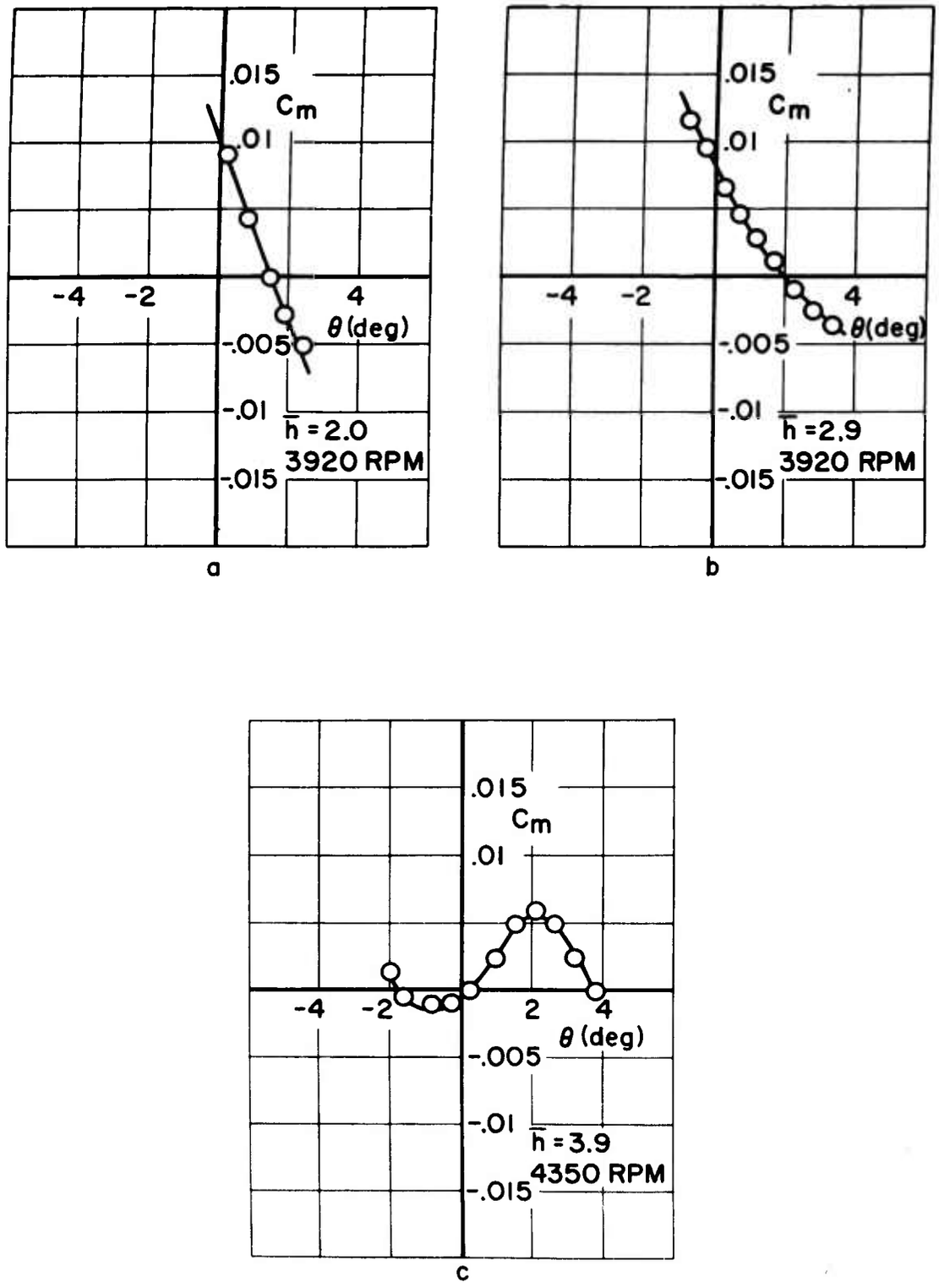

FIGURE 21 EXPERIMENTAL MOMENT VS. ATTITUDE CURVES

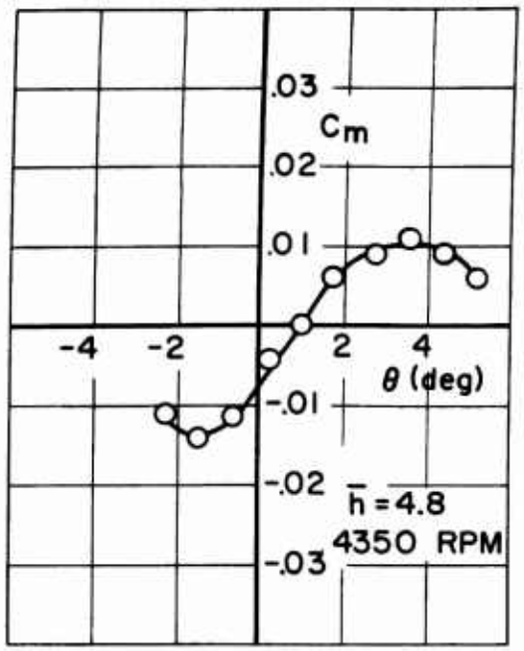

d

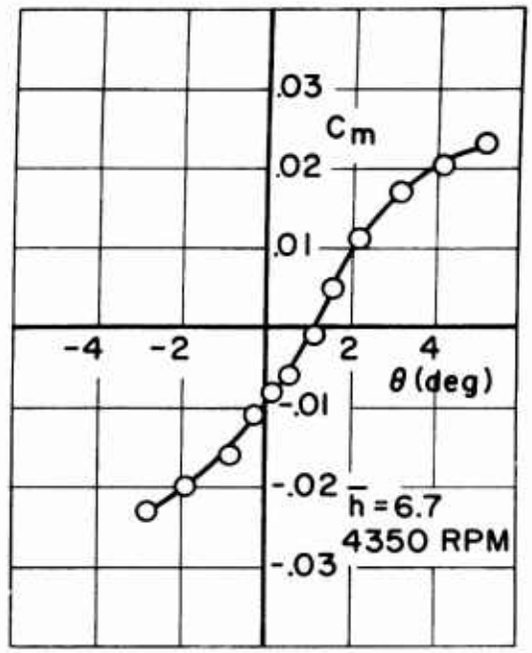

e

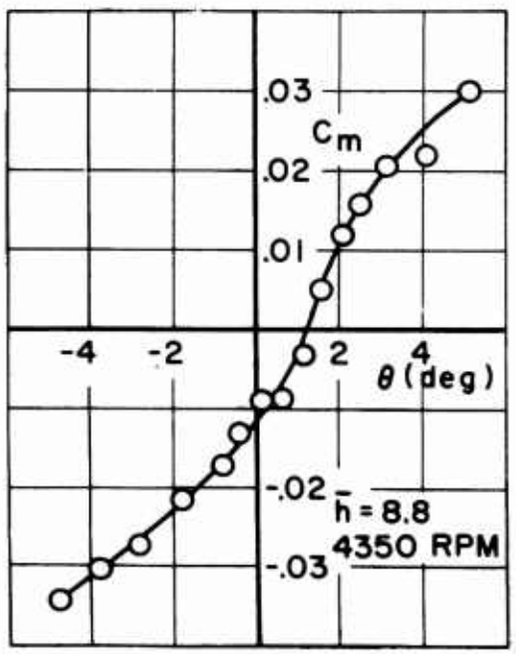

f

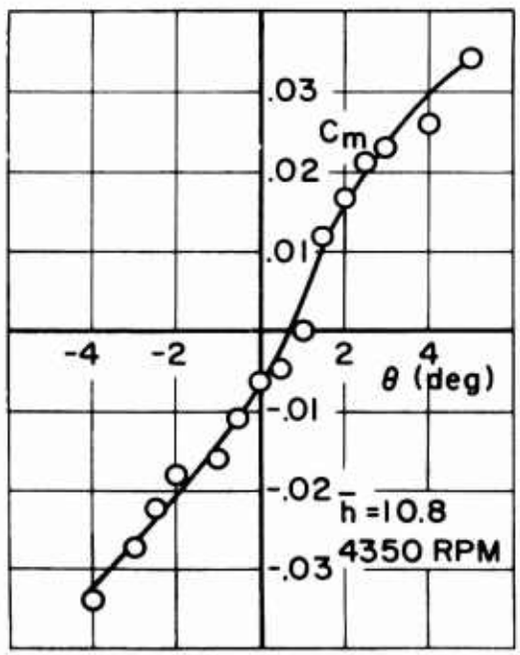

g

FIGURE 21 (cont.)

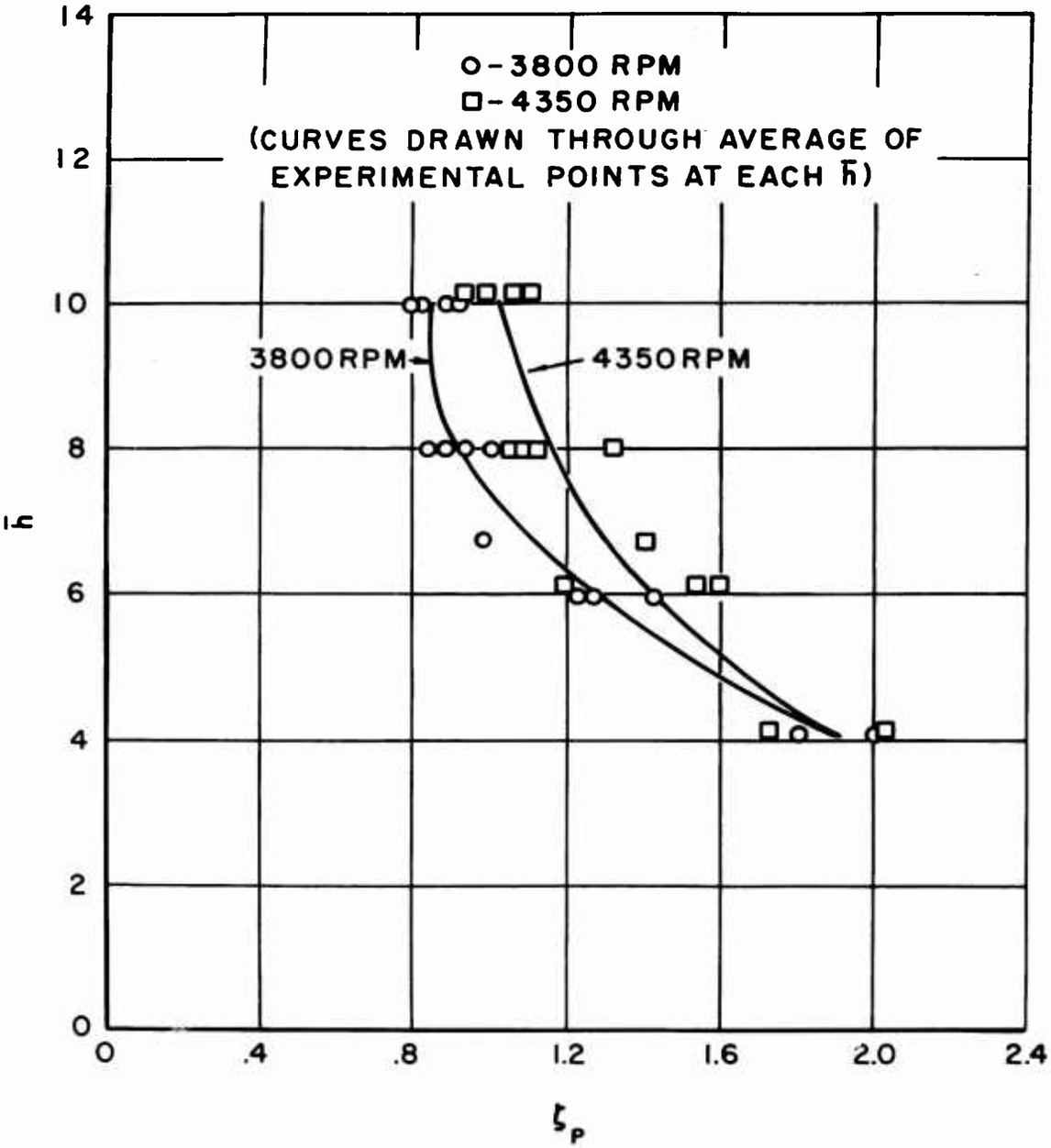

FIGURE 22 EXPERIMENTAL PITCH DAMPING

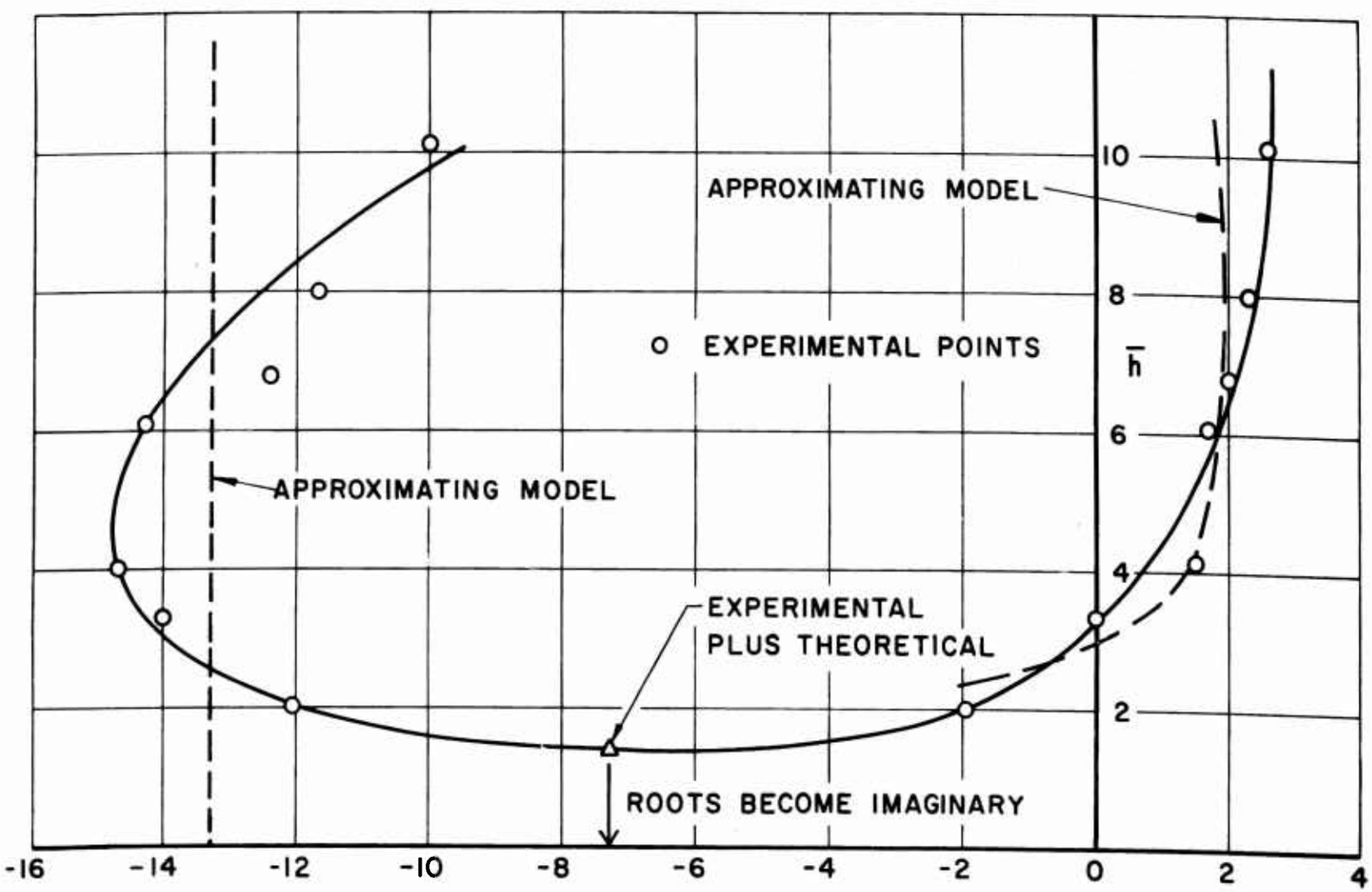

FIGURE 23 CHANGE OF PITCHING MODE WITH HEIGHT

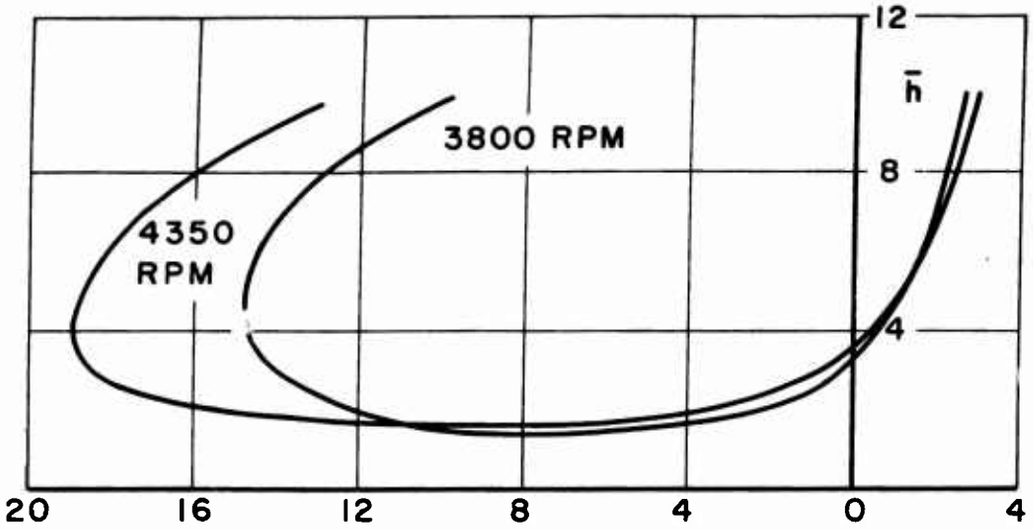

FIGURE 24 EFFECT OF RPM ON PITCHING MODE (EXPERIMENTAL)

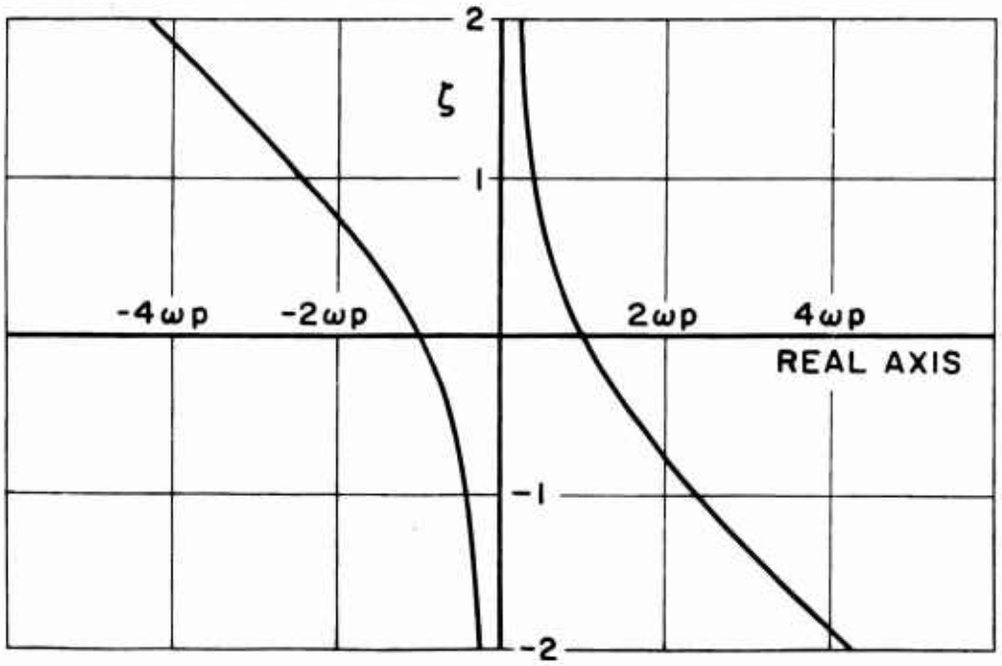

FIGURE 25 EFFECT OF DAMPING ON STATICALLY UNSTABLE SECOND ORDER SYSTEM

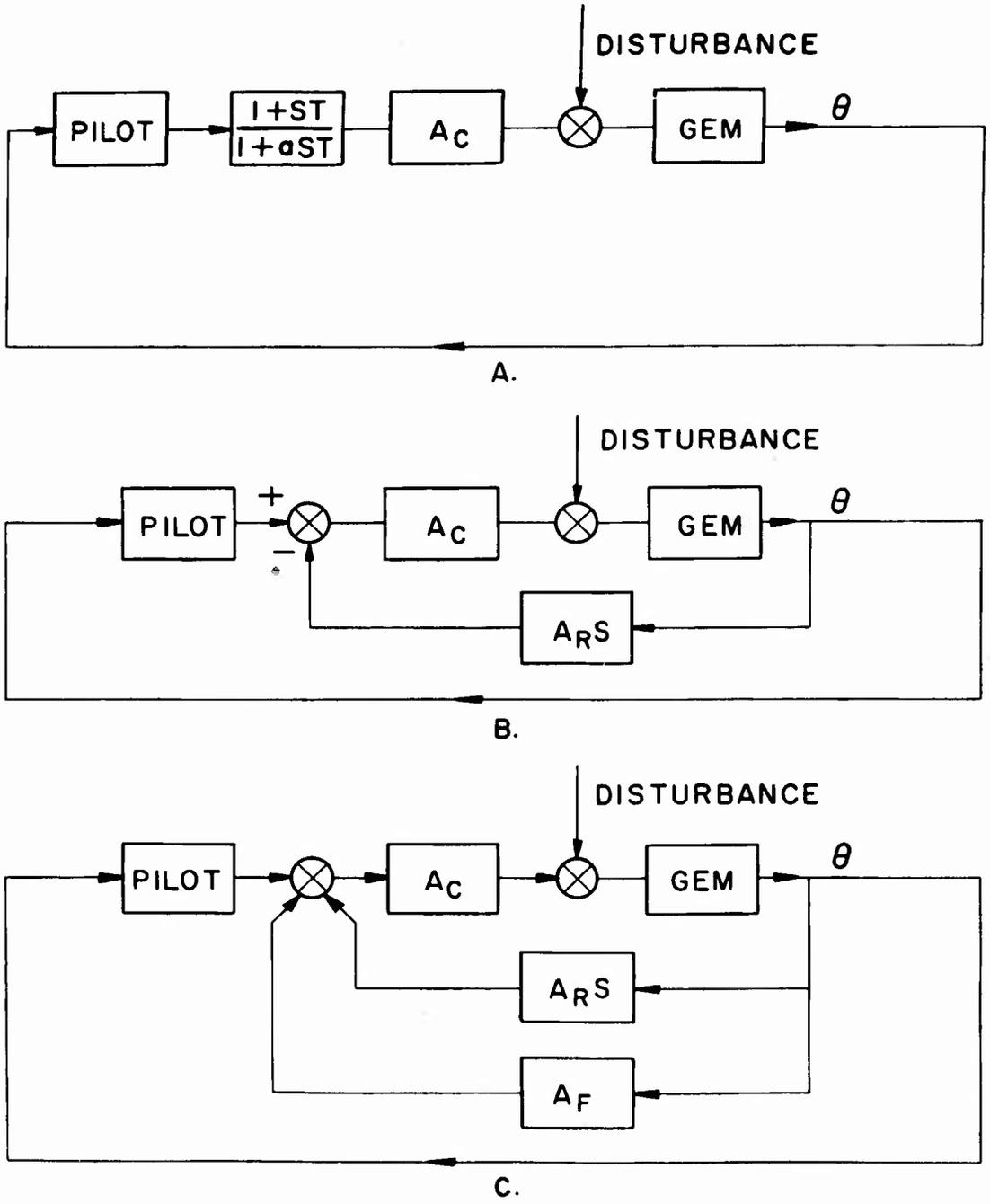

FIGURE 26 FEEDBACK CONFIGURATIONS

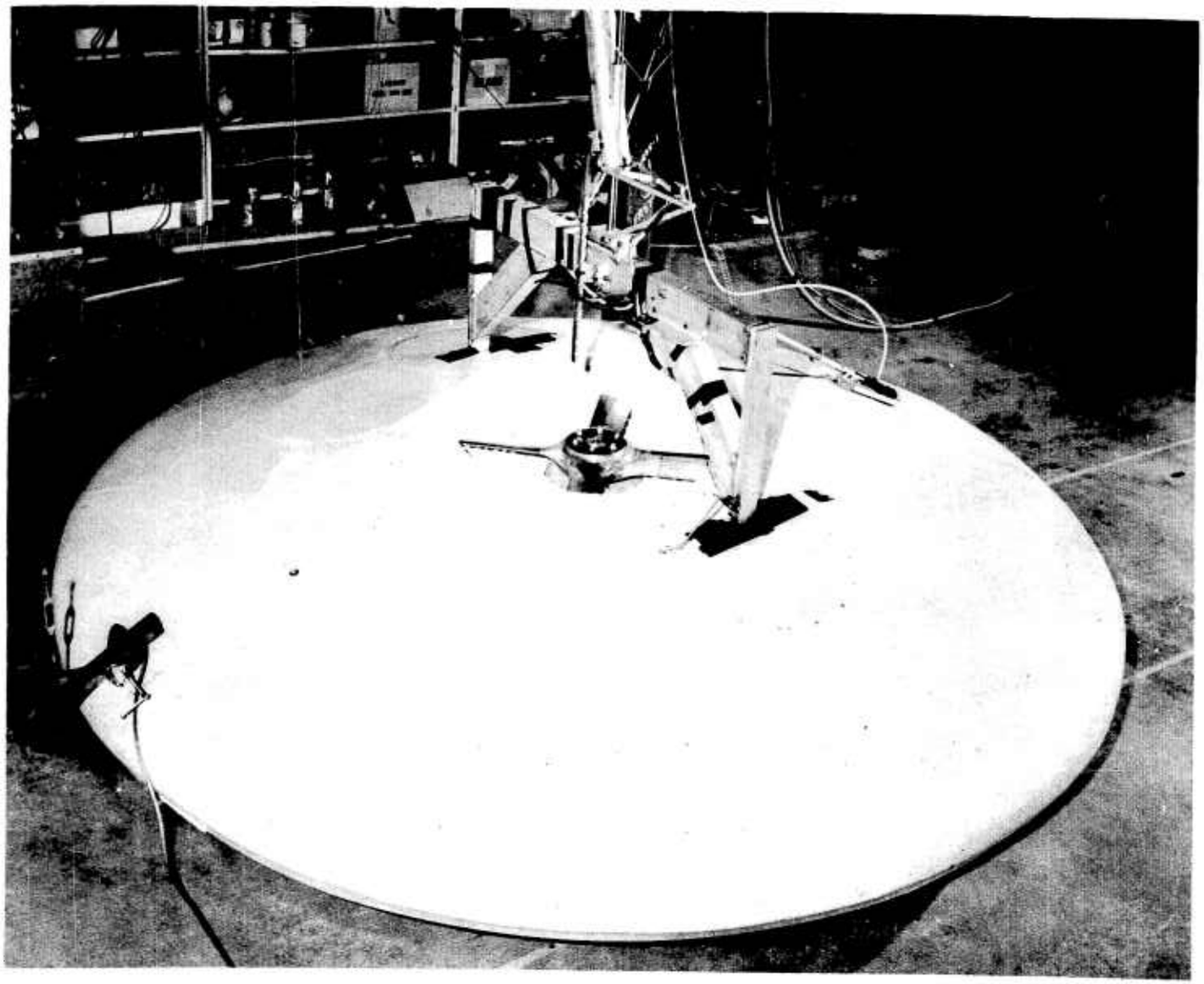

Figure 27. Close-up View of the Model

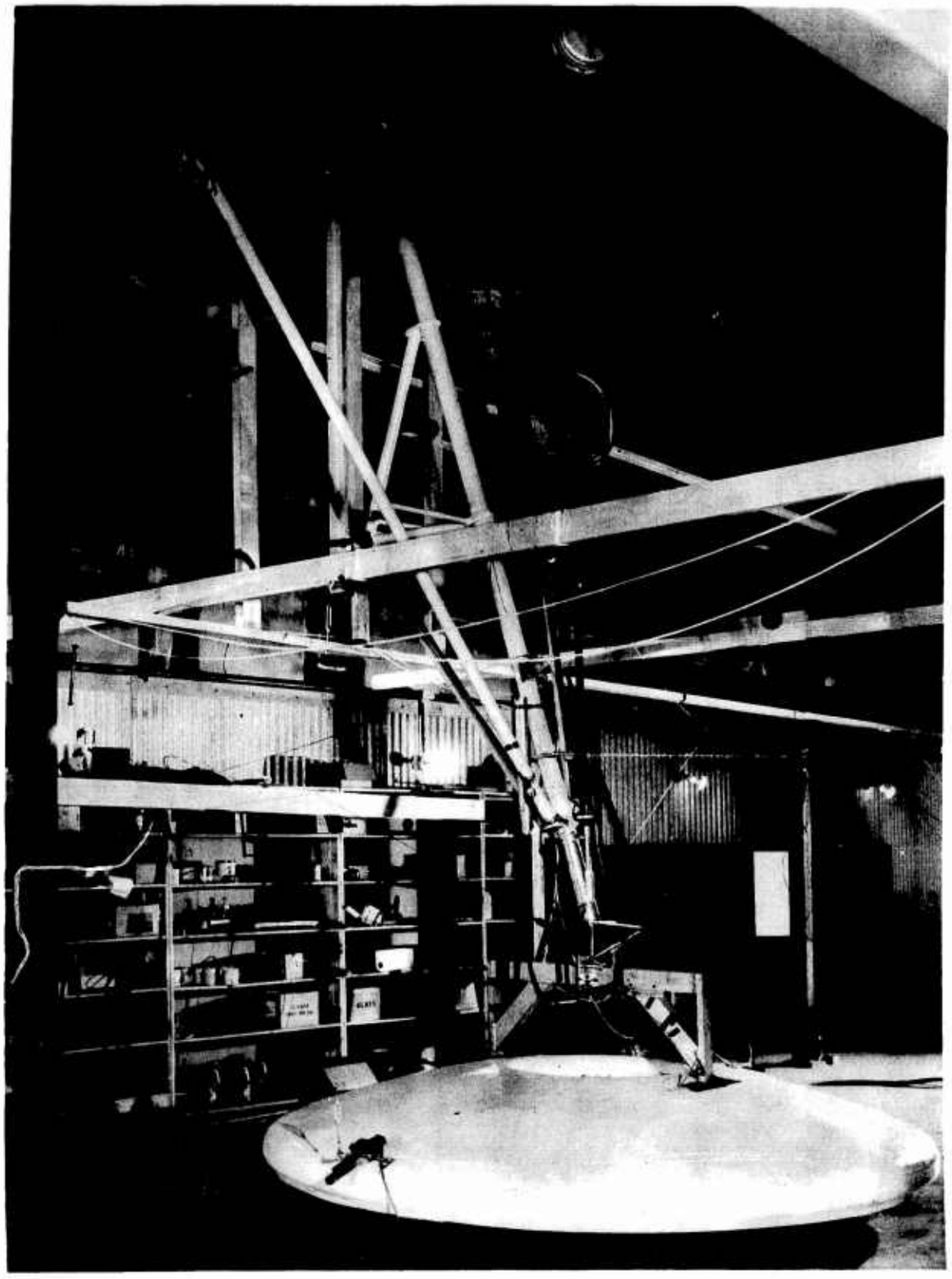

Figure 28. Model and Test Setup

AIART PROGRAM
Technical Report
Distribution List

	ADDRESS	NO. OF COPIES
1.	Chief of Transportation Department of the Army Washington 25, D.C. ATTN: TCACR	2
2.	Commander Wright Air Development Division Wright-Patterson Air Force Base, Ohio ATTN: WCLJA	2
3.	Commanding Officer U.S. Army Transportation Research Command Fort Eustis, Virginia ATTN: Research Reference Center ATTN: Aviation Directorate	4 3
4.	U.S. Army Representative HQ AFSC (SCS-3) Andrews Air Force Base Washington 25, D.C.	1
5.	Director Air University Library ATTN: AUL-8680 Maxwell Air Force Base, Alabama	1
6.	Commanding Officer David Taylor Model Basin Aerodynamics Laboratory Washington 7, D.C.	1
7.	Chief Bureau of Naval Weapons Department of the Navy Washington 25, D.C. ATTN: Airframe Design Division ATTN: Aircraft Division ATTN: Research Division	 1 1 1
8.	Chief of Naval Research Code 461 Washington 25, D.C. ATTN: ALO	1

	ADDRESS	NO. OF COPIES
9.	Director of Defense Research and Development Room 3E - 1065, The Pentagon Washington 25, D.C. ATTN: Technical Library	1
10.	U.S. Army Standardization Group, U.K. Box 65, U.S. Navy 100 FPO New York, New York	1
11.	National Aeronautics and Space Administration 1520 H Street, N. W. Washington 25, D.C. ATTN: Bertram A. Mulcahy Director of Technical Information	5
12.	Librarian Langley Research Center National Aeronautics & Space Administration Langley Field, Virginia	1
13.	Ames Research Center National Aeronautics and Space Agency Moffett Field, California ATTN: Library	1
14.	Armed Services Technical Information Agency Arlington Hall Station Arlington 12, Virginia	10
15.	Office of Chief of Research and Development Department of the Army Washington 25, D.C. ATTN: Mobility Division	1
16.	Senior Standardization Representative U.S. Army Standardization Group, Canada c/o Director of Weapons and Development Army Headquarters Ottawa, Canada	1
17.	Canadian Liaison Officer U.S. Army Transportation School Fort Eustis, Virginia	3

	ADDRESS	NO. OF COPIES
18.	British Joint Services Mission (Army Staff) DAQMG (Mov & Tn) 1800 "K" Street, N. W. Washington 6, D.C. ATTN: Lt. Col. R.J. Wade, R.E.	3
19.	Office of Technical Services Acquisition Section Department of Commerce Washington 25, D.C.	2
20.	Librarian Institute of the Aeronautical Sciences 2 East 64th Street New York 21, New York	2
21.	Chief U.S. Army Research and Development Group (Europe) ATTN: USATRECOM Liaison Officer APO 757 New York, New York	1

AD_____ Accession No. _____

Princeton University Aero. Eng. Dept., Princeton, N.J.

STABILITY AUGMENTATION OF GROUND EFFECT MACHINES -T.A. Dukes C.R. Hargraves

Report No. 601, April 1962
127 pp.-illus.

Contract No. DA44-177-TC-524
Project No. 9-38-01-000, TK902
Unclassified Report

UNCLASSIFIED

1. Ground Effect Machines - Stability
2. Automatic Control - Ground Effect Machines
3. Contract No. DA44-177 TC-524

AD_____ Accession No. _____

Princeton University Aero. Eng. Dept., Princeton, N.J.

STABILITY AUGMENTATION OF GROUND EFFECT MACHINES -T.A. Dukes C.R. Hargraves

Report No. 601, April 1962
127 pp.-illus.

Contract No. DA44-177-TC-524
Project No. 9-38-01-000, TK902
Unclassified Report

UNCLASSIFIED

1. Ground Effect Machines - Stability
2. Automatic Control - Ground Effect Machines
3. Contract No. DA44-177 TC-524

AD_____ Accession No. _____

Princeton University Aero. Eng. Dept., Princeton, N.J.

STABILITY AUGMENTATION OF GROUND EFFECT MACHINES -T.A. Dukes C.R. Hargraves

Report No. 601, April 1962
127 pp.-illus.

Contract No. DA44-177-TC-524
Project No. 9-38-01-000, TK902
Unclassified Report

UNCLASSIFIED

1. Ground Effect Machines - Stability
2. Automatic Control - Ground Effect Machines
3. Contract No. DA44-177 TC-524

AD_____ Accession No. _____

Princeton University Aero. Eng. Dept., Princeton, N.J.

STABILITY AUGMENTATION OF GROUND EFFECT MACHINES -T.A. Dukes C.R. Hargraves

Report No. 601, April 1962
127 pp.-illus.

Contract No. DA44-177-TC-524
Project No. 9-38-01-000,TK902
Unclassified Report

Unclassified

1. Ground Effect Machines - Stability
2. Automatic Control - Ground Effect Machines
3. Contract No. DA44-177 TC-524

This is a study of feedback control for the stabilization of a GEM. The study is limited to over land operation, to hovering and low forward velocities. Expressions for the frequency and damping of the heave motion and for the attitude moment derivative are derived, using the principle of momentum balance. The influence of physical parameters and scaling is discussed. The equations of forward flight are developed. The results of a series of experiments on an 8' diameter GEM model are in satisfactory agreement with predictions. They also show considerable damping of the attitude motion. An attitude and rate feedback control system was devised, considering the adaptability of the human pilot and the disturbing moments. Preliminary synthesis brings out the significance of the moment control lag and variation of the moment control effectiveness. It is suggested that open loop gain adjustments can be expected to provide satisfactory compensation for parameter changes.

This is a study of feedback control for the stabilization of a GEM. The study is limited to over land operation, to hovering and low forward velocities. Expressions for the frequency and damping of the heave motion and for the attitude moment derivative are derived, using the principle of momentum balance. The influence of physical parameters and scaling is discussed. The equations of forward flight are developed. The results of a series of experiments on an 8' diameter GEM model are in satisfactory agreement with predictions. They also show considerable damping of the attitude motion. An attitude and rate feedback control system was devised, considering the adaptability of the human pilot and the disturbing moments. Preliminary synthesis brings out the significance of the moment control lag and variation of the moment control effectiveness. It is suggested that open loop gain adjustments can be expected to provide satisfactory compensation for parameter changes.

This is a study of feedback control for the stabilization of a GEM. The study is limited to over land operation, to hovering and low forward velocities. Expressions for the frequency and damping of the heave motion and for the attitude moment derivative are derived, using the principle of momentum balance. The influence of physical parameters and scaling is discussed. The equations of forward flight are developed. The results of a series of experiments on an 8' diameter GEM model are in satisfactory agreement with predictions. They also show considerable damping of the attitude motion. An attitude and rate feedback control system was devised, considering the adaptability of the human pilot and the disturbing moments. Preliminary synthesis brings out the significance of the moment control lag and variation of the moment control effectiveness. It is suggested that open loop gain adjustments can be expected to provide satisfactory compensation for parameter changes.

This is a study of feedback control for the stabilization of a GEM. The study is limited to over land operation, to hovering and low forward velocities. Expressions for the frequency and damping of the heave motion and for the attitude moment derivative are derived, using the principle of momentum balance. The influence of physical parameters and scaling is discussed. The equations of forward flight are developed. The results of a series of experiments on an 8' diameter GEM model are in satisfactory agreement with predictions. They also show considerable damping of the attitude motion. An attitude and rate feedback control system was devised, considering the adaptability of the human pilot and the disturbing moments. Preliminary synthesis brings out the significance of the moment control lag and variation of the moment control effectiveness. It is suggested that open loop gain adjustments can be expected to provide satisfactory compensation for parameter changes.

UNCLASSIFIED